



DISSERTATION
der Fakultät für Biologie
der Ludwig-Maximilians-Universität München

EXPLORING *Synechocystis* PCC 6803 AS
A SYNTHETIC BIOLOGY PLATFORM TO
STUDY PLANT PHOTOSYNTHESIS

Vorgelegt von: Chiara GANDINI
Tag der Abgabe: 30.05.2017

Diese Dissertation wurde angefertigt
unter der Leitung von Prof. Dario Leister
im Bereich von Fakultät für Biologie
an der Ludwig-Maximilians-Universität München

Erstgutachter: Prof. Dario LEISTER
Zweitgutachter: Prof. Dr. Jörg NICKELSEN

Tag der Abgabe: 30.05.2017
Tag der mündlichen Prüfung: 06.11.2017

ERKLÄRUNG

Ich versichere hiermit an Eides statt, dass meine Dissertation selbständig und ohne unerlaubte Hilfsmittel angefertigt worden ist. Die vorliegende Dissertation wurde weder ganz, noch teilweise bei einer anderen Prüfungskommission vorgelegt. Ich habe noch zu keinem früheren Zeitpunkt versucht, eine Dissertation einzureichen oder an einer Doktorprüfung teilzunehmen.

München, den 29.05.2017

Summary

In plants, oxygenic photosynthesis occurs in chloroplasts, specialized organelles that are remainders of an ancient cyanobacterium endosymbiont. Today, understanding the biogenesis and repair of photosynthetic complexes of land plants is of crucial importance to improve crops yields and biofuel production. However, the study of plant photosynthesis is hampered by the inherent technical and biological limitations of plant model organisms. Hence, a new approach to investigate plant photosynthesis must emerge. A promising but challenging approach would be the reconstitution of plant-like photosynthetic complexes in a prokaryotic chassis such as the model cyanobacterium *Synechocystis* PCC 6803.

In this work, the feasibility to use *Synechocystis* as a chassis to study plant photosynthesis is explored by three approaches. First, a method to construct cDNA expression libraries from the model plant *Arabidopsis thaliana* to complement photosynthetic mutants of *Synechocystis* is described. A tailor-made cDNA expression vector was constructed and a procedure for synthesis and cloning of cDNA fragments implemented. The boosted *Synechocystis* transformation efficiency by two orders of magnitude enabled the construction of a representative cDNA library. Second, the reconstitution in *Synechocystis* of the light harvesting complexes (LHC) from *Arabidopsis* was attempted. The genes *cpSRP43*, *cpSRP54*, *cpFtsY* and *Alb3*, shown previously to help the LHC reconstitution *in vitro*, together with the structural gene *Lhcb1*, were cloned in *Synechocystis* within a synthetic construct. However, not all the foreign proteins accumulated successfully. Further analysis revealed that the gene sequence optimization affected transcripts stability. Third, a *Synechocystis* mutant for SynPAM71, a putative manganese (Mn) transporter, was characterized. The loss of SynPAM71 function induces Mn²⁺ sensitivity, reduces accumulation of PSI, and impairs PSII activity. SynPAM71 was found in both plasma and thylakoid membrane fractions. These data suggest that SynPAM71 is a Mn²⁺ exporter that protects the cytoplasm from the detrimental effects of excess Mn²⁺ by shunting it into periplasmic and luminal compartments. This latter study highlighted differences in Mn homeostasis between *Arabidopsis* and *Synechocystis*.

Zusammenfassung

In Pflanzen findet oxygene Photosynthese in den Chloroplasten, spezialisierten Organellen, die Relikte eines ursprünglich Cyanobakterien-ähnlichen Endosymbionten sind, statt. Heute ist das Verständnis der Biogenese und Reparatur von photosynthetischen Komplexen in Landpflanzen von entscheidender Bedeutung für die Verbesserung der Ernteerträge und der Produktion von Biokraftstoffen. Das Studium der pflanzlichen Photosynthese wird jedoch durch die inhärenten technischen und biologischen Einschränkungen pflanzlicher Modellorganismen behindert. Daher bedarf es eines neuen Ansatzes zur Untersuchung der pflanzlichen Photosynthese. Ein vielversprechender, aber anspruchsvoller, Ansatz wäre die Rekonstitution von pflanzenähnlichen photosynthetischen Proteinkomplexen in einem prokaryotischen Chassis wie dem Modell-Cyanobacterium *Synechocystis*.

In dieser Arbeit wird die Möglichkeit, *Synechocystis* als Chassis zu verwenden, um die Pflanzen-Photosynthese zu untersuchen, durch drei Ansätze erforscht. Zuerst wird ein Verfahren zur Konstruktion von cDNA-Expressionsbibliotheken aus der Modellpflanze *Arabidopsis* zur Komplementierung photosynthetischer Mutanten von *Synechocystis* beschrieben. Es wurde ein entsprechender cDNA-Expressionsvektor konstruiert und ein Verfahren zur Synthese und Klonierung von cDNA-Fragmenten implementiert. Eine Steigerung der *Synechocystis*-Transformationseffizienz um zwei Größenordnungen ermöglichte die Konstruktion einer repräsentativen cDNA-Bibliothek. Zweitens wurde eine funktionale Rekonstitution der Lichtsammelkomplexe (LHC) von *Arabidopsis* in *Synechocystis* angestrebt. Die Gene *cpSRP43*, *cpSRP54*, *cpFtsY* und *Alb3*, die eine LHC-Rekonstitution *in vitro* erlauben, wurden zusammen mit dem Strukturgen *Lhcb1* in einem synthetischen Konstrukt in *Synechocystis* kloniert. Allerdings wurden nicht alle exogenen Proteine erfolgreich akkumuliert. Weitere Analysen zeigten, dass die erfolgte Codon-Optimierung für die Destabilisierung der Transkripte verantwortlich sein könnte. Drittens wurde eine *Synechocystis*-Mutante für SynPAM71, einen mutmaßlichen Mangan (Mn)-Transporter, charakterisiert. Der Verlust der SynPAM71-Funktion induziert Mn²⁺-Sensitivität, reduziert die Akkumulation von PSI und beeinträchtigt

tigt die PSII-Aktivität. SynPAM71 wurde sowohl in Plasma- als auch in Thylakoid-Membranfraktionen gefunden. Diese Daten deuten darauf hin, dass SynPAM71 ein Mn^{2+} Exporter ist, der das Cytoplasma vor schädlichen Wirkungen von überschüssigem Mn^{2+} schützt, indem es die Kationen in periplasmatische und lumenale Kompartimente schleust. Zudem wurden Unterschiede hinsichtlich der Mn-Homöostase zwischen *Arabidopsis* und *Synechocystis* gefunden.

Contents

Summary	i
Zusammenfassung	iii
Abbreviations	xii
1 Introduction	1
1.1 Oxygenic photosynthesis	1
1.2 Oxygenic photosynthesis in land plants and cyanobacteria .	2
1.3 Significance of photosynthesis domestication	5
1.4 Plant photosynthesis in the light of synthetic biology	6
1.5 <i>Synechocystis</i> PCC6803 as the prokaryotic chassis to study plant photosynthesis	7
1.6 Aim of the work	8
1.6.1 Shotgun functional complementation of <i>Synechocystis</i> phototrophic mutants with a cDNA library from <i>Arabidopsis</i>	9
1.6.2 Expression and stabilization of functional LHCII in <i>Synechocystis</i>	10
1.6.3 The Mn transporter SynPAM71 is required to main- tain Mn homeostasis in <i>Synechocystis</i>	14
2 Materials and Methods	17
2.1 Materials	17
2.2 Methods used in the cDNA library preparation	17
2.2.1 RNA extraction from <i>Arabidopsis</i>	17
2.2.2 Preparation of pUR and derivative vectors for cloning	20
2.2.3 Construction of pUR2LT	20
2.2.4 Synthesis of double-stranded <i>Arabidopsis</i> cDNA . . .	20
2.2.5 Cloning cDNAs into pUR2LT and transformation of <i>E. coli</i> -donor	22
2.2.6 Measuring the DNA transfer efficiency	23

2.2.7	Conjugal transfer of a cDNA library	23
2.2.8	Calculation of the number of clones required to obtain a representative cDNA library	24
2.2.9	Growing <i>Synechocystis</i> strains	25
2.2.10	Generation <i>Synechocystis</i> Δ <i>psaD</i> and Δ <i>psaD</i> express- ing AtPsaD with or without cTP	25
2.2.11	Immunoblot analysis	26
2.2.12	RNA extraction from <i>Synechocystis</i>	26
2.2.13	Transcript analysis by northern blot	27
2.3	Methods used to reconstitute functional LHCI in <i>Synechocystis</i>	28
2.3.1	Growing <i>Synechocystis</i> strains	28
2.3.2	Generation of pDS433, p54Y and pDESTLhcb1 vectors	28
2.3.3	Synthetic LHC gene cluster and generation of pUR- CLHCop	32
2.3.4	DNA extraction and genotyping of <i>Synechocystis</i> strains	32
2.3.5	Immunoblot analysis	32
2.3.6	Transcript analysis	33
2.3.7	Accession numbers	33
2.4	Methods used for the characterization of <i>Synechocystis</i> knock- out for the putative Mn transporter SynPAM71	36
2.4.1	<i>Synechocystis</i> growth conditions	36
2.4.2	Construction of Δ <i>SynPAM71</i> and the complemented strain F <i>SynPAM71H</i>	36
2.4.3	Pigment analysis	37
2.4.4	Thylakoids isolation and BN-PAGE	37
2.4.5	Immunoblot analysis	37
2.4.6	Determination of total metal concentrations in whole cells and thylakoids	38
2.4.7	SEC-ICP-QQQ-MS measurements	39
2.4.8	Oxygen evolution measurements	39
2.4.9	Accession Numbers	39
3	Results	41
3.1	Shotgun functional complementation of <i>Synechocystis</i> photo- synthetic mutants with a cDNA library from <i>Arabidopsis</i> .	41
3.1.1	Improving <i>Synechocystis</i> transformation efficiency . .	41
3.1.2	cDNA synthesis and construction of a replicative cDNA expression vector for <i>Synechocystis</i>	43
3.1.3	Cloning the cDNA into pUR2LT and creation of a cDNA library in <i>E. coli</i> -donor	46
3.1.4	Complementation of Δ <i>psaD</i> with a cDNA library from <i>Arabidopsis</i>	49

3.1.5	Complementation of other <i>Synechocystis</i> mutants . . .	53
3.2	Expression and stabilization of functional LHCII in <i>Synechocystis</i>	55
3.2.1	First strategy: introducing the LHC operon into the genome of <i>Synechocystis</i>	55
3.2.2	Second strategy: generation of a <i>Synechocystis</i> strain harbouring a synthetic gene cluster for LHC reconstitution	57
3.2.3	Analysis of <i>Synechocystis</i> strains harbouring the synthetic gene cluster for LHC reconstitution	59
3.3	The transporter SynPAM71 is required to maintain Mn homeostasis in <i>Synechocystis</i>	63
3.3.1	Identification of SynPAM71 and construction of <i>Synechocystis</i> Δ SynPAM71	63
3.3.2	Δ SynPAM71 is sensitive to increased Mn ²⁺ concentrations	66
3.3.3	Accumulation of photosynthetic supercomplexes is reduced in the mutant	67
3.3.4	Lack of SynPAM71 affects PSII photochemistry . . .	70
3.3.5	Δ SynPAM71 cytoplasm, thylakoids and PSII protein complexes are enriched in Mn	73
3.3.6	SynPAM71 is predominantly located in the plasma membrane of <i>Synechocystis</i>	74
4	Discussion	79
4.1	Shotgun functional complementation of <i>Synechocystis</i> photosynthetic mutants with a cDNA library from <i>Arabidopsis</i> . .	79
4.2	Expression and stabilization of functional LHCII in <i>Synechocystis</i>	81
4.3	The transporter SynPAM71 is required to maintain Mn homeostasis in <i>Synechocystis</i>	84
5	Conclusion	88
	Appendices	89
A	Complete sequence of the synthetic construct used for LHC reconstitution in <i>Synechocystis</i>	90
B	Raw data for element analysis in WT and ΔSynPAM71 <i>Synechocystis</i> strains	94

List of Figures

1.1	Oxygenic photosynthesis in land plants.	2
1.2	Protein complexes of the photosynthetic apparatus of <i>Arabidopsis</i> and of <i>Thermosynechococcus elongatus</i>	3
1.3	Model of the Lhcb crystal structure and a schematic representation of the chloroplastic SRP pathway.	12
3.1	<i>Synechocystis</i> transformation by natural DNA uptake and conjugation.	42
3.2	Scheme depicting the SMART TM method to synthesize cDNA.	45
3.3	Map and cloning site of the pUR2LT vector to express cDNA libraries in <i>Synechocystis</i>	47
3.4	PCR analysis of cDNA inserts in pUR2L as in <i>E. coli</i> donor	48
3.5	Generation of <i>Synechocystis</i> Δ <i>psaD</i>	50
3.6	Sequence alignment of <i>psaD</i> proteins from <i>Arabidopsis</i> (<i>At_psaD</i>) and <i>Synechocystis</i> (<i>Syn_psaD</i>).	51
3.7	Immunoblot analysis and phenotypic characterization of <i>Synechocystis</i> Δ <i>psaD</i> expressing <i>AtPsaD</i> +cTP and <i>AtPsaD</i> -cTP.	52
3.8	Scheme for the introduction of the LHC operon into the genome of <i>Synechocystis</i>	56
3.9	Maps of the synthetic LHC gene cluster and the final vector pURCLHC.	58
3.10	Genotyping and immunoblot analysis of the heterologous proteins expressed from LHCgc in two WT_LHC strains.	60
3.11	pURCLHCgc transcripts analysis of <i>Synechocystis</i> WT and two WT_LHC strains.	61
3.12	Transcripts analysis of LHCgc genes in different <i>E. coli</i> strains.	62
3.13	Sequence alignment of SynPAM71 with its (predicted) chloroplast-localized homologs from <i>A. thaliana</i> , <i>AtPAM71</i> and <i>AtPAM71HL</i>	64
3.14	Generation of the Δ <i>SynPAM71</i> strain.	65
3.15	Initial characterization of Δ <i>SynPAM71</i>	68

3.16	Immunoblot analysis of proteins from WT and the mutant strain separated by SDS-PAGE	69
3.17	Immunoblot analysis of proteins from WT and mutants strains separated by second dimension (BN-PAGE and subsequently SDS-PAGE)	70
3.18	Analysis of protein complexes accumulation in <i>Synechocystis</i> WT cells grown in toxic amounts of Mn.	72
3.19	Analysis of total element concentrations in WT and Δ <i>SynPAM71</i> whole cells and isolated membrane fractions and SEC-ICP-QQQ-MS profiles for WT and Δ <i>SynPAM71</i>	75
3.20	Assignment of Mn and Fe peaks in SEC-ICP-MS profiles to thylakoid complexes and other fractions.	76
3.21	Mn ₁ peak overlays with a P peak.	77
3.22	FSynPAM71H functional complements the mutant phenotype in Mn toxic conditions. Sucrose step density gradient suggests that SynPAM71 is enriched in plasma membranes	78
4.1	Schematic view of Mn homeostasis in <i>Synechocystis</i> grown in Mn-sufficient conditions.	87

List of Tables

2.1	Plasmids used to construct a cDNA library in <i>Synechocystis</i>	18
2.2	Bacterial strains used to construct a cDNA library in <i>Synechocystis</i>	19
2.3	List of primers used in the cDNA library project. Small caps indicate RNA sequence. Bracketed subscripts indicate the number of times the previous base is repeated in the primer.	29
2.4	Plasmids used for expression of LHCs into <i>Synechocystis</i> . .	30
2.5	Bacterial strains used to develop a method for a cDNA library in <i>Synechocystis</i>	31
2.6	List of primers used in the LHC project.	34
2.7	Continue - List of primers used in the LHC project.	35
2.8	List of primers used in the SynPAM71 library project.	40
3.1	Frequency of transformation by conjugation through tri-parental mating between <i>E. coli</i> and <i>Synechocystis</i>	44
3.2	Optimization of ligation conditions between <i>Arabidopsis</i> cDNAs and pUR2LT.	46
3.3	List of some cDNAs retrieved from complemented Δ <i>psaD</i> . .	54
3.4	Growth rates and pigment analysis of WT and Δ <i>SynPAM71</i> . .	67
3.5	Rates of oxygen evolution in WT, Δ <i>SynPAM71</i> and <i>psaA</i> ^{prim} strains, and WT cells grown in 20-fold Mn (WT 20xMn). . .	72
B.1	Raw data for element analysis in whole cell samples of <i>Synechocystis</i> WT and Δ <i>SynPAM71</i> mutant.	95
B.2	Raw data for element analysis in isolated membrane fractions of <i>Synechocystis</i> WT and Δ <i>SynPAM71</i> mutant.	96
B.3	ANOVA <i>P</i> -values calculated for element ratios in whole cell samples of WT and Δ <i>SynPAM71</i> <i>Synechocystis</i> strains.	97
B.4	ANOVA <i>P</i> -values calculated for element ratios in isolated membrane fractions of WT and Δ <i>SynPAM71</i> <i>Synechocystis</i> strains.	98

Abbreviations

Amp	Ampicillin
APC	Allophycocyanin
BG11	Blue Green 11 (growth medium)
BiFC	Bimolecular fluorescence complementation
BN-PAGE	Blue-native PAGE
BPV	Biophotovoltaic
CAO	Chlorophyllide <i>a</i> oxygenase
CAT	Chloramphenicol acetyl transferase
CBC	Clavin Benson cycle
cDNA	Complementary DNA
CDS	Coding DNA sequence
CFU	Colony forming unit
Chl <i>a</i>	Chlorophyll <i>a</i>
Chl <i>b</i>	Chlorophyll <i>b</i>
Cm	Chloramphenicol
CRISPR-Cas	Clustered regularly interspaced short palindromic Repeats - CRISPR associated
cTP	Chloroplast target peptide
Cytb ₆ f	Cytochrome c ₆ f
Cytc ₆	Cytochrome c ₆
DNA	Deoxyribonucleic acid
dNTP	deoxynucleotide triphosphate
ds/ss cDNA	double strand/single strand complementary DNA
DTT	Dithiothreitol
EC	Efficiency of conjugation
FAD	Flavin adenine dinucleotide
FD	Ferredoxin
FNR	Ferredoxin-NADP ⁺ reductase
FT	Frequency of transformation
GT	Glucose tolerant
GTP	Guanosine triphosphate
HL	High light (100 μmol photons m ⁻² s ⁻¹)
Km	Kanamycin
LAHG	Light activated heterotrophic growth
LHCII	Light harvesting complex II
LL	Low light (5 μmol photons m ⁻² s ⁻¹)
MMLV-RT	Moloney murine leukemia virus - reverse transcriptase

mRNA	messenger RNA
NADP ⁺	Nicotinamide adenine dinucleotide phosphate
NL	Normal light (50 $\mu\text{mol photons m}^{-2} \text{s}^{-1}$)
OD	Optical density
OEC	Oxygen evolving complex
ON	Overnight
PC	Plastocyanin
PSI	Photosystem I
PSII	Photosystem II
PV	Photovoltaic
RNA	Ribonucleic acid
RT	Room temperature
RuBisCo	Ribulose-1,5-bisphosphate carboxylase/oxygenase
SDS	Sodium dodecyl sulfate
SDS-PAGE	SDS - Polyacrylamide gel electrophoresis
SEC-ICP-QQQ-MS	Size exclusion column - inductively coupled plasma - triple quadrupole - mass spectrometry
SMART	Switching Mechanism At the 5' end of the RNA Transcript
Sp	Spectinomycin
SRP	Signal recognition pathway
SynBio	Synthetic biology
TALEN	Transcription activator-like effector nuclease
TE	Transformation Efficiency
TM	Transmembrane domain
UTR	Untranslated region
WT	Wild-type
ZEP	Zeaxanthin epoxidase
ZFN	Zinc finger nuclease

Chapter 1

Introduction

1.1 Oxygenic photosynthesis

Photosynthesis is a biological process by which the energy of the sun is captured and stored as electrochemical gradients and/or in chemical bonds by an organism. This energy is in turn used to drive the energy-required processes of life.

In particular, oxygenic photosynthesis produces dioxygen as byproduct and evolved in cyanobacteria around 2.4-2.35 billion years ago [1], determining the direction of the evolution of life on Earth. In oxygenic photosynthesis the energy of sunlight is captured to extract electrons from water, channelling them through two photosystems that work in series (photosystem II, PSII, and photosystem I, PSI) to generate reducing power and high-energy chemical bonds as final products.

The process of oxygenic photosynthesis as occurs in land plants is shown in Figure 1.1. In plants, photosynthesis takes place inside specialized organelles called chloroplasts, that are remainders of an ancient cyanobacterium endosymbiont. Inside the chloroplasts, the photosynthetic apparatus is embedded in distinct membranes, called thylakoids. The energy of photons gathered by light harvesting complexes (LHC) is funneled to the chlorophyll P680 of PSII, which ejects one electron to consecutively reduce the electron acceptors pheophytin, Q_A and the plastoquinone (PQ), bound to the PSII Q_B site. The electron hole of the chlorophyll P680⁺ is filled by an electron of the nearby redox-active-tyrosine (T_Z), which in turn is reduced by the oxygen-evolving-complex (OEC) that is able to harvest electrons from the oxidation of water. Through the action of the OEC, four successive photooxidation reactions from PSII oxidize two molecules of water to produce dioxygen and four protons. While oxygen diffuses in the atmosphere, protons remain in the internal compartment delimited by the thylakoid membranes (lumen), building up an electrochemical gra-

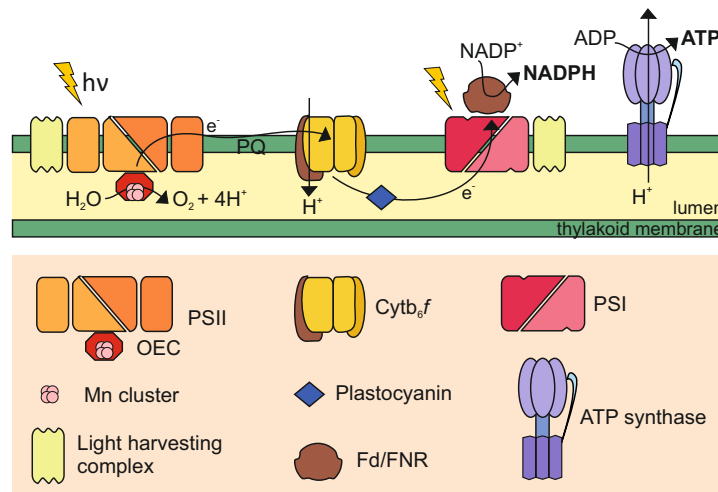


Figure 1.1: Oxygenic photosynthesis in land plants. See text for details.

dient. The extracted electrons are transferred from PSII to cytochrome b_6f (Cyt b_6f) via the soluble electron carrier PQ and from Cyt b_6f to PSI from the small soluble protein plastocyanin (PC) (Fig. 1.1). The electron transfer along Cyt b_6f further contributes to build up an electrochemical gradient in the lumen (Fig. 1.1). The PSI complex catalyze the oxidation of PC and the reduction of ferredoxin (Fd) at the non-luminal side of PSI (Fig. 1.1). The photochemistry of PSI is initiated by the P700 chlorophyll- a (Chl a) dimer, that transfer electrons to a Chl a monomer (A_0) which then reduces sequentially the phylloquinone A_1 , three iron-sulfur complexes and ferredoxin (Fd). Fd, in turn, reduces NADP⁺ in a reaction mediated by ferredoxin-NADP⁺ reductase (FNR) to yield the final product NADPH (Fig. 1.1). The dissipation of the luminal proton gradient is coupled with the enzymatic synthesis of ATP by the multiprotein complex of ATP synthase. The high-energy chemical bonds of ATP and the reducing power of NADPH are then used for the metabolic processes of the cell, among which the incorporation of CO₂ into carbohydrates in the Calvin-Benson cycle (CBC).

1.2 Oxygenic photosynthesis in land plants and cyanobacteria

Chloroplasts are specialized organelles originated from an ancient endosymbiotic event between an ancestral cyanobacterium and a heterotrophic eukaryote [3] [4]. During evolution, cyanobacterial genes were transferred to the nucleus of the host. Therefore, cyanobacterial nuclear genes encode for

proteins which are imported, post-translationally, back into the chloroplast (Fig. 1.2, upper panel).

Although the endosymbiotic event occurred around 1.5 billion years ago, the photochemistry of photosynthesis, and the processes of electron transport and ATP synthesis are clearly conserved between cyanobacteria and land plants [2] (Fig. 1.2). The subunit composition of the photosynthetic apparatus reveals little differences (Fig. 1.2). The photosynthetic machineries between photosynthetic organisms show such a high degree of similarity that their subunits could be exchanged among different photosynthetic organisms. It has been shown that four subunits (PsbA -D1-, PsbD -D2-, CP43, CP47) of the PSII core of the model green alga *Chlamydomonas reinhardtii* could be replaced by the homologous subunits from three different green algae, reconstituting the photosynthetic activity to 85, 55, and 53% of the wild-type level [5]. Furthermore, the PSII core subunit D1 of the cyanobacterium *Synechocystis* could be replaced by the homologous subunit of the land plant *Poa annua*, resulting in a functional chimeric PSII [6]. Recently, it was also shown that a *Synechocystis* mutant of the PSI core subunit PsaA of *Synechocystis* could be partially rescued by the homologous protein PsaA from *Arabidopsis* [7]. Despite the evolutionary distance, *Synechocystis* D1 shares 83% amino acid identity with the D1 from *Poa annua* (81% with the D1 from *Arabidopsis*), and *Synechocystis* PsaA shares 80% amino acid identity with the homolog from *Arabidopsis*.

Despite strong similarities, the photosynthetic machineries of cyanobacteria and plants display some differences (Fig. 1.2). Peripheral antenna complexes evolved multiple times to adapt to different light environments [8]. Cyanobacteria such as *Synechocystis* contain phycobilisomes, huge soluble protein complexes that absorb 550-650 nm wavelengths, while land plants contain LHCs, membrane-embedded protein complexes that absorb blue (around 440 nm) and red (around 660 nm) photons (Fig. 1.2). Furthermore, the assembly and repair of photosystems is an elaborate process that depends on the action of a plethora of different assembly factors that coordinate the assembly of stable intermediate modules. Several common intermediate modules have been found between cyanobacteria and plants, and indeed a large set of assembly factors was found conserved between these organisms [9] [10] [11]. However, some diversification occurs during the evolution, and some assembly and repair factors has been found in plants but not in cyanobacteria and *vice versa* [9] [10]. This discrepancy might reflect the evolution of novel plant-specific assembly factors that either substituted cyanobacterial counterparts or evolved in response to the new conditions of life on land [12].

Although photosynthesis is one of the best understood and most studied

biological process, the biogenesis and assembly of photosystems are still poorly understood. Moreover, we lack the ability to extensively engineer the photosynthetic apparatus of land plants to exploit this formidable biological tool for mankind needs.

1.3 Significance of photosynthesis domestication

Understanding the molecular mechanisms involved in the assembly and repair of photosynthetic machineries will be critical to either improve photosynthetic efficiency to enhance crop yield and biofuel production or to use photosystems for *in vitro* applications.

Crop yield depends on four parameters: i) the incident solar radiation, ii) the efficiency with which the crop intercepts that radiation, iii) the efficiency in converting the intercepted radiation into biomass (conversion efficiency) and iv) the partition of the biomass into the harvested part of the plant (grains). Traditional plant breeding and selection used throughout the Green Revolution could not overcome the limitations of photosynthetic conversion because the photosynthetic apparatus is highly conserved within and among different cultivars [13] [14]. Hence, conversion efficiency is the only parameter that remained significantly lower its theoretical limit [15] [16]. Conversion efficiency hinge on photosynthetic performance in converting the radiant energy into biomass. Improvements of photosynthetic performance would aim at engineering the light and carbon capture and conversion [14]. In particular, the targets for enhancing light conversion would focus on i) lowering the light absorptivity in order to decrease deleterious photooxidations and the pathways involved in their quenching [14] [16] ii) the introduction of exogenous photosystems that are not in competition for the quality of photons absorbed [14]. These strategies all rely on the radical redesign of the plant photosynthetic apparatus, and will require plant genetic engineering at an unprecedented scale.

In addition, food availability and therefore prices are affected by the cost of fossil fuels, in particular the price of crude oil. Fossil fuels are used for agricultural machines and means for food transport and are therefore pivotal to keep the low prices of food. However, conventional oil resources are at an advanced stage of depletion, hence liquid fuels will become more expensive [17]. Biofuels are a valid alternative when they do not compete for arable lands. Biofuels are compounds derived from recently lived organisms and therefore have a low impact on the rise of carbon emission in the atmosphere. Biofuels are produced from either lignocellulosic biomass from agricultural left-overs [18], from algae

or cyanobacteria [19] [20], or from non-edible oil seeds (an example is the biodiesel production from the *Jatropha* tree seeds [21]). Yet, biofuels production rely on the efficiency of photosynthetic conversion. Therefore, concomitantly with improving engine-technology for using biofuels, improvement of photosynthesis would be crucial to sustain the nascent biofuel-based economy.

Furthermore, identify the still unknown accessory factors necessary for assembly and repair of photosystems would pave the way for exploiting photosystems for *in vitro* applications. For instance, electrons produced from the photosynthetic apparatus can be harvested by biophotovoltaic devices (BPVs) [22] [23] [24]. In BPVs photosynthetic electrons can be harvested applying photosystems on the surface of electrodes [25] [24]. The main disadvantage of BPVs is their poor stability over time, when compared to other inorganic photovoltaic systems [26]. Since photosystems are sophisticated multisubunit protein complexes that need the help of many accessory factors to assemble them correctly, the photosystems used in BPVs are extracted from cyanobacteria or plants. Many of the factors for assembly and repair of photosystems have not been identified yet [11], leaving the *in vitro* assembly and repair of functional photosystems for *in vitro* applications, such as for BPV, an open challenge.

1.4 Plant photosynthesis in the light of synthetic biology

The radical redesign of the photosynthetic apparatus will require genetic engineering at an unprecedented scale, which poses various technical challenges that can not be fulfilled by directly engineering plants [14]. In fact, even if directed genome engineering techniques has been successfully applied in plants (e.g. CRISPR-Cas systems [27], TALEN [28] or ZFN [29] proteins), engineering a complicated process such as plant photosynthesis is still challenged by inherent difficulties in handling complex organisms such as the plant model organism *Arabidopsis*: long generation times (1.5 month for wild-type *Arabidopsis*), difficulty of screening libraries of mutants or to pursue adapted evolution on a sufficient number of individuals, and inability to grow them heterotrophically over generations. This latter ability is extremely useful when trying to dissect and engineering photosynthetic complexes.

Furthermore, forward and reverse genetic screenings could still be used to find new players involved in photosynthesis, but setting up the appropriate screening procedure to identify new factors that fine-tune the photosynthetic process or help the assembly of photosystems is challenging,

moreover when the desired phenotype is the result of gene redundancy.

Hence, a new strategy to study photosynthesis is necessary. One promising but challenging approach would be the tentative assembly of a plant-like photosynthetic apparatus in a orthogonal biological system (chassis) easier to handle than plants, such as a cyanobacterium. Indeed, a cyanobacterium would provide not only thylakoid membranes for specific structural support to the plant photosystems, but also a number of evolutionary conserved accessory factors that could help their assembly and stabilization [10]. Concepts of design, chassis, orthogonality and parts are borrowed from the science of engineering. Indeed, a new-born branch of biology, named Synthetic Biology (SynBio), used these concepts to try to dissect biological systems with the final aim to either re-design or building them up from scratch.

This approach would help to i) isolate the plant-specific accessory factors involved in the photosystem assembly and repair and ii) the extensive engineering of the plant-specific photosynthetic apparatus in a prokaryotic chassis (e.g. for high irradiance tolerance), with the final purpose to re-introduce it back to the original plant organism. A promising chassis to pursue this goal is the model cyanobacterium *Synechocystis* [11] [10] [14].

Concepts of design, chassis, orthogonality and parts are borrowed from the science of engineering. A new-born branch of biology, named Synthetic Biology (SynBio), use these concepts to dissect biological systems with the final aim of either re-design or building them up from scratch.

1.5 *Synechocystis* PCC6803 as the prokaryotic chassis to study plant photosynthesis

Synechocystis is a freshwater cyanobacterium that performs oxygenic photosynthesis. *Synechocystis* has a duplication time as short as 6 hours and it is naturally competent, meaning that it takes up DNA from the environment without requiring chemical or electrical treatments. If the engulfed DNA contains regions identical to genome, homologous recombination occurs, resulting in the introduction of the exogenous DNA into specific regions of the genome, hence specific knock-outs can be created by homologous recombination. Since *Synechocystis* carries more than one copy of the genome (ranging from 5 to 20 copies, depending on lab strain and conditions [30]), the growth in more stringent conditions is required (e.g. increasing the antibiotic concentration over time) in order to isolate homozygous mutants. In addition, a glucose-tolerant strains are available [31] which can grow heterotrophically [32]. Furthermore, there are extensive molecular biology tools available (although not as well characterized and defined as for

Escherichia coli). All these characteristics make *Synechocystis* a convenient organism to study oxygenic photosynthesis.

Indeed, not only *Synechocystis* has been extensively used to study photosynthesis but it is also the cyanobacterium in which SynBio concepts to study photosynthesis has been tested the most [33] [34]. Some plant-specific components, such as a protein of the core of PSII (*psbA*, D1) [6], the enzyme to synthesize chlorophyll-*b* (chlorophyllide-*a* oxygenase, CAO) [35], and the plant peripheral antenna (*Lhcb1*) [36] have been already introduced into *Synechocystis* with various degree of success. In particular, the D1 protein from *Poa annua* could reconstitute functional *Poa-Synechocystis* hybrid PSII complexes [6], the accumulation of the CAO protein from *Arabidopsis* converted almost all chlorophyll-*a* (Chl-*a*) into chlorophyll-*b* (Chl-*b*), which, in turn, replaced almost all the Chl-*a* molecules in the endogenous functional photosystems [35]. The expression of the *Lhcb1* peripheral antenna gene from *Arabidopsis* did result in the accumulation of a Lhcb1 protein fragment [36].

Hence, among the commonly studied cyanobacteria, *Synechocystis* is by far the most suitable species in which plant-like photosystems could be introduced and in which could be foreseen a functional complementation with cDNA libraries and extensive engineering of the plant photosystems through adaptive evolution or direct protein engineering [11] [10].

1.6 Aim of the work

The work presented here is part of a long-term project in which *Synechocystis* is used as a chassis to study the assembly of *Arabidopsis* photosynthetic complexes.

In line with the previous works of Viola [37] and Vamvaka [38], this dissertation further explores how extensively *Synechocystis* could be exploited as a synthetic biology platform to study plant photosynthesis. In particular, three projects are discussed:

Shotgun functional complementation of *Synechocystis* photosynthetic mutants with a cDNA library from *Arabidopsis* A method to implement the construction of cDNA libraries in *Synechocystis* is described. This method paves the way to isolate new genes involved in photosynthesis through heterologous functional complementation of *Synechocystis* photosynthetic mutants with cDNA libraries from land plants such as *Arabidopsis*;

Expression and stabilization of functional LHCII in *Synechocystis* The coding sequence of *Lhcb1*, the peripheral antenna of *Arabidopsis*, to-

gether with the genes coding for the *Arabidopsis* signal recognition particle pathway (SRP) were introduced into *Synechocystis* to tentatively express, stabilize and insert the plant-type peripheral antenna into *Synechocystis*;

The transporter SynPAM71 is required to maintain Mn homeostasis in *Synechocystis* Mn is the crucial divalent metal constituting the oxygen evolving complex (OEC) at the luminal side of PSII. In organisms that perform oxygenic photosynthesis, regulation of Mn homeostasis is essential. The characterization of a *Synechocystis* knock-out mutant for SynPAM71, a novel identified key player in Mn homeostasis in *Synechocystis*, is described. Further, differences between Mn homeostasis of *Arabidopsis* and *Synechocystis*, are highlighted and discussed.

1.6.1 Shotgun functional complementation of *Synechocystis* photosynthetic mutants with a cDNA library from *Arabidopsis*

Interspecies (or heterologous) functional complementation is one of the most powerful methods to isolate unknown genes of which the protein product shares the same molecular function in different organisms.

As early as 1976, yeast genomic DNA was used to complement an auxotrophic mutation in *E. coli* [39]. However, bacteria do not harbour eukaryotic specific post transcriptional modifications (e.g. splicing). Therefore, as soon as methods to synthesize double-stranded complementary DNA (ds cDNA) and to clone DNA fragments in plasmids [40] were available, a number of groups independently attempted to establish methods for cDNA cloning [41] [42] [43]. Since then, many genes have been isolated and characterized in *E. coli* by interspecies complementation.

The methods described in the work of Maniatis and Gubler [42] [44] were the most widely used, until few years after the first published method, a new method relying on the introduction of polymerase chain reaction (PCR) to clone cDNA starting from minute amounts of mRNA was established [45]. Still, the high mutation rate of the polymerases employed hampered the reliability and widespread of such technique [45]. The advent of high-fidelity thermostable polymerases, almost a decade later, finally satisfied the concerns raised about the high mutation rate introduced in the amplified cDNAs, and methods such as the cDNA cloning exploiting the 5' oligo-capping [46] [47], or the Switching Mechanism At the 5' end of the RNA Transcript (SMARTTM) [48] started to be used to construct cDNA libraries.

Besides the advances in cDNA synthesis, another step forward in cDNA library construction was the use of the bacteriophage λ as vector to take advantage of the high efficiency and reproducibility of the in vitro packaging into infectious virus particles, which gave the best results in terms of transformation efficiency in *E. coli* when compared to plasmid transformation [49] [50].

All the cDNA libraries constructed to date were mostly accomplished in the model bacterium *E. coli* or in model unicellular eukaryotes, such as *Saccharomyces cerevisiae* [50]. Recently, the possibility to construct cDNA libraries in plant protoplasts became also available, after the implementation of method to efficiently transform plant protoplasts [51] [52].

In fact, the success of interspecies functional complementation methods strongly rely on the availability of three distinct tools i) tailored molecular biology tools for cloning and expression of cDNA libraries (e.g. specific expression vectors) ii) a method to efficiently transform the final host iii) a robust, sensitive and specific selective assay to identify the complemented clones.

High efficiency of transformation and tailored molecular biology tools are indeed extensively available for model organisms such as *E. coli* or *S. cerevisiae* [50]. However, since in these model organisms it is not possible to exploit the power of heterologous functional complementation to study photosynthesis, a model organisms which harbours photosynthetic complexes has to be used as final host, such as the model cyanobacterium *Synechocystis*.

Contrary to *E. coli*, *Synechocystis* lacks many molecular biology tools useful for constructing cDNA libraries. Moreover, the transformation efficiency of *Synechocystis* is low compared to *E. coli*. In this work these issues have been addressed and a method to construct expression cDNA libraries in *Synechocystis* is described.

1.6.2 Expression and stabilization of functional LHCII in *Synechocystis*

In this project the introduction of the functional peripheral antenna complexes of *Arabidopsis* into *Synechocystis* have been attempted.

Peripheral antenna complexes have evolved to enhance the capture of photons for photosynthesis. Peripheral antenna complexes are remarkably diverse among photosynthetic organisms and indeed they were invented multiple times in the course of evolution to adapt photosynthetic organisms to different light environments (see Fig.1.2).

Phycobilisomes are *Synechocystis* peripheral antenna. Phycobilisomes are huge (3-7 MDa) soluble protein complexes which covalently bind bilin

chromophores by thioether bonds. The core antennas of *Synechocystis* PSI and PSII are embedded in chlorophyll-*a* (Chl*a*), absorbing blue (443 nm, measured as free pigment in pyridine [53]) and red photons (671 nm [53]). Due to bilins, phycobilisomes extend the photons absorption to wavelengths that spans between 550 to 650 nm. Green algae and plants harbour instead a set of membrane-embedded peripheral antenna complexes, called light harvesting complexes (LHCs), which room both Chl*a* and chlorophyll *b* (Chl*b*) as light-gathering pigments and therefore enhance the photon harvest for blue (443 and 473 nm for Chl*a* and Chl*b*, respectively [53]) and red (671 and 655 nm [53]) photons.

Swapping peripheral antennas between photosynthetic organisms has the potential to tune the quality of the absorbed wavelengths used to drive the photosynthetic process. A *Synechocystis* strain harbouring functional LHCs in place of phycobilisomes, could harvest photons in the range of the chlorophyll absorption. Concerning practical applications, such a *Synechocystis* strain could be useful to increase biomass in bioreactors when used in mixed *Synechocystis* cultures. A LHCs-containing *Synechocystis* strain and a *Synechocystis* containing phycobilisomes would indeed be "transparent" to each other, avoiding photon competition when grown in the same bioreactor.

Interestingly, if the LHCs accumulation into *Synechocystis* will not occur, the created *Synechocystis* strain could be used as a chassis to isolate still unknown plant-specific factors involved in the process of reconstitution of LHCs into thylakoid membranes exploiting the cDNA expression library described in section 3.1.

Lhcs proteins are encoded by several nuclear genes in *Arabidopsis* and can be either associated with PSI (LHCI complexes constituted by Lhca proteins which are encoded by the *lhca* genes) or with PSII (LHCII complexes constituted by lhcb proteins, encoded by the *lhcb* genes). Most of the photons converted to biochemical energy and biomass through photosynthesis are harvested by the major antenna LHCII. The functional unit of LHCII antenna is the trimer, with each monomer constituted by three transmembrane helices embedded by numerous pigments (Fig. 1.3A). LHCII is constituted by the nuclear-encoded proteins Lhcb1, Lhcb2, Lhcb3. Among these, Lhcb1 is the most abundant form and is the only Lhc protein able to form functional homotrimers [54] [55].

All *Lhcs* are nuclear genes, hence they are transcribed and translated in the cytoplasm of the plant cell. Lhcs are thus posttranslationally delivered to the chloroplast due to an N-terminal chloroplast target peptide (cTP), and there are imported across the envelope membranes. Once in the stroma, several factors are involved in integrating and assembling LHCs

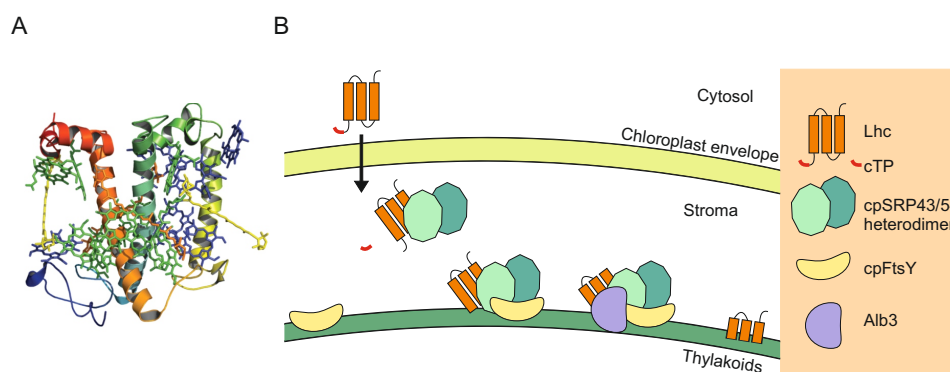


Figure 1.3: Model of the Lhcb crystal structure and a schematic representation of the chloroplastic SRP pathway. **A.** Crystal structure of the Lhcb monomer from pea embedded with pigments. The protein chain is colored from blue (N-terminal) to red (C-terminal). Chl*a* are shown in green, Chl*b* in blue, luteins in orange and other carotenoids in yellow. Reproduced from [8]. **B.** Model for the post-translational insertion of Lhcs into thylakoids via the SRP pathway. After the transport through the TIC/TOC complex of the envelope membranes (not shown), and the cleavage of the cTP targeting signal, the binding with cpSRP43 prevents the aggregation on Lhcs in the stroma. cpSRP43/54 heterodimer is then responsible for the Lhc delivery to the thylakoids, guided by cpFtsY. On the thylakoids, Alb3 supports the proper insertion of the Lhcs. Figure adapted from [56].

into thylakoid membranes. Two pathways, the signal recognition particle (SRP)- and the chlorophyllide-*a* oxygenase(CAO)-dependent pathways, have been suggested to be responsible for the delivery of Lhcs into the thylakoids membranes [57] [58]. The SRP pathway is to date by far the most studied and understood pathway and is depicted in Fig. 1.3B.

When the Lhc proteins leave the envelope, they are transferred to the soluble transit complex cpSRP (constituted by the proteins cpSRP43 and cpSRP54) via the small LTD protein [57] [59] [60] [61]. The transit complex, loaded with one Lhc protein, is then recruited to the thylakoid membrane by the SRP receptor cpFtsY and there the membrane insertase Alb3 arranges the proper insertion and folding of Lhc into the thylakoid membrane [60]Fig. 1.3B.

Among the proteins involved in Lhcs post-translational integration in thylakoids, only cpSRP43 appears to be unique to the chloroplast, where it has been shown to act as a Lhc-specific chaperone, preventing and resolving Lhcs aggregation in the chloroplast stroma [59] [62] [63]. The protein cpSRP43 tightly interacts and coordinates all the proteins involved in the process, serving as a hub for the transport of Lhcs into thylakoids [60]. Indeed, cpSRP43 possesses three chromodomains (CD) and four ankyrin repeats that provide a robust scaffolds for various protein interactions [64].

Two out of three CDs have been shown to interact with the chloroplast-specific C-terminal tails of cpSRP54 and Alb3 [62], while the ankyrin repeats are responsible for the binding of the highly conserved DPLG motif in the L18 region connecting TM1 and TM3 of Lhcb1 [64]. Hence, despite homologues of Alb3, cpSRP54 and cpFtsY have been found in other organisms, including cyanobacteria, the chloroplast-specific SRP pathway seems to have evolved for the particular high-throughput delivery of the abundant LHCs to the thylakoid membranes.

Strikingly, it has been shown that in the presence of cpSRP43, cpSRP54 and cpFtsY, GTP and plant thylakoids, the purified proteins LHC are integrated into thylakoid membranes [65].

Therefore, a functional biological module for the LHCII homotrimer insertion into *Synechocystis*, composed of the genes encoding for Lhcb1, cpSRP43, cpSRP54, cpFtsY and Alb3, could be envisioned.

To introduce functional Lhcs into *Synechocystis*, another consideration has to be taken into account. Each of the Lhcs monomers, composing the trimeric LHCII, contains three transmembrane helices embedded with numerous pigments: eight molecules of Chla, six of Chlb and four carotenoids, of which two are luteins, one neoxanthin and the fourth positioned at the monomer-monomer interface was interpreted as a xanthophyll-cycle carotenoid (antheraxanthin or violaxanthin) [66] (Fig.1.3B). All these pigments are important structural elements for Lhcs. Pigments have been shown to be essential in the Lhc apoprotein folding and stabilization in both *in vitro* and *in vivo* studies [67] [68] [69]), although the exact process through which the various pigments are inserted in the apoprotein *in vivo* remains to be elucidated [70].

In order to ensure the proper LHCII assembly in *Synechocystis*, all these pigments must be provided. *Synechocystis* contains only Chla as chlorophyll and β -carotene, zeaxanthin, echineone and myxoxanthophylls as carotenoids [71]. *Synechocystis* does not contain Chlb and the required xanthophylls. However, it has been shown that plant-specific pigments can be extracted from plant thylakoids and supplemented to the growth medium of *Synechocystis*, from which they are incorporated inside the cyanobacterium [36]. Although the external supplementation of pigments could be initially pursued, the final goal will be to have a stable production of these pigments in the LHCs-bearing *Synechocystis* strain.

A stable production of Chlb has been already achieved in *Synechocystis* [72] [35] and the generation of a lutein-containing *Synechocystis* strain has been recently obtained in our laboratory [38], despite the recombinant strain produce only traces of it. The enzyme zeaxanthin epoxidase (ZEP), responsible to convert zeaxanthin into violaxanthin and antheraxanthin in

Arabidopsis, was also introduced in *Synechocystis* [38]. The introduction of the xanthophyll-cycle should be sufficient to initially stabilize the LHCs [73]. However, the introduction of ZEP into *Synechocystis* produced neither violaxanthin or antheraxanthins, but instead unknown xanthophylls, probably because ZEP prefers other *Synechocystis* endogenous xanthophylls as substrates [38].

In 1999 He and co-workers [36] already attempted to introduce LHCI into *Synechocystis*. In their work, the *Lhcb1* gene alone was introduced in *Synechocystis* genome replacing the native *PsbA3* gene, so that *Lhcb1* could be expressed under the strong P_{psbA3} promoter. Whilst the *Lhcb1* transcript was detected, the full-length *Lhcb1* protein was not stable in the mutant. Interestingly, a small ~ 8 kDa immuno-reactive peptide was found accumulating in the membrane fraction only when plant pigments were externally supplied [36]. Thus, it was suggested that the *Lhcb1* protein was unstable in *Synechocystis*. Not all the components of the cpSRP pathway were known at that time, and the *Lhcb1* protein instability could have been the result of the lack of a stabilizing protein environment such as the one created by the transit complex, inducing *Lhcb1* degradation.

Given the apparent simplicity of the SRP pathway, its good characterization and its successful partial reconstitution *in vitro*, together with the possibility to initially feed the final Lhcs-expressing *Synechocystis* strain with the required plant pigments, we attempted to introduce LHCI in *Synechocystis* through the concert expression of *Lhcb1* and the proteins involved in the SRP pathway (cpSRP43, cpSRP54, cpFtsY, Alb3).

1.6.3 The Mn transporter SynPAM71 is required to maintain Mn homeostasis in *Synechocystis*

In all the organisms that perform oxygenic photosynthesis isolated so far, manganese (Mn) is an essential constituent of the Mn_4O_5Ca cluster at the donor side of PSII and therefore indispensable for oxygenic photosynthesis. However, very little is known about how Mn is transported, delivered and retained in photosynthetic cells. In the cyanobacterium *Synechocystis*, the inorganic Mn cluster is coordinated with specific amino acids in the PSII core protein subunits D1 and CP43 (*PsbA* and *PsbC*, respectively), and is shielded from the luminal environment by the extrinsic proteins *PsbO*, *PsbU* and *PsbV* [74] [75]. In flowering plants and green algae, *PsbU* and *PsbV* have been replaced by the proteins *PsbP* and *PsbQ*, respectively. Cyanobacteria harbor homologs of *PsbP* and *PsbQ*, called CyanoP (*PsbP*-like) and CyanoQ (*PsbQ*-like). In *Synechocystis*, CyanoP and CyanoQ have been shown to participate in regulating and stabilizing the donor side of PSII complexes (CyanoQ) and/or the early assembly of PSII complexes (CyanoP) [76] [77] [78] [79].

The importance of Mn in oxygenic photosynthesis is underlined by the fact that, in *Synechocystis*, Mn accumulates to a level that is 100 times higher than that found in the non-oxygenic photosynthetic purple bacterium *Rhodobacter capsulatus* [80].

The ability to control metal allocation is essential for cell survival, therefore the control over the Mn shuffling around the cells has to be strictly regulated by tailored import/export mechanisms, metal sequestration systems and adaptation of metabolism [81].

Despite the importance of Mn in oxygenic photosynthesis, the processes involved in its transport, sequestration and delivery to its final protein acceptors within the cell are far from being understood. In *Synechocystis*, efforts to dissect the mechanisms of Mn transport and homeostasis have revealed that this cyanobacterium stores Mn in the periplasmic space, either bound to the outer membrane or to dedicated Mn storage proteins, such as MncA [80] [82]. From the periplasmic space Mn^{2+} can enter the cytoplasm via two distinct high-affinity transport systems [83] [84]. The first is an ABC-type transporter encoded by the *mntCAB* operon, which is induced by Mn deficiency and can be competitively inhibited by Cd^{2+} , Zn^{2+} and Co^{2+} [84]. The expression of the *mntCAB* operon is regulated by the ManS/ManR sensor-transducer system. When the extracellular concentration of Mn is not limiting, ManS is activated by binding Mn^{2+} , and a signal is transmitted to ManR, which represses the transcription of *mntCAB* [85]. The second transport system, whose molecular nature remains unclear, is induced in the presence of micromolar Mn^{2+} concentrations and exhibits high specificity towards Mn^{2+} [84]. The regulation of this Mn import system is influenced by the ManSR system [86], but also by RfrA (a member of the pentapeptide repeat family of proteins), although the molecular mechanisms underlying the latter are still unknown [87]. Furthermore, this import system is in part inhibited by the PSII inhibitor DCMU, suggesting the existence of a regulatory mechanism that depends on photosynthetic electron transport [80].

Together with these transport mechanisms for Mn, the system used to deliver Mn^{2+} to its major recipient, PSII, has just begun to emerge in *Synechocystis*. The tetratricopeptide repeat protein PrtA has been shown to be responsible of the pre-loading of Mn^{2+} into D1 of *Synechocystis* [88].

Recently, a protein involved in the uptake of Mn^{2+} (and potentially also of Ca^{2+}) into the thylakoid lumen of *Arabidopsis*, named PAM71, was characterized [89] [90]. PAM71 belongs to the evolutionarily conserved UPF0016 family of membrane proteins, homologues of which are thought to mediate Ca^{2+} and/or Mn^{2+} transport across Golgi membranes in yeasts and humans [91] [92].

In *Arabidopsis* as well as in other land plants, PAM71 is present in a small family of proteins. In *Arabidopsis*, in particular, PAM71 is part of a family of 5 proteins, two of which located in the chloroplast. However, in *Synechocystis*, only one PAM71 homolog is present (hereafter called SynPAM71). The investigation of the primordial version of this class of proteins could suggest how Mn transport and handling evolved in photosynthetic organisms. Therefore, a mutant in *Synechocystis* for SynPAM71 was created and characterized.

Chapter 2

Materials and Methods

2.1 Materials

Standard chemicals were purchased from Roth (Karlsruhe, Germany), Duchefa (Haarlem, Netherlands), Applichem (Darmstadt, Germany), Serva (Heidelberg, Germany), Invitrogen (Darmstadt, Germany) and Sigma-Aldrich (Steinheim, Germany). Restriction enzymes were purchased from New England Biolabs (Ipswich, MA, USA). Polymerases employed in this study were: Taq DNA polymerase from QIAGEN (Venlo, Netherlands) and Phusion high-fidelity polymerase from NEB. Reverse transcriptase MMLV, Advantage PCR and size fractionation CHROMA SPIN-400 columns were purchased by Clontech. The DNA molecular weight markers employed in this study was GeneRuler™ 1 kb Plus DNA ladder (Thermo Scientific, Rockford, USA); the protein molecular weight marker was PageRuler pre-stained marker (10 to 170 kDa) purchased from Thermo Scientific. All the primers were purchased from Metabion GmbH (Martinsried, Germany). Antibodies used to immunodecorate western-blot membranes: α psaD (Agrisera, Sweden). Plasmids used in this study are listed in table 2.1 and bacterial strains in table 2.5.

2.2 Methods used in the cDNA library preparation

2.2.1 RNA extraction from *Arabidopsis*

Leaves from 3-weeks old plants grown in 12 h light/12 h dark cycle were harvested and immediately frozen in liquid nitrogen. Leaves were ground in a mortar in liquid nitrogen. 1/3 of a 2 ml reaction tube was filled with the powder and 700 μ L TRIzol reagent added. The suspension was vortexed for 2 min at RT and centrifuged 10 min at 4°C, 12000xg. The supernatant was mixed with equal volume of chloroform, vortexed for 1

Table 2.1: Plasmids used to construct a cDNA library in *Synechocystis*

Plasmid	Characteristics	Selection	Source
pUR	pYZ derived, mobilizable plasmid	Km ^R , Sp ^R	Prof. Dr. Annegret Wilde (Justus-Liebig University, Giessen) [93]
pUR2	pUR without <i>SfiI</i> site in the backbone	Km ^R , Sp ^R	this study
pUR2D+	pUR2 expressing AtPsaD with cTP	Km ^R , Sp ^R	this study
pUR2D-	pUR2 expressing AtPsaD without cTP	Km ^R , Sp ^R	this study
pUR2LT	pUR2 with modified cloning site: ribosomal sliding site (T ₁₃) downstream ATG, <i>SfiI</i> A and <i>SfiI</i> B as cDNA cloning sites	Km ^R , Sp ^R	this study
pICH69822	Destination vector for Golden Gate Cloning	Km ^R	E. Weber (Icon Genetics GmbH, Halle)
pCMpsaD	pICH69822 with <i>psaD</i> flanking regions and chloramphenicol acetyltransferase (<i>cat</i>) resistance cassette, obtained from <i>Synechocystis</i> Δ <i>ygf48</i>	Km ^R , Cm ^R	This study

Table 2.2: Bacterial strains used to construct a cDNA library in *Synechocystis*.

Strain	Characteristics	Selection	Source
<i>E. coli</i> DH5 α	used for cloning procedures, fhuA2 lac Δ U169 phoA glnV44 Φ 80' lac Δ M15 gyrA96 recA1 relA1 endA1 thi-1 hsdR17 F- mcrA Δ (mrr-hsdRMS-mcrBC), Φ 80lacZ Δ M15 Δ lacX74 recA1 endA1 araD139 Δ (ara, leu)7697 galU galK λ - rpsL nupG tonA		Invitrogen
MegaX DH10B TM T1 ^R			
Helper	harbouring fertility RP4 plasmid [94] (IncP α group)	Km ^R , Amp ^R	Prof. Annegret Wilde (Justus-Liebig Uni- versity, Giessen)
<i>Synechocystis</i> PCC6803 GT	Glucose tolerant		Prof. H. Pakrasi (Washington University, St. Louis, Missouri)
$\Delta ycf48$	impaired in PSII assembly	Cm ^R	Prof. J. Komenda (Center Algatech, Tře- boň, Czech Republic)
$\Delta psdD$	light sensitive, impaired growth in ab- sence of glucose	Cm ^R	This study
$\Delta psdA\Delta tpsaD+cTP$	impaired growth in absence of glucose	Cm ^R , Km ^R , Sp ^R	This study
$\Delta psdA\Delta tpsaD-cTP$	Salt sensitive	Cm ^R , Km ^R , Sp ^R	This study
$\Delta curt$		Km ^R	Prof. Nickelsen (Ludwig Maximilian Uni- versity, Munich, Germany)
$\Delta SynPAM71$	Mn ²⁺ sensitive	Km ^R	This study (see section 3.3)

min and centrifuged again as before. The supernatant was then mixed with equal volume of phenol/chloroform/isoamylalcohol, vortexed for 1 min and centrifuged as before. The supernatant fractions were collected taking care to leave the intact interphase, which contained genomic DNA. The RNA was precipitated ON at -20°C adding the equal volume of ethanol 95 % and 1/2 volume of sodium acetate pH 5.2. The next day the RNA was pelleted centrifuging 30 min, 4°C, 12000xg, washed in ethanol 70 % and resuspended in 20 μ L of water.

2.2.2 Preparation of pUR and derivative vectors for cloning

pUR and derivative vectors are large and low copy number plasmids. In order to obtain sufficient quantity for cloning procedures, pURs production was done via chloramphenicol amplification as reported in [49]. Briefly, ON cultures were diluted 1:10 in fresh media and the culture was incubated until OD₆₀₀ 0.6 was reached. 25 ml of this culture were inoculated in 0.5 L of LB broth and the culture until it reached OD₆₀₀ 0.4, and chloramphenicol (170 μ g/mL final concentration) was added to the culture. After ON incubation at 37° with vigorous shaking (300 rpm/min), the plasmid was isolated with standard protocols.

pUR2LT was digested with *Sfi*I overnight at 50°C and dephosphorylated by CIP 30 min at 37°C. The digested plasmid was precipitated overnight at -20°C in presence of 1/10 NaOAc (3 M, pH 4.8), 1.3 μ L glycogen (20 μ g/ μ L) and 2.5 vol. of ice-cold 95 % ethanol. The plasmid was resuspended in 10 μ l nuclease free water.

2.2.3 Construction of pUR2LT

The *Sfi*I site present in the pUR backbone was deleted via overlapping PCR: 4-5 and 6-7 pairs of primers were used to produce the first round of amplicons and primers 4 and 7 were used to amplify the final fragments which were cloned in pUR via *Eco*O109I and *Xho*I digestion, giving pUR2. Primers 8-9 were used to amplify the *hfr* gene from the pUR vector, introducing the ribosomal slip site at the 5' of and the asymmetrical *Sfi*I restriction sites at 5' and 3' of the *hfr* sequence, giving rise to the cDNA library expression vector pUR2LT.

2.2.4 Synthesis of double-stranded *Arabidopsis* cDNA

The protocol that was used to synthesize and clone the ds cDNA into pUR2LT via a modified SMARTTM protocol is described here in detail.

First-strand synthesis In a PCR tube, 1 μg of total RNA was mixed with 1 μL of Fts primer, 1 μL Switch primer and water up to 5 μL . The contents were incubated for 2 min at 72° in a thermal cycler and cooled on ice for 2 min. To this solution were added 2 μL of 5X First-strand buffer, 1 μL DTT (20 mM), 1 μL dNTPs (10 mM) and 1 μL of SMARTScribe MMLV Reverse transcriptase (Clontech). The solution was mixed gently by pipetting and incubated for 1h at 42°C. The tube was placed on ice to terminate the first-strand synthesis, 1 μL of NaOH (25 mM) was added and the solution incubated at 68°C for 30 min to completely degrade the RNA. After this step the tube was put on ice.

Second-strand synthesis The thermal cycler was pre-heated to 95°C. To 11 μL of the first-strand cDNA were added: 71 μL of deionized water, 10 μL of Advantage 2 PCR buffer, 2 μL of dNTPs (10 mM), 2 μL of anchor primer, 2 μL of Fst primer and 2 μL of Advantage 2 Polymerase mix (Clontech). The reaction mixture was subjected to a thermal cycling with the following program:

72°C	10 min
95°C	20 sec
10-12 cycles:	
95°C	5 sec
68°C	8 min

After the synthesis of the ds cDNA, 5 μL of sample was analyzed on a 1 % agarose/EtBr gel, alongside with a 1-kb DNA size marker. The agarose gel contained 0.1 $\mu\text{g}/\text{mL}$ of EtBr and 0.1 μg of DNA marker was loaded (to reduce background signal). If the band pattern was satisfactory, the cDNA was stored in -20°C.

Proteinase K digestion To remove polymerase and RT activities from the reaction, the mixture was subjected to proteinase K digestion. Proteinase k (20 $\mu\text{g}/\mu\text{L}$) was added to 50 μL of amplified ds cDNA, and the mixture was incubated at 45° for 20 min (in a 0.5 mL tube). The volume of the solution was brought to 100 μL with water and the same volume of phenol:chloroform:isoamyl alcohol was added, the solution was mixed by gentle continuous inversion for 1-2 min and centrifuged at 14000 rpm (table-top centrifuge) for 5 min to separate phases. The top (aqueous) layer was moved to a clean tube discarding the interface and lower layers. 100 μL of chlorophorm:isoamyl alcohol was added, mixed gently, centrifuged and collected as before. 10 μl of NaOAc, 1.3 μl of glycogen (20 $\mu\text{g}/\mu\text{L}$), and 260 μL of

room-temperature 95% EtOH was added to the collected sample to precipitate DNA, and the mixture was centrifuged 14000xg for 20 min. The pellet was washed with 80 % EtOH, dried for 10 min and resuspended in 79 μ L of deionized water.

SfiI digeston To digest the cDNA, 79 μ L of purified ds cDNA were mixed with 10 μ L of CutSmart buffer and 10 μ L of Sfi enzyme (NEB) and incubated at 50°C for 2 hr. 2 μ L of xylene cyanol dye were added to the reaction mixture.

cDNA size fractionation CHROMA SPIN-400 (Clontech) were used to separate the digested cDNA from digestion fragments and cDNA fragments. The matrix was resuspended thoroughly until the flow rate reached the optimal parameters of 1 drop evert 40-60 sec. The column matrix was washed with 70 0 μ L TE buffer (10 mM Tris-HCl pH 8.0, 1.0 mM EDTA, 0.2 filtered). When the buffer stopped dripping out, the cDNA was applied on the matrix surface and allowed to be completely absorbed, other 100 μ L of buffer were applied on the surface and allowed to be completely absorbed. 600 μ L of TE buffer were applied on top of the column and 16 drops were collected. 3 μ L of each drop are analyzed on agarose gel (prepared as described before) alongside a 1-kb DNA size marker (0.1 μ g). The gel was run 10 min, 150V. Usually, the first four fractions containing the cDNA were collected in a clean 1.5-ml tube. To precipitate the DNA, 1/10 NaOAc (3 M, pH 4.8), 1.3 μ L glycogen (20 μ g/ μ L) and 2.5 vol. of ice-cold 95 % ethanol were added to the collected fractions, and the cDNA was precipitated ON at -20°C. The cDNA was pelleted at 14000 rpm for 20 min at RT, and resuspended in 10 μ L with nuclease-free water.

2.2.5 Cloning cDNAs into pUR2LT and transformation of *E. coli*-donor

To clone the cDNAs into pUR2LT, the molar ratio of vector to insert should be 1:2, as determined empirically (see Table 3.2). The molarity of cDNA was calculated from the average size (ca. 1000 bp, as visually determined in Fig. 3.2). Since the vector is 9 times as large as the average insert, the vector to cDNA ratio in micrograms is 9:2. Vector and cDNAs were incubated ON at 16°C. 1.25 μ L of T4 ligase (NEB) was used in 20 μ L reaction.

5 aliquots of *E. coli* MegaX DH10BTM T1^R electrocompetent cells (Invitrogen) were transformed with 3.5 μ L of ligation mixture following the protocol provided by the supplier. The transformed cells were incubated 1

h at 37°C without antibiotic for recovery. After 1 h incubation in 1 mL recovery media, 10^{-3} and 10^{-4} dilutions were plated to count the efficiency of transformation, the rest of the culture was directly used for the triparental mating conjugation. The serial dilutions were performed in minimal M9 media [49] in order to prevent further *E. coli* duplication. CFU on plates were counted only if $30 < \text{CFU} < 300$.

2.2.6 Measuring the DNA transfer efficiency

Bacteria can acquire exogenous DNA in three different ways: conjugation, transduction and transformation. In bacterial transformation, cells take up free DNA directly from their environment (naturally, or helped by treatments as heat shock or electroporation). The efficiency of transformation is defined as:

$$\text{Efficiency of transformation} = \frac{\text{number of transformants}}{\mu\text{g DNA}}$$

In conjugation and in transduction the DNA is exchanged between two biological systems (bacteria to bacteria and virus to bacteria respectively). The efficiency of the DNA exchange is defined by the frequency of transformation:

$$\text{Frequency of transformation} = \frac{\text{number of transformants}}{\text{number of recipients}}$$

where *number of recipients* is the initial number of bacteria subjected to conjugation or transduction.

In the conjugation protocol described in this chapter, a cDNA plasmid library is first transferred by electroporation to an *E. coli* parental strain, which then transfer the library by conjugation to the *Synechocystis* strain (transconjugant). Therefore, the efficiency of conjugation could be defined as:

$$\text{Efficiency of conjugation} = \frac{\text{number of transconjugants}}{\mu\text{g DNA}}$$

where the *number of transconjugants* are the number of the obtained *Synechocystis* transconjugants and the $\mu\text{g DNA}$ are the μg of DNA used to transform the *E. coli* parental strain by electroporation. The above defined efficiency of conjugation allows to compare transformation and conjugation performances in terms of $\mu\text{g DNA}$ used.

2.2.7 Conjugal transfer of a cDNA library

After 1h recovery of the *E. coli* donor transformed with the cDNA library, the culture was diluted to 10 mL in LB medium and incubated for 3.5 h with

kanamycin 100 μM . A overnight culture of *E. coli* helper strain was diluted 1:40 and incubated 2.5 h without antibiotics. After this incubation period, both cultures were gently harvested (2000 \times g, 10 min), resuspended in 0.5 mL, mixed together in a 2 mL reaction tube, centrifuged (2000 \times g, 5 min). The pellet was resuspended in 100 μL , distributed on little rectangles of sterile nitrocellulose filter on top of LB agar plates without antibiotics, and incubated at 30°C for 1 h. The filters were washed in a 2 mL eppi with 1 mL LB. 1 mL of *Synechocystis* at OD₇₃₀ 0.8-0.9 was added to the transconjugant, and after centrifugation (2000 \times g, 5 min) the cells were resuspended in 30 μL of BG11 and distributed on nitrocellulose filters as before, on top of a BG11 agar plate containing 5 % LB medium without antibiotics. The plate was incubated overnight at 30°C in dim light. The filters were washed in a 2 mL eppi with BG11 medium and the cell suspension plated on BG11 agar plate containing 10 mM sodium arsenate to inhibit *E. coli* growth, the appropriate antibiotic (low starting concentration) and incubated in suitable screening conditions. To calculate the efficiency of transformation, at the end of each step serial dilutions were plating in the following conditions: after the helper-donor conjugation completed, the culture was plated on LB agar plates containing spectinomycin and ampicillin; after the *E. coli* donor transconjugants-*Synechocystis* conjugation, cells were plated on BG11 agar plates containing the appropriate antibiotics for selection.

2.2.8 Calculation of the number of clones required to obtain a representative cDNA library

A typical eukaryotic cell contains up to 30,000 different transcribed sequences [49] (*Arabidopsis* contains around 27,000 protein-coding genes [95]), but the number of mRNA species per cell is much higher due to differential splicing [49] [96]. Moreover, not all of these transcribed sequences are represented equally, at the steady state. A cell contains 5-15 abundant species of mRNA which constitutes 10-20% of the total mRNA pool, 200-500 intermediately expressed mRNA that comprise the 40-60% of the mRNA pool, and 10,000 to 20,000 rare mRNA species (<10 copies per cell) that may account for 20-40% of the mRNA pool [97] [98].

The number of clones required to ensure that also low-abundant transcripts are represented in a cDNA library can be calculated as follow:

$$N = \frac{\ln(1 - P)}{\ln(1 - [1/n])} \quad (2.1)$$

where N is the number of clones required, P is the probability desired (usually set to 0.99) and $1/n$ is the fraction of the total mRNA population that is represented by a single type of mRNA. Therefore, to achieve a

99% probability of obtaining a cDNA clone of a rare mRNA ($P=0.99$, $n=10,000/0.3$ considering the rare mRNAs represents 30% of the mRNA pool and 10,000 different mRNA belong to this class), N should be at least 1.5×10^5 with 10^6 clones recommended [49] [48].

2.2.9 Growing *Synechocystis* strains

Unless otherwise stated, *Synechocystis* sp. PCC 6803 glucose-tolerant wild type (GT, Himadri Pakrasi, Department of Biology, Washington University, St. Louis) and mutant strains were grown at $50 \mu\text{mol photons m}^{-2} \text{ s}^{-1}$ light at $22 \text{ }^\circ\text{C}$ in BG11 medium containing 5 mM glucose [99]. Liquid cultures were shaken at 120 rpm. For growth on plates, 1% (w/v) agar was added to the BG11 medium.

2.2.10 Generation *Synechocystis* ΔpsaD and ΔpsaD expressing AtPsaD with or without cTP

The Figure 3.5 shows the inactivation of the *psaD* gene. To generate pCMpsaD, the upstream and downstream regions of *psaD* and the chloramphenicol resistance cassette, were amplified using primers from # 10 to # 15 listed in Table 2.3 using WT or Δycf48 *Synechocystis* genomes, respectively (genomes were isolated according to [100]). The amplified fragments were assembled into pCMpsaD using the one-step Golden-Gate assembly strategy [101] using the plasmid pICH69822 as backbone. *Synechocystis* was transformed with pCMpsaD purified from 100 ml of the appropriate *E. coli* culture with QIAGEN (Venlo, Netherlands) Midiprep kit. 10 mL of *Synechocystis* at OD_{730} 0.8 were harvested by centrifugation and resuspended in 1/20 volume of BG11. Around $2 \mu\text{g}$ of plasmid DNA per transformation were added to the cells. Transformations were incubated in light for 5 h, of which the last 3 h with shaking. For recovery, fresh BG11 was added and the transformations were incubated ON in the dark with shaking at $30 \text{ }^\circ\text{C}$. On the next day, cells were collected by centrifugation at $4500 \times g$ for 10 min, resuspended in a small volume of fresh BG11 medium and plated on BG11 agar plates containing $2 \mu\text{g/mL}$ of chloramphenicol. For complete segregation of the mutant, increasing chloramphenicol (up to $20 \mu\text{g/ml}$ concentration) and incubation in LAHG condition (Light Activated Heterotrophic Growth: darkness, unless 5 min of light per day [32]) were used.

To construct *Synechocystis* strains harbouring *Arabidopsis* genes, *AtpsaD* was amplified from *Arabidopsis* cDNA using primers # 18 and # 19 or # 20 and # 19 for *AtPsaD* with and without cTP, respectively (primers sequence is reported in Table 2.3). The fragments were digested with *NdeI* and *BamHI*

and subsequently cloned in pUR2, creating pUR2D+ and pUR2D- vectors (Table 2.1). The constructs were transformed in *Synechocystis* Δ psaD by conjugation.

2.2.11 Immunoblot analysis

To prepare total protein samples, cells were resuspended in homogenization buffer (HB, 0.4 M sucrose, 10 mM NaCl, 5 mM MgCl₂, 20 mM Tricine pH 7.9, 10 mM Na-ascorbate, 10 mM NaF) and disrupted with glass beads in a cooled TissueLyser (QIAGEN). The crude extract was centrifuged for 2 min at 16000xg, to pellet unbroken cells and the glass beads. The supernatant constituted the total protein extract used in immunoblot analysis. Protein samples used for immunoblot analysis were resuspended in 225 mM Tris-HCl pH 6.8, 50 mM DTT, 10 % [w/v] SDS, 50 % [v/v] glycerol and 0.05% [w/v] bromophenol blue, incubated at 85°C for 10 min, centrifuged at 16,000xg to remove the insoluble fraction and fractionated on 12% Tris-glycine SDS-PAGE gels. PsaD proteins were detected using psaD antibody (Agrisera, Vannas, Sweden) in combination with α -rabbit IgG HRP (Sigma), and visualized with the Pierce enhanced chemiluminescence system (Thermo Fisher Scientific).

2.2.12 RNA extraction from *Synechocystis*

Cells (50 ml) were harvested by centrifugation and pellets were redissolved by adding 700 μ L TRIzol reagent, vortexed for 1 min, transferred in 1.5 mL tubes and frozen in liquid nitrogen. After freezing, the tubes were incubated at 70 °C to thaw, vortexed again and frozen in liquid nitrogen again (two times). The thawed suspension was centrifuged 10 min at 4°C, 12000xg. The supernatant was mixed with equal volume of chloroform, vortexed for 1 min and centrifuged again as before. The supernatant was mixed with equal volume of phenol/chloroform/isoamylalcohol, vortexed for 1 min and centrifuged as before. The supernatant fractions were collected taking care to leave the interphase intact, which contained genomic DNA. The RNA was precipitated ON at -20°C adding the equal volume of ethanol 95% and 1/2 volume of sodium acetate pH 5.2. The next day the RNA was pelleted centrifuging 30 min, 4°C, 12000xg, washed in ethanol 70 % and resuspended in 20 μ L of water. RNA quality was checked by nanodrop analysis and agarose gel before performing northern blotting.

2.2.13 Transcript analysis by northern blot

Northern blot analyses were performed according to [49] loading 15 μg of total RNA, using *psaD* redioactive probe synthesized from the *psaD* amplicon (from primers 19-20, Table 2.3). To 15 μL of RNA, 15 μl of formamide, 4 μl of formaldehyde and 3 μl of 10x MEN (0.2 M MOPS, 50 mM Na-acetate, 10 mM EDTA; pH 7.0) buffer were added. The samples were incubated at 65 °C for 15 min and afterwards put on ice for 5 min. Then 8 μl of 6x loading dye were added, the samples were loaded on an agarose gel (2% agarose, 6% formaldehyde, 1x MEN buffer) and then ran at 40 V for 3 h. The gel was then blotted on a positively-charged nylon membrane (Hybond N+; GE Healthcare, Freiburg, Germany) by using the capillary transfer technique. A glass plate was placed on top of a glass basin filled with 20x SSC buffer (2 M NaCl, 0.2 M Na-citrate; pH 7.0). A paper bridge was placed on top of this plate, consisting of 1 piece of Whatman paper (3 MM) slightly larger than the gel and long, in order to reach into the 20x SSC buffer in the basin. The bridge was wetted with 10xSSC and, on top of that, 2 pieces of Whatman paper of the same size of the gel and also wetted with 10xSSC were placed. Air bubbles were carefully removed and the gel was placed upside down on the paper and then, on its back side, the positively charged nylon membrane upfront pre-incubated in 2x SSC buffer. On top of the membrane 2 further sheets of Whatman paper were added, also pre-wetted in 2x SSC buffer and a stack of paper towels about 10 cm tall. A weight of about 400 g was placed on top of the sandwich, to drive the flux of the blotting buffer via capillary force. The capillary transfer was allowed to run over night for approximately 16 h. The membrane was UV-crosslinked. For the pre-hybridization-step the hybridization buffer was preheated to 60 °C. 20 mL of hybridization buffer and 160 μl of previously denaturated (100 °C, 5 min) herring sperm DNA (10 ng/ μl) were added. The tube was incubated in a rotating oven at 60 °C overnight. For probe preparation approximately 100 ng of PCR-product were filled up to 12 μl with ddH₂O, denaturated at 100 °C for 5 min and cooled down on ice for 5 min. Afterwards, 4 μl of 1x NEBuffer 2, 1 μl of Klenow DNA polymerase, 33 μM dNTPs (without CTP) and 3 μl of radioactive ³²P-dCTP were added to the probe followed by incubation over night at room temperature. For probe purification, Illustra MicroSpin™ G-25 Columns were used according to instructions from the producer. For the washing step the washing buffer (0.1% SDS, 0.2 M NaCl, 20 mM NaH₂PO₄, 5 mM EDTA; pH7.4) was pre-warmed in a water bath to 60 °C. The probe was discarded and 10 ml of washing buffer were added and further incubated at 65°C. The washing buffer was kept at 60°C. After 30 min the washing buffer was exchanged and the tubes were put back

to 60 °C for 15 min. The membrane was then exposed to a radioactive sensitive screen overnight. Primers used to amplify the probes are listed in Table 2.3. Signals were acquired and quantified with a phosphor imager and IMAGEQUANT (Typhoon, GE Healthcare).

2.3 Methods used to reconstitute functional LHCII in *Synechocystis*

2.3.1 Growing *Synechocystis* strains

Unless stated otherwise, growth conditions of *Synechocystis* strains was performed as reported in section 2.2.9.

2.3.2 Generation of pDS433, p54Y and pDESTLhcb1 vectors

The plasmid pDS433 was assembled by Golden-Gate cloning [101]. The genes for cpSRP43, cpSRP54, cpFtsY were amplified from cDNA of *Arabidopsis* prepared as reported in section 2.2.4, the double selection cassette containing kanamycin resistance (nptI, for positive selection) and the levansucrase (sacB, for negative selection) was amplified from the plasmid pRL250 (prof. Wolk, Michigan State University) [102], and the downstream and upstream regions of the neutral site (slr0168) were amplified from *Synechocystis* genome (genome isolation performed according to [100]). The plasmid p54Y harbour the genes *cpSRP54*, *cpFtsY* (amplified from *Arabidopsis* cDNA) and *lhcb1* (amplified from pDS433, used as the upstream region for homologous recombination) and downstream region of the neutral site (amplified from *Synechocystis* WT genome). p54Y was assembled by Golden-Gate cloning using BsmBI in place of BsaI, since *cpSRP54* and *cpFtsY* genes contain many BsaI sites into their CDSs. The primers used to construct the plasmid vectors are listed in Table 2.7.

pDESTLhcb1 vector was constructed for other means, but in this work was used to analyze the transcript expression of the *lhcb1* non-codon optimized gene. pDESTLhcb1 was assembled by Golden-Gate cloning in the backbone of the suicide vector pICH69822. The assembled fragments are, in order, 600 bp of the upstream region of *slr0168* (neutral site, NS), the P_{psbA2} promoter, *lhcb1* gene from *Arabidopsis*, 600 bp of the downstream region of *slr0168* (neutral site, NS). The DNA fragments were amplified by PCR using the primers from # 31 to # 40 listed in Table 2.7.

Table 2.3: List of primers used in the cDNA library project. Small caps indicate RNA sequence. Bracketed subscripts indicate the number of times the previous base is repeated in the primer.

No.	Primer name	Sequence (5' → 3')	Comments
1	Fst	ATTCTAGAGGCCCGAGGGCCGACATGT ₍₃₀₎ VN	Bold: <i>Sfi</i> site
2	Switch	AAGCAGTGGTATCAACGCAGAGTGGCCATTATGGCCGGGG	Bold: <i>Sfi</i> site, lower case: NTPs
3	Anchor	AAGCAGTGGTATCAACGCAGAGT	
4	Sfi mut1 FW	CCAGAAGGATGAGCCCG	
5	Sfi mut1 RV	CTGGCCGCCACATGAG	Bold: point mutation introduced in <i>Sfi</i> site
6	Sfi mut2 FW	CTCATGTGGCCGCCAG	Bold: point mutation introduced in <i>Sfi</i> site
7	Sfi mut2 RV	AGCATCCATGTTGGAAATTTAATC	
8	CS cDNA FW	TTTT CATA IGT ₍₁₃₎ GGCC ATT AI GGCC CC AGATT TG ATAGCGGATT AC CC	Bold: <i>NdeI</i> site, <i>Sfi</i> site
9	CS cDNA RV	TTTTGGAT CC GGCC GA GGCC GC CTAAGGGT AG GG TA ATG	
10	UR psaD FW	TTTGG TC TC TA GGTCCGCT TA GGGT AG GG AG	Bold: <i>BsaI</i> site, italics: sticky end
11	UR psaD RV	TTTGG TC TC TA GGGAT GA AAATGGAA TT TCATA AGG	Bold: <i>BsaI</i> site, italics: sticky end
12	CMr FW	TTTGG TC TC TC CCCT TG ACTCGGAT GT TTA ACCG	Bold: <i>BsaI</i> site, italics: sticky end
13	CMr RV	TTTGG TC TC TA CGTT TG AT TC CCGG CG	Bold: <i>BsaI</i> site, italics: sticky end
14	DR psaD FW	TTTGG TC TC TA CGTT TC TGGCT CT ACT TG CT TGC	Bold: <i>BsaI</i> site, italics: sticky end
15	DR psaD RV	TTTGG TC TC TA AGCAT GAGG ATGG TCC AC CTG	Bold: <i>BsaI</i> site, italics: sticky end
16	SynpsaD FW	ACAGAACT CT TGGACA ACCC	Bold: <i>BsaI</i> site, italics: sticky end
17	SynpsaD RV	CTAGACCT CG TAGGGGG CTT TAC	
18	AtpsaD cTP FW	TTTT CATA IGATGG CC AACT CA AGCC CG	Bold: <i>NdeI</i> site
19	AtpsaD cTP RV	TTTTGGAT CC TTACA AA T CATA ACTTT TG TTGG CC AG	Bold: <i>BamHI</i> site
20	AtpsaD w/ocTP FW	TTTT CATA IGATGGCC GAG AAA AC AGAT TCC TC	Bold: <i>NdeI</i> site
21	pUR2LT colony FW	CGAGTTTT TC AG CA AGAT ACCG	
22	pUR2LT colony RV	CCATGAAA AA T AC CA TG CT CAG	
23	AtpsaD int FW	ACGCC AC CG CA G CTAG	
24	AtpsaD int RV	AGAC CA AC CA CT CT CT CT CT CTG	

Table 2.4: Plasmids used for expression of LHCs into *Synechocystis*

Plasmid	Characteristics	Selection	Source
pICH69822	Destination vector for Golden Gate Cloning	Km ^R	E. Weber (Icon Genetics GmbH, Halle)
pDS433	<i>cp5RP43</i> , <i>Alb3</i> , <i>lhcb1</i> , <i>nptII/sacB</i> cassette, upstream and downstream regions of <i>Synechocystis slr0168</i> (neutral site)	Km ^R , backbone pICH69822	This work
p54Y	<i>cp5SRP54</i> , <i>cpFtsY</i> , <i>lhcb1</i> , downstream region of <i>Synechocystis slr0168</i> (neutral site)	Km ^R	This work
pRL250	<i>nptII/sacB</i> double selection cassette	kan ^R , suc ^S	P. Wolk (Michigan State University)
pURC	pUR2L with chloramphenicol resistance cassette from <i>Synechocystis Δycf48</i> in place of the Sp and Kan resistance cassettes	Cm ^R	This work
pUCLHCop	Genescript synthesized LHCgc, cloned in pUC	Amp ^R	This work (Genescript)
pURCLHCop	Genescript synthesized LHCgc cloned in pURC	Cm ^R	This work
pDESTLhcb1	Lhcb1 gene under the P _{psbA2} promoter, flanked with upstream and downstream <i>Synechocystis slr0168</i> (neutral site) fragments, backbone pICH69822	Kan ^R	This work

Table 2.5: Bacterial strains used to develop a method for a cDNA library in *Synechocystis*.

Strain	Characteristics	Selection	Source
<i>E. coli</i> DH5 α	used for cloning procedures, fhuA2 lac Δ U169 phoA glnV44 Φ 80' lacZ Δ M15		
Helper	gyrA96 recA1 relA1 endA1 thi-1 hsdR17 harbouring fertility RP4 plasmid [94] (IncP α group)	Km ^R , Amp ^R	Prof. Annegret Wilde (Justus-Liebig Uni- versity, Giessen)
LHCgc	harbouring pURCLHC	Cm ^R	this work
<i>Synechocystis</i> PCC6803 GT	Glucose tolerant		Prof. H. Pakrasi (Washington University, St. Louis, Missouri)
$\Delta ycf48$	used to amplify chloramphenicol resis- tance cassette	Cm ^R	Prof. J. Komenda (Center Algatech, Tře- boň, Czech Republic)
DS433	harbouring <i>cpSRP43</i> , <i>Alb3</i> , <i>llcb1</i> , <i>nptI/sacB</i> cassette, in place of <i>slr0168</i> (neutral site)	Km ^R	This work
WT_LHCgc	WT harbouring pURCLHC	Cm ^R	This work

2.3.3 Synthetic LHC gene cluster and generation of pURCLHCop

The *Arabidopsis* genes sequences were acquired from the National Center for Biotechnology Information (NCBI, with accession numbers indicated in section 2.3.7), *Synechocystis* promoters sequences were gathered as indicated in [20]. All the CDSs contain a RBS and relative spacer upstream of the starting codon. The viral terminator OOP was inserted at the end of each transcriptional unit [93]. The final LHCgc sequence was sent to Genscript (Piscataway, NJ, USA) to be synthesized. All the CDSs were optimized for expression in *Synechocystis*. In particular, each CDS was corrected regarding codon usage bias, GC content, mRNA secondary structures, internal chi sites and ribosomal binding sites, RNA instability motifs, repeat sequences and restriction sites (*BsaI*, *KpnI*, and *BamHI* sites were removed). *BsaI* were removed in order to be able to use the synthetic operon in Golden-Gate cloning. LHCgc sequence details are reported in section A.

2.3.4 DNA extraction and genotyping of *Synechocystis* strains

Synechocystis DNA extraction was performed using the xanthogenate method, according to [100]. 2 mL of exponentially growing liquid cultures were pelleted and resuspended in 50 μ l of TE buffer (10 mM Tris/HCl pH 7.4, 1 mM EDTA pH 8.0) containing 100 μ g/ml RNase A (DNase-free). 750 μ l XS buffer (1 % calciummethylxanthogenate, 100 mM Tris/HCl pH 7.4, 20 mM EDTA pH 8.0, 1% SDS, 800 mM NH₄OAc) was added to each sample and the well-mixed tubes were incubated at 70 ° for 2 h to dissolve membranes. The suspensions were then vortexed for 10 sec, incubated on ice for 30 min and centrifuged for 10 min at 13000xg. The supernatant was transferred into a new tube and DNA was precipitated by adding 0.7 volumes of isopropanol, and pelleted centrifuging for 10 min at 12000xg. The DNA was washed with 70% ethanol and resuspended in 100 μ l of nuclease-free H₂O.

The DNA was used to check the presence of the genes carried by pURCLHC by PCR. The primers used for genotyping are reported in Table 2.7 and are the couples 19-20 (cpSRP43), 21-22 (cpSRP54), 23-24 (Lhcb1), 25-26 (cpFtsY) and 27-28 (Alb3).

2.3.5 Immunoblot analysis

The total protein extraction was performed as in section 2.2.11. To further separate soluble from insoluble proteins, the crude protein extract was centrifuged 16,000 x g for 45 min at 4 °. The obtained pellet (insoluble material) and supernatant (soluble material) were separated in different reaction tubes. The insoluble material was washed three times with 500 μ l

of Tricine buffer (5 mM Tricine, 10 mM NaF), each time centrifuging 16,000 × g for 15 min at 4 °, while the soluble material (deep blue colored due to the presence of phycobilisomes) was centrifuged again at 16,000 × g for 30 min at 4 °, the eventual pellet discarded and the supernatant retained. Protein quantification was done using BCA protein assay (Thermo Fischer Scientific). After samples normalization according to protein, were resuspended in 225 mM Tris-HCl pH 6.8, 50 mM DTT, 10% [w/v] SDS, 50% [v/v] glycerol and 0.05% [w/v] bromophenol blue, incubated at 85°C for 10 min, centrifuged at 16,000xg to remove eventual membranes and fractionated on 12% Tris-glycine SDS-PAGE gels.

Proteins of interest were detected using antibodies against Lhcb (Agrisera), cpSRP43, cpSRP54, Alb3, cpFtsY (Prof. Danja Schünemann, Ruhr-Universität Bochum), in combination with α -rabbit IgG HRP (Sigma), and visualized with the Pierce enhanced chemiluminescence system (Thermo Fisher Scientific).

2.3.6 Transcript analysis

RNA extraction from *Synechocystis* strains was performed as reported in section 2.2.12. Single stranded cDNA was synthesized with Maxima First Strand cDNA Synthesis Kit (Thermo Fischer scientific). The primers combinations #3-#4, #5-#6, #7-#8 reported in Table 2.7 (to amplify cpSRP43, Alb3, Lhcb1 respectively) were used in the PCR on the prepared genomic, RNA and cDNA samples in order to analyze transcripts accumulation in *Synechocystis* DS433.

Northern blotting was performed as described in section 2.2.13. Radioactive probes were synthesized from PCR amplicons from primers combinations #19-#20, #21-#22, #23-#24, #25-#26, #27-#28 (for cpSRP43, cpSRP54, Lhcb1, cpFtsY, and Alb3 probes, respectively) and primers combination #29-#30 for psaD+. The primers sequences are listed in Table 2.7.

2.3.7 Accession numbers

Sequence data were obtained from the National Center for Biotechnology Information (NCBI) under the following accession numbers: *Arabidopsis thaliana* NC_003071.7 (At2g47450, cpSRP43); *Arabidopsis thaliana* NM_120476 (At5g03940, cpSRP54); *Arabidopsis thaliana* NP_566056 (At2g45770, cpFtsY); *Arabidopsis thaliana* NP_174286 (At1g29930, Lhcb1, CAB1); *Arabidopsis thaliana* NP_180446 (At2g28800, Alb3).

Table 2.6: List of primers used in the LHC project.

No.	Primer name	Sequence (5' → 3')	Comments
1	URns FW	TTTGGTCTCTAGGTGATCGCGTTTGTGTGGC	Bold: <i>Bsal</i> site
2	URns RV	TTTTGGTCTCTGGAGATTAAITTCACACAGTAATATTTTCAC	Bold: <i>Bsal</i> site
3	cpSRP43 FW	TTTTGGTCTCTCCAAATGGCCCGGTACAAAGAAAC	Bold: <i>Bsal</i> site
4	cpSRP43 RV	TTTTGGTCTCTTCAITTCATTGTTGTTG	Bold: <i>Bsal</i> site
5	ALB3RBS FW	TTTTGGTCTCTAATAAGCAATGTTCAGCTTAAACGAGATTCTC	Bold: <i>Bsal</i> site; italics: RBS
6	ALB3 RV	TTTTGGTCTCTTAGACACAGTGGCTTTCGGCTTC	Bold: <i>Bsal</i> site
7	Lhcb1RBS FW	TTTTGGTCTCTAATAAGCAATGGCATCTGAAGTCCCTTGGAAG	Bold: <i>Bsal</i> site; italics: RBS
8	Lhcb1 RV	TTTTGGTCTCTAACCCTTCCGGGAACAAAG	Bold: <i>Bsal</i> site
9	DRns FW	TTTTGGTCTCTAATGACAGATTTTCAGGTAATGCTTAACAC	Bold: <i>Bsal</i> site
10	DRns RV	TTTTGGTCTCTAAGCCAGTACCACCTGAAGGATTACG	Bold: <i>Bsal</i> site
11	Lhcb1 FW	TTTTCGTCTCTAAGTATGGCATCTGAAGTCCCTTGGAAG	Bold: <i>BsmbI</i> site
12	Lhcb1 RV	TTTTCGTCTCTTCACTTTCGGGAACAAAG	Bold: <i>BsmbI</i> site
13	cpSRP54RBS FW	TTTTCGTCTCTGTGAAGAAGCAATGGCCGAGATGTTTGGTTCAG	Bold: <i>BsmbI</i> site; italics: RBS
14	cpSRP54 RV	TTTTGGTCTCTTTAGTTACCAGAGCCGGAAGC	Bold: <i>BsmbI</i> site
15	cpFtsYRBS FW	TTTTCGTCTCTTAAAGAAATGGCAACTTCTTCTGCTCAC	Bold: <i>BsmbI</i> site; italics: RBS
16	cpFtsY RV	TTTTCGTCTCTTAAAGAAATATAGCAITTCACAAAAAGC	Bold: <i>BsmbI</i> site
17	DRns FW	TTTTCGTCTCTTAAAGCCCAITGTACGTTGTTACG	Bold: <i>BsmbI</i> site
18	DRns RV	GGCCGATATTTGAAGTGAAG	Bold: <i>BsmbI</i> site
19	cpSRP43 FW	CATGCACACCTTTCACCC	
20	cpSRP43 RV	CCACCCTTAATGTGAAATTTGG	
21	cpSRP54 FW	CTAACAATTCCGGCCGCTTC	
22	cpSRP54 RV	CATAGTCGTTGGCCATG	
23	Lhcb1 FW	CCAGCCACCCGATTAACC	
24	Lhcb1 RV	TGATTAATGATTTGTGGCCGTG	
25	cpFtsY FW	GCTTTCCTTACAGGCAATTCATTTTC	
26	cpFtsY RV	AACAAGTGAATTTAACCGCAAAATTTGG	
27	Alb3 FW	TTTACTGGTGTACTGGAAGC	
28	Alb3 RV	TTTACTGGTGTACTGGAAGC	

Table 2.7: Continue - List of primers used in the LHC project.

No.	Primer name	Sequence (5' → 3')	Comments
29	psaD+ FW	TTTTCATATGATGGCAACTCAAGCCGC	
30	psaD+ RV	TTTGGATCCTTACAAATCATAAATTTGTTGGCCAG	
31	ur NS FW	TTTGGTCTCTIAGGTACATTTGACCTGTGTGCTGGAAATG	Bold: <i>Bsal</i> site
32	ur NS RV	TTTGGTCTCTTTGGGAGATTAATTCAACAGTAAATTTTCACAAAAG	Bold: <i>Bsal</i> site
33	psbA2P FW	TTTGGTCTCTCCCATGGAAAACGACAATTAC	Bold: <i>Bsal</i> site
34	psbA2P RV	TTTGGTCTCTTTGGTTATAATTCCTTATGTATTTG	Bold: <i>Bsal</i> site
35	LHCB1.1 FW	TTTGGTCTCTCCAAATGGCATCAGAAGTCCTTGG	Bold: <i>Bsal</i> site
36	LHCB1.1 RV	TTTGGTCTCTTCACATTTCCGGGAACAAAAG	Bold: <i>Bsal</i> site
37	KANN cassette FW	TTTGGTCTCTGTGAGGAATTCGATTGATCCGTC	Bold: <i>Bsal</i> site
38	KANN cassette RV	TTTGGTCTCTAAACCGCAAAAGAAAATGCC	Bold: <i>Bsal</i> site
39	dr NS FW	TTTGGTCTCTGTTTCTCAGGGGCATTATCGGAG	Bold: <i>Bsal</i> site
40	dr NS RV	TTTGGTCTCTAAGCTACAAACAGGGTTTGCCCC	Bold: <i>Bsal</i> site

2.4 Methods used for the characterization of *Synechocystis* knock-out for the putative Mn transporter SynPAM71

2.4.1 *Synechocystis* growth conditions

Unless stated otherwise, glucose-tolerant wild-type (WT) (Himadri Pakrasi, Department of Biology, Washington University, St. Louis) and mutant strains of *Synechocystis* sp. PCC 6803 were grown under 50 $\mu\text{mol photons m}^{-2} \text{ s}^{-1}$ light at 22 °C in BG11 medium containing 5 mM glucose [99]. In cation feeding experiments, *Synechocystis* was grown in modified BG11 media containing increasing concentrations (10-, 20- and 50-fold the standard dose) of CaCl_2 , CuSO_4 , MgSO_4 , SnSO_4 , Fe-EDTA and MnCl_2 . To make Mn-free medium, MnCl_2 was omitted from the microelement stock. BG11 medium containing 20-fold Mn is referred in the text as 20xMn medium. Growth curves were recorded in a Multi-Cultivator MC 1000-OD (Photon Systems Instruments).

2.4.2 Construction of $\Delta\text{SynPAM71}$ and the complemented strain FSynPAM71H

Deletion of *sll0615* was performed by homologous recombination using plasmid pK71 (Figure 3.14), which was constructed by Golden Gate assembly [101] using pICH69822 as a plasmid backbone (E. Weber, Icon Genetics GmbH, Halle). The fragments upstream and downstream of *sll0615* were amplified with the primer pairs 1-2 and 3-4 respectively (Table 2.8), with *Synechocystis* genomic DNA as template. The kanamycin cassette was amplified using the primer pair 5-6, using plasmid pRL250 as template (P. Wolk, Michigan State University). PCR was performed by standard procedures using Phusion high-fidelity DNA polymerase (New England Biolabs). Primers used in this study are listed in Table 2.8. The final pK71 was used to transform *Synechocystis* as described previously [7]. Complete segregation of the mutant was obtained under LAHG conditions (light-activated heterotrophic growth) [32], by stepwise increase of the kanamycin concentration (up to 200 $\mu\text{g/ml}$) in the growth medium. Since the mutant gives rise to revertants if continuously cultivated for 3-4 months, all experiments were started from freshly grown glycerol stock. The correlation between OD and number of cells of mutant and WT was determined using a Thoma cell-counting chamber. $\Delta\text{SynPAM71}$ was complemented using a self-replicative plasmid (pUR, (Wiegard et al., 2013) expressing SynPAM71 fused to an N-terminal FLAG tag 18 (present in the pUR backbone) and a C-terminal 6xHis tag. The amplicon FSynPAM71H was obtained using the

primers pair 7-8 (see Table 2.8), digested with NdeI and BamHI and cloned downstream of the PpetJ promoter in pUR. Δ SynPAM71 was then transformed by conjugation as reported previously [103] and transformants were selected on kanamycin and spectinomycin-containing BG11 agar plates. The resulting complemented strain was named FSynPAM71H.

2.4.3 Pigment analysis

Pigment analysis was done as reported before [104]. Briefly, 1 mL of culture at OD₇₅₀ 0.5 was pelleted, resuspended in 1 mL 100% methanol and incubated on ice in the dark for 30 min. The solution was centrifuged at 16,000xg for 10 min at 4°C, and the supernatant used to measure chlorophyll and carotenoids as previously described [105].

2.4.4 Thylakoids isolation and BN-PAGE

To prepare thylakoid samples, cells were resuspended in homogenization buffer (HB, 0.4 M sucrose, 10 mM NaCl, 5 mM MgCl₂, 20 mM Tricine pH 7.9, 10 mM Na-ascorbate, 10 mM NaF) and disrupted with glass beads in a cooled TissueLyser (QIAGEN). The crude extract was centrifuged for 2 min at 16000xg, to pellet unbroken cells and the glass beads. The supernatant constituted the total protein extract used in Western blot analysis. The thylakoids were isolated by centrifuging the supernatant at 16000xg at 4°C for 1 h. Thylakoids were washed and resuspended in Tricine buffer (5 mM Tricine, 10 mM NaF). The protein concentration was determined using the Pierce BCA Protein Assay (Thermo Fisher Scientific). For ICP-QQQ-MS and BN-PAGE analyses, the thylakoids were solubilized by incubation with 2% [w/v] n-dodecyl β -D-maltoside (DDM) in darkness for 10 min on ice, and insoluble material was removed by centrifugation at 16,000xg at 4°C for 10 min. For BN-PAGE, a one-tenth volume of sample buffer (200 mM Bis-Tris, pH 7.0, 75% [w/v] sucrose, and 1 M ϵ -amino-n-caproic acid) was added to each thylakoid sample and 50 μ g of protein was applied to each lane of an 0.75-mm thick, 4-12% polyacrylamide gradient gel (20x20 cm). Electrophoresis was performed at 4°C at 50V, overnight.

2.4.5 Immunoblot analysis

Protein extraction was performed as reported in section 2.2.11. Individual proteins of interest were detected using antibodies raised against PsaA, PsaB, PsaD, CP47, CP43, PsbO, PsbP-like (CyanoP) and APC (Agrisera) His-tag (Sigma), in combination with α -rabbit IgG HRP (Sigma) or α -mouse IgG (Sigma) and visualized with the Pierce enhanced chemiluminescence

system (Thermo Fisher Scientific). For second dimension gel analysis, proteins in strips of the BN gel were solubilized for 30 min at 25°C with mild shaking in 66 mM NaCO₃, 5% SDS, 100 mM DTT and loaded onto of a 4-12% SDS-PAGE gradient gel (20x20 cm). Silver staining was performed as previously reported [106]. Comparisons between band intensities in Western blots were done with ImageJ software.

2.4.6 Determination of total metal concentrations in whole cells and thylakoids

The measurements was done by Dr. Sidsel Birkelund Schmidt (University of Copenhagen). Total metal concentrations in whole cells and thylakoids of WT and the $\Delta SynPAM71$ mutant were determined using inductively coupled plasma-mass spectrometry (ICPMS)(Agilent 8800 ICP-QQQ-MS, CA, USA) of samples that had been normalized with respect to protein concentration. WT and $\Delta SynPAM71$ cultures were harvested at OD₇₅₀ 0.8-0.9 and carefully washed three times in EDTA buffer (20 mM Tricine pH 7.9, 5 mM EDTA), and in Tricine 20 mM pH 7.9. The cell pellets constituted whole cell samples, from which thylakoids were isolated as described above. The concentration of protein in the whole cell sample was determined after incubation with lysozyme for 30 min and disruption of the cells in a high-pressure homogenizer (Microfluidizer Processor M-110L, IDEX). Complete breakage was verified by light microscopy, and the protein concentration was measured with the BCA assay. Three technical replicates for each of three biological samples were prepared for whole cells and thylakoids from WT and $\Delta SynPAM71$, respectively. Cells corresponding to ~73 mg of protein and thylakoids corresponding to ~0.73 mg of protein were then transferred to Teflon vials and digested with ultrapure acids in a mixture consisting of 2:1 (v/v) HNO₃ and H₂O₂ using a pressurized microwave oven (Ultra-WAVE, Milestone srl, Sorisole, Italy) as described previously [107]. After digestion, all samples were diluted with double-distilled water to a final HNO₃ concentration of 3.5% before ICP-MS analysis. The accuracy and precision of the measurements was estimated by the analysis of certified reference material (apple leaf, NIST 1515, National Institute of Standards and Technology, Gaithersburg, MD, USA). Data were accepted if the accuracy was above 90% of certified reference values. ICP-MS data were analyzed by two-factor ANOVA in order to determine the significance of genotypic variance. The data used in ANOVA were obtained from two independent experiments, each consisting of three independent preparations for each strain.

2.4.7 SEC-ICP-QQQ-MS measurements

The measurements were done by Dr. Sidsel Birkelund Schmidt (University of Copenhagen). Solubilized thylakoid proteins were passed through a 0.45 μm nylon membrane filter (Q-max RR syringe filters, Frisenette, DK) and 50 μg of total protein was applied to a size-exclusion column (BioBasic SEC 1000, Thermo Scientific, USA) using an inert HPLC system (Ultimate 3000, Dionex, Thermo Scientific, CA, USA). The column temperature was held at 6°C during analysis. Protein elution was performed with 25 mM Bis-Tris (Sigma-Aldrich, BioXtra) pH 7 (adjusted with TFA) containing 0.03% β -DM as the mobile phase. The outlet of the column was coupled to a triple-quadrupole ICP-MS (Agilent 8800 ICP-QQQ-MS, CA, USA) for online detection of metal binding in the size-fractionated photosynthetic complexes. The ICP-QQQ-MS was operated in MS/MS scan mode with oxygen as the reaction gas, and the following oxide and nonoxide ions were monitored: $^{24}\text{Mg}^+$, $^{47}\text{PO}^+$, $^{48}\text{SO}^+$, $^{55}\text{Mn}^+$, and $^{72}\text{FeO}^+$. The integration time was 0.1 s per element. The plasma conditions and ion lenses were tuned on a daily basis for robust plasma conditions and maximum sensitivity.

2.4.8 Oxygen evolution measurements

Oxygen evolution was assayed using a Clark-type electrode (Oxygraph, Hansatech). WT and $\Delta\text{SynPAM71}$ cultures in late exponential phase (OD_{750} 0.8-0.9) were harvested and resuspended at OD_{750} 5 in BG11 medium without glucose. Cells were kept in the dark for 30 min prior to measurement. Oxygen evolution was measured without the addition of an external acceptor, PSII activity was measured adding 5 mM 2,6-dimethoxybenzoquinone (DMBQ) and 15 mM ferricyanide. Cells were illuminated at 300 $\mu\text{mol photons m}^{-2} \text{ s}^{-1}$ provided by a Fiber Illuminator FL-440 (Walz). The strain $\text{psaA}^{\text{prim}}$, which was light sensitive [7], was adapted to growth in dim light before the measurements.

2.4.9 Accession Numbers

Sequence data were obtained from the National Center for Biotechnology Information (NCBI) under the following accession numbers: *Synechocystis* sp. PCC 6803 substr. GT-I BAL30131 (sll0615); *Arabidopsis thaliana* NP_564825.1 (At1g64150, PAM71); *Arabidopsis thaliana* NP_193095 (At4g13590, PAM71-HL).

Table 2.8: List of primers used in the SynPAM71 library project.

No.	Primer name	Sequence (5'→3')	Comments
1	UR0615FW	TTGGTCTCTAGGTTTGACCAGGGAATTTGGTTG	Bold: <i>Bsal</i> site
2	UR0615RV	TTTGGTCTCTTCACAGATCAGCCAGGAACAGAGC	Bold: <i>Bsal</i> site
3	DR0615FW	TTTGGTCTCTGTGACTCGGATTTGCAGATCAAC	Bold: <i>Bsal</i> site
4	DR0615RV	TTTGGTCTCTAAGCAGCCCAAAAAAGCGAATGG	Bold: <i>Bsal</i> site
5	KanFW	TTTGGTCTCTGTGAGGAATTCGATTCGCGTC	Bold: <i>Bsal</i> site
6	KanRV	TTTGGTCTCTAAACCGCAAAAAGAAAAATGCC	Bold: <i>Bsal</i> site
7	tagFW	TTTTGAATTCATGCTGACCGCTTTTACTG	Bold: <i>EcoRI</i> site
8	tagRV	TTTTGGATCCCTAGTGATGGTGATGATGTGCAATCTTTGGTCCACC	Bold: <i>BamHI</i> site, Italics: 6xHis

Chapter 3

Results

3.1 Shotgun functional complementation of *Synechocystis* photosynthetic mutants with a cDNA library from *Arabidopsis*

3.1.1 Improving *Synechocystis* transformation efficiency

A library having at least 10^6 independent clones should be representative of the mRNA complexity of an organism (see section 2.2.8 and [108] [48] [49]). Therefore, obtaining a good transformation efficiency of the final host is pivotal in order to achieve the high number of transformants required.

The transformation efficiency (TE, defined in section 2.2.6) using natural competence mainly depends on two factors i) the employed *Synechocystis* strain and ii) the length, form and concentration of the provided DNA. In particular, for a given strain and a plasmid, the TE shows a positive correlation with the DNA concentration, up to a saturation point [109] [110] [111]. The natural transformation reaches TE that vary between 10^2 to 10^4 CFU (measured with WT and plasmid, for the protocol see 2.4.2), in good accordance with the values reported in literature [111]. Therefore, in order to reach 10^6 clones which are required to have a good cDNA library coverage, the transformation should be considerably scaled up. The major issue in scaling up the transformation procedure is providing enough DNA to the cells to be transformed, meaning that the cDNA should be synthesized in amounts of micrograms, ligated to a vector and the ligation mixture provided to the cells. In addition, this procedure could work only if the final aim is the insertion of the DNA into the chromosome. Using natural transformation for a self-replicative plasmid in *Synechocystis* rely on molecular mechanisms that hamper the transformation with a heterologous pool of plasmid, as it is the case of a plasmid library. In order to reconstitute

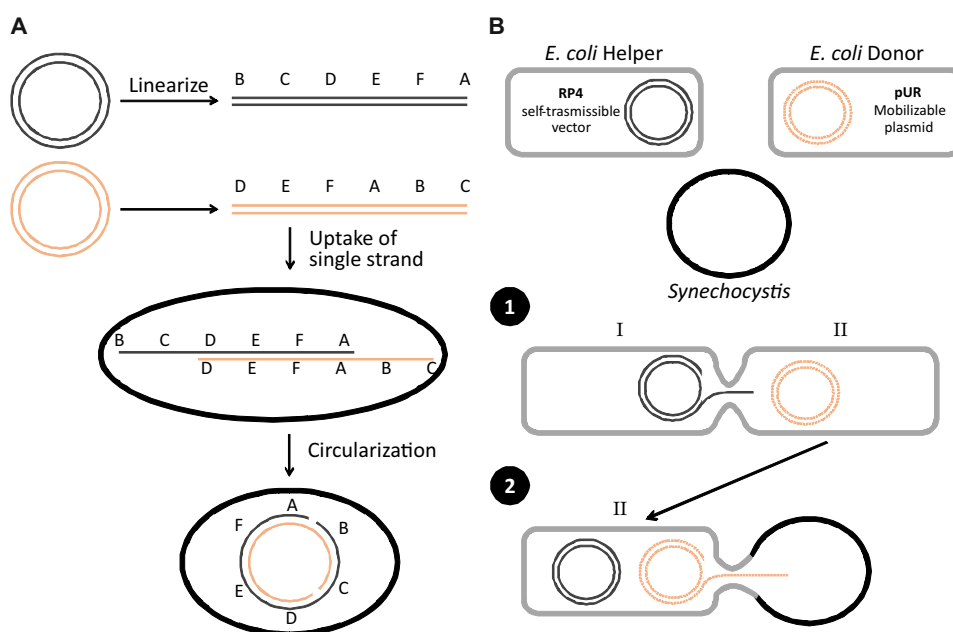


Figure 3.1: A. Transformation by plasmid DNA in natural transformation. Multiple linearized single-stranded plasmids enter in the same cell and anneal. The remaining gaps are filled by cellular DNA repair system and nicks are sealed by DNA ligase. B. Conjugal transfer via triparental mating. In step 1, the self-transmissible plasmid RP4 from the *E. coli*-helper (parent I) is transferred to the *E. coli*-donor (parent II). In step 2, RP4 transfers the mobilizable plasmid pUR into *Synechocystis* (final transconjugant). Pictures adapted from [112].

a plasmid within the cell, at least two single-stranded identical plasmids have to enter inside the cell, anneal and be reconstituted by the cellular DNA repair systems and DNA ligase (Fig.3.1A).

Synechocystis can be also transformed using conjugation. Conjugation in *Synechocystis* is performed via triparental mating, as shown in Fig. 3.1B. As the name implies, three different bacterial strains participate in the mating. The first strain contains a self-transmissible plasmid, the second contains a mobilizable plasmid (which can be mobilized only in the presence of a self-transmissible plasmid) and the third strain is the final recipient. Frequency of transformation (FT, for the definition see section 2.2.6) of triparental mating in *Synechocystis* has been reported to be 10^{-3} [103], although FT between bacterial species as been reported to reach values near 1 [113]. Constructing a cDNA library employing conjugation means that the cDNA plasmid library has to be transformed first in the *E. coli* donor strain, which, after mating with the *E. coli* helper strain, would transfer the library to *Synechocystis*. Since *E. coli* transformation reaches TE of 3×10^{10} (best available on the market MegaX DH10TM T1R ElectrocompTM Cells [114]), the

first bacterial transformation (*E. coli* donor) with the plasmid library would not suffer the DNA concentration constraints of *Synechocystis* natural competence. Hence, the *E. coli* donor is transformed with the plasmid library, care has to be taken in maintaining the high number of transconjugants up to the final *Synechocystis* host.

To test whether conjugation could be used to efficiently transform *Synechocystis* with a cDNA library, FT between the *E. coli*-donor strain MegaX DH10TM T1R ElectrocompTM Cells (containing the mobilizable plasmid pUR) and *E. coli*-helper and between *E. coli*-donor and *Synechocystis* were calculated. The FT was tested in different incubating conditions, in order to optimize the transformation procedure. The major increase in frequency was obtained when both matings (*E. coli*-*E. coli* and *E. coli*-*Synechocystis*) were performed on nitrocellulose filters (Table 3.1). Altering the incubation time or temperature during matings or modifying the ratio between parent strains, did not add significant improvements (data not shown).

The use of nitrocellulose filter could better immobilize the parents during the mating, increasing the initial attachment or stability of the conjugative pilus during the mating, in turn increasing the DNA transfer efficiency. Usually, nitrocellulose filters are not used during *E. coli* intraspecies conjugation, because of the high frequency of transformation obtained between *E. coli* strains. Using the filter during the conjugation between helper and donor *E. coli* parent strains it was possible to reach high FT (Table 3.1). In the mating between *E. coli*-donor and *Synechocystis*, 1/10 of the recipient *Synechocystis* did not survived the mating and a proportion that varies between 1/3 and 1/10 of the survivors were actually transformed. Therefore, once transformed in *E. coli*-donor, 1 out of 100 mobilizable plasmids could be transferred up to the final *Synechocystis* recipient.

3.1.2 cDNA synthesis and construction of a replicative cDNA expression vector for *Synechocystis*

Double-stranded (ds) cDNAs from *Arabidopsis* were synthesized using the Switching Mechanism At the 5' end of the RNA Transcript (SMARTTM) method [48], briefly described in Fig. 3.2.

In SMARTTM cDNA synthesis the fraction of cDNAs containing intact long coding sequences (CDSs) was found enriched compared to other methods [48]. This advantage is not trivial, since the presence of full-length cDNAs is pivotal in order to achieve expression of whole proteins for successful functional complementation. Furthermore, during the SMARTTM cDNA synthesis an asymmetrical *Sfi*I restriction site (*Sfi*IA and B, Fig. 3.2A)

Table 3.1: Frequency of transformation by conjugation through triparental mating between *E. coli* and *Synechocystis*. The efficiencies are calculated as averages of 2 different transformation using nitrocellulose filter in both mating. No R: Number of recipients; No TC: number of transconjugants; FT: Frequency of transformation.

Strain	Strain	No R	No TC	FT
-	<i>E. coli</i> -donor (pUR)	2.4×10^8	-	
<i>E. coli</i> -helper (RP4)	-	7.4×10^8	-	
<i>E. coli</i> -helper (RP4)	<i>E. coli</i> -donor (pUR)	-	1.9×10^8	0.3
<i>E. coli</i> -helper (RP4)	<i>E. coli</i> -donor (pUR)	1.9×10^8	-	
-	<i>Synechocystis</i>	1.4×10^7	-	
<i>E. coli</i> -donor (pUR)	<i>Synechocystis</i>	-	2×10^6	0.14

is incorporated at the 5' and 3' ends of cDNA fragments, in order to allow the directional cloning into expression vectors.

The *Synechocystis* replicative expression vector pUR [93] was chosen as a backbone to construct the expression plasmid for the cDNA library.

pUR is a mobilizable plasmid that belongs to the group of pVZ-derived vectors [93] which are constituted by the replicon of the self-transmissible RSF1010 plasmid (IncW group) [103] [116]. Thanks to its origin of replication *oriV* and its trans-acting factors (the *rep* genes, see Fig. 3.3, [117]), pUR can be maintained in a broad range of gram-negative bacteria, including cyanobacteria [116]. Mobilizable plasmids, such as pUR, can not organize their transfer between bacteria since they lack the genes required building up the conjugative pilus. Instead, mobilizable plasmids contain a set of genetic features (including the *oriT* sequence -site of plasmid transfer initiation- and a series of *mob* genes, Fig. 3.3) required to prepare the plasmid for the conjugative transfer, which is accomplished by a trans-acting self-transmissible plasmid (the helper plasmid RP4, of the IncP group).

In order to perform the cloning of the cDNA fragments into pUR, some modifications of the vector backbone were necessary. First, pUR was modified deleting a *SfiI* restriction site present in the backbone. Second, downstream the promoter, after the ATG starting codon, a ribosomal slipping site (stretch of 13 consecutive Ts), was added. Ribosomal slipping site would induce a variation in codon reading frame of the downstream cloned cDNA. The cloned cDNA would indeed contains stretches of 5' untranslated regions (UTR) that could hamper the start at the right codon reading frame.

pUR harbour the copper repressible P_{petJ} promoter to drive protein expression. In *Synechocystis*, P_{petJ} induce the expression of c_6 , a redox carrier between cythochrome b_6f and PSI that substitute plastocyanin in

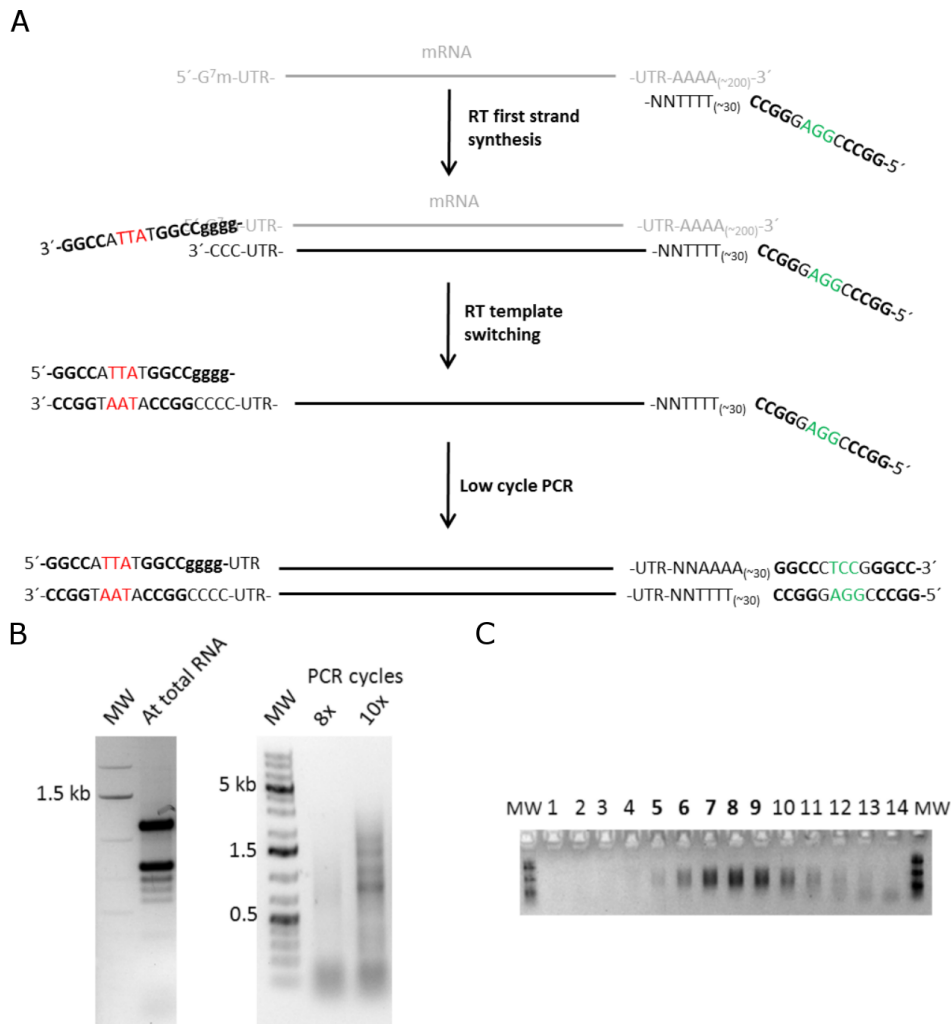


Figure 3.2: **A.** SMARTTM method to synthesize cDNA. *Arabidopsis* RNA is retro-transcribed with MMLV reverse transcriptase (RT) using poly-T anchored primers that anneal on the poly-A tail of mRNA transcripts. MMLV-RT adds additional dCTPs which are not encoded by the template. A second primer harboring a strand of GTP anneals to the added dCTP. MMLV-RT switches the template and copies the rest of the primer. A proof-reading polymerase-mix amplifies the transcribed sequences. The two primers introduce distinct SfiI restriction sites (labelled in green and red in the figure) at each cDNA end. This allow the subsequent directional cloning into a plasmid. **B.** Total RNA extracted from *Arabidopsis*. The visible bands are rRNA, which constitute 75% of the total RNA [115]. **C.** cDNA after two different low-cycles PCR (8 and 10 amplification cycles). Most abundant transcripts appear as distinct bands, rRNA is degraded during the cDNA synthesis. **D.** Scheme of SfiI recognition site. **E.** Fractions collected after size fractionation of SfiI-digested double-stranded cDNA. Eluted fractions are analysed on gel and the 5 fractions with appropriate size are collected and pooled (in this example fractions from 4 to 8).

Table 3.2: Optimization of ligation conditions between *Arabidopsis* cDNAs and pUR2LT. Different molar ratios between vector and insert were probed (indicated in bold). For each indicated molar ratio, different DNA concentrations were also probed (ng, each ligation was performed in 20 μ l reaction). Ligations were performed over night at 16°C. Values shown for transformation efficiency (TE) are averages of two independent transformations of *E. coli* DH5 α home-made chemically competent cells. A negative control made with 200 ng of digested pUR2LT without insert resulted in 4 CFU.

ng pUR2LT	ng cDNA	TE
2:1 vector:insert		
200	11	2.8x10 ⁴
500	27.7	1.5x10 ⁴
1000	55.5	2x10 ⁴
1:1 vector:insert		
200	22	4x10 ⁴
1:2 vector:insert		
200	44	2x10 ⁴
500	110.8	1.8x10 ⁵

copper starvation conditions. Albeit proteins are well expressed by P_{petJ} in copper starvation, a basal activity of the promoter was detected also in the presence of copper (using standard BG-11 growth medium, see section 3.1.4 and also [118]). This P_{petJ} basal activity has been shown to be sufficient for the complementation of null mutants [118]. This, together with the flexibility of having a library under an inducible promoter, prompt us to maintain the P_{petJ} promoter to drive the expression of the cDNA library.

The obtained cDNA library expression vector was named pUR2LT (Fig.3.3).

3.1.3 Cloning the cDNA into pUR2LT and creation of a cDNA library in *E. coli*-donor

In order to find the best conditions to ligate cDNAs into pUR2LT, a series of test ligation reactions were set up as reported in Table 3.2, and transformed in *E. coli* DH5 α home-made chemically competent cells (Table 3.2).

The ligation reactions reported in Table 3.2 were transformed in *E. coli* DH5 α home-made chemically competent cells. The best transformation was obtained using 0.5 μ g of *Sfi*I-digested pUR2LT with a vector to insert ratio equal to 1:2. Meaning that, as the vector is about 9 times as large as the average insert (as determined on agarose gel, Fig. 3.2B), the vector to insert ratio in micrograms will be 9:2. However, the number of *Synechocystis*

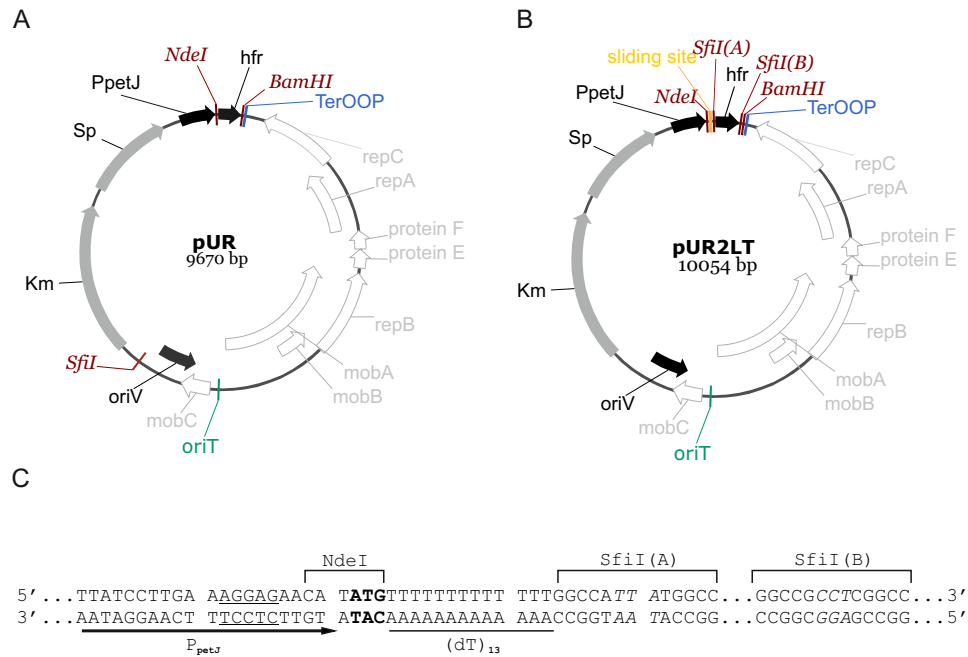


Figure 3.3: Map and cloning site of the pUR2LT vector for cDNA expression libraries in *Synechocystis*. **A.** map of the original vector pUR. **B.** map of the cDNA libraries expression vector pUR2LT. P_{petJ} : copper repressible promoter; Red: restriction sites, Yellow: ribosome sliding site, hfr: gene that will be substituted by the cDNA library; TerOOP: transcriptional terminator; *mob* genes, and *oriT*: genetic features required for the transfer of pUR vectors by the helper plasmid; *rep* genes and *oriV*: genetic features required for broad-host range replication of the plasmid; *protein F* and *protein E*: genes with unclear function; Km: kanamycin resistance cassette; Sp: spectinomycin resistance cassette. **C.** Sequence of the cloning site of pUR2LT. Underlined, the core of the Shine-Dalgarno sequence of the promoter P_{petJ} . Bold: Starting codon ATG, followed by a slip site (stretch of dTs) that cause ribosomes to shift codon reading frames. Italics, the sticky ends that are left after *SfiI* digestion of *SfiI*(A) and *SfiI*(B) recognitions sites.

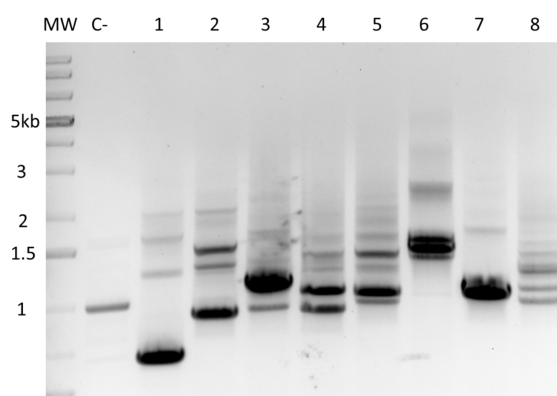


Figure 3.4: PCR analysis of cDNA inserts in pUR2L in *E. coli* donor. 8 pooled colony PCR each from 5 different *E. coli*-donor colonies transformed with the plasmid cDNA library from *Arabidopsis* were loaded on an agarose gel. To amplify the cDNA inserts, a pair of primers (21-22) on the pUR2L backbone, flanking the cDNA insert, were used. C-: negative control.

clones required to obtain a cDNA library which is representative of the mRNA complexity of a eukaryotic cell is at least 2 orders of magnitude higher than the number reported in Table 3.2.

MegaX DH10BTM T1^R electrocompetent cells (Invitrogen) were used to increase the TE of the *E. coli* donor. Using this competent cells, libraries with an average of 9×10^6 *E. coli* donor transformants were obtained (averaged over 10 libraries, with a range of 1.4×10^5 to 2.6×10^7 transformants). Considering that 1 out of 100 of the mobilizable plasmid would be transferred to the *Synechocystis* recipient, the efficiency of conjugation (defined as described in section 2.2.6) would be 1.5×10^5 , reaching the number predicted with the equation ???. Since each ligation mixture used to transform the *E. coli* donor contained $0.6 \mu\text{g}$ DNA, the efficiency of conjugation reached is 1.5×10^7 (which is comparable with the efficiencies previously reported for cDNA plasmid libraries in *E. coli* [50]).

To test the quality of the inserts, a subset of transformants were screened by colony PCR to amplify the cDNA inserts. The sizes of the inserts was found to be between 0.6 and 5 kb as shown in fig.3.4. Some of the inserts were sequenced and 6 out of 10 were found to contain whole transcripts. This was in line with what was reported before about SMARTTM cDNA libraries [48].

Interestingly, some chloroplast-encoded sequences were also found in the library (see Table3.3). Presumably, the poly-T primer employed in the cDNA synthesis (Fig. 3.2) anneals also to the poly-A degradation signal of chloroplast transcripts [119], including these sequences into the library.

3.1.4 Complementation of Δ *psaD* with a cDNA library from *Arabidopsis*

As proof of concept, the quality of the cDNA library was tested complementing a *Synechocystis* *psaD* knock-out. PsaD is a small soluble protein located at the stroma side of PSI and it is responsible, together with PsaE and PsaC, for the efficient transfer of electrons between PSI and ferredoxin (Fd) which in turn will reduce, in a reaction mediated by the ferredoxin-NADP oxidoreductase (FNR), NADP⁺ to NADPH (Fig. 1.1).

Synechocystis Δ *psaD* was already generated and described by Chitnis and co-workers [120]. *Synechocystis* Δ *psaD* showed a strong growth impairment when incubated in autotrophic conditions (in glucose-deficient growth conditions). The inability of *Synechocystis* Δ *psaD* to grow in autotrophic conditions could be used to set up an efficient screening to test a functional complementation by an *Arabidopsis* cDNA library.

A *Synechocystis* *psaD* knock-out strain was generated substituting the gene *psaD* (*slr0737*) with a chloramphenicol acetyl-transferase (CAT) cassette. The complete knock-out mutant was obtained in LAHG conditions (Light Activated Heterotrophic Growth [32]) and it was verified by genomic PCR and northern analysis (Fig. 3.5).

Synechocystis PsaD shows 65% identity and 75% similarity to the *Arabidopsis* protein homolog PsaD (henceforth *AtpsaD*, Fig. 3.6). Therefore, a functional complementation of *Synechocystis* Δ *psaD* by *AtPsaD* is expected. However, cDNA prepared from eukaryotes harbours not only the CDS, including target peptides (to be expected for chloroplast proteins), but also both 5' and 3' untranslated regions (UTRs). In order to determine whether i) *AtPsaD* from *Arabidopsis* can complement *Synechocystis* Δ *psaD* and if ii) the presence of UTRs and/or chloroplast target peptides (cTPs) could influence the complementation, two different *Synechocystis* Δ *psaD* strains harbouring *AtPsaD* with and without chloroplast target peptide (hereafter named *AtPsaD*+cTP and *AtPsaD*-cTP strains, respectively) were generated. The expression of *AtPsaD*+/-cTP genes was confirmed via western blot analysis using an antibody raised against *AtPsaD* (Fig. 3.7A).

The viability of *Synechocystis* WT, Δ *psaD* and Δ *psaD* harbouring *AtPsaD*+cTP or *AtPsaD*-cTP was tested by drop test. Each strain was grown in liquid media, brought to 0.25 OD₇₅₀, spotted on BG-11 plates for heterotrophic or autotrophic conditions and incubated in different light intensities. *Synechocystis* Δ *psaD* showed a drastic growth impairment in autotrophic conditions (confirming what was previously found [120]). Additionally, it displayed sensitivity to the transition to strongest light intensities. The mutant showed drastic growth impairment when moved from 5 μ mol photons m⁻² s⁻¹ (low light, LL) to 50 μ mol photons m⁻² s⁻¹

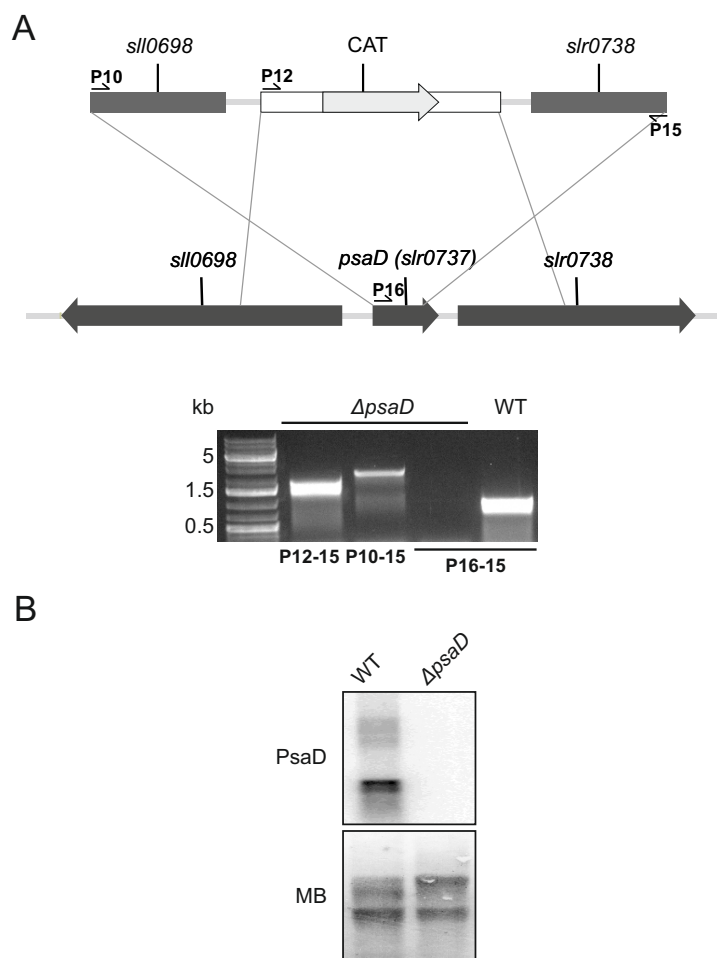


Figure 3.5: Generation of *Synechocystis* Δ *psaD*. **A.** *psaD* (*slr0737*) was substituted with a *CAT* cassette by homologous recombination. The absence of *psaD* was confirmed by genomic PCR using the primers shown in the scheme (sequence of primers is reported in Tab.2.3). **B.** Northern blot analysis confirmed the absence of the *psaD* transcript in *Synechocystis* Δ *psaD*. The probe used to detect *psaD* was synthesized using the primer combination #16-#17, listed in Table 2.3.

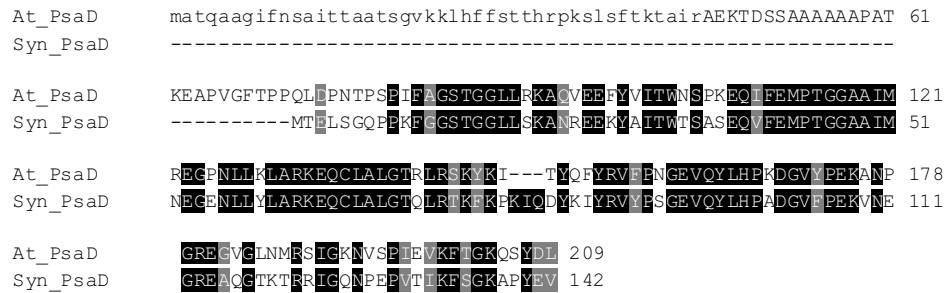


Figure 3.6: Sequence alignment of *psaD* proteins from *Arabidopsis* (*At_psaD*) and *Synechocystis* (*Syn_psaD*). Amino acids similarities and identities are highlighted in gray and black shading, respectively. Chloroplast target peptide (cTP) predicted by ChloroP is indicated in lower case letters.

light intensity (normal light, NL) (Fig. 3.7B). The expression of *AtPsaD*-cTP rescued the mutant, both in autotrophic and in NL conditions. Interestingly, while the introduction of *AtPsaD*+cTP did not restore the autotrophic growth of the mutant, it reduced the light sensitivity of the mutant to a certain extent (up to 50 but not up to 100 $\mu\text{mol photons m}^{-2} \text{s}^{-1}$, as shown in Fig. 3.7B).

The introduced cTP constitutes 30% of the expressed protein *AtPsaD*+cTP. Presumably, the cTP steric hindrance at the N-terminal part of the protein affects the docking site to PSI, causing a transient attachment to PSI, which, albeit helping to dissipate a moderate electron flow (produced in NL conditions), it does not sustain a higher electron flow (produced in HL conditions) possibly causing over-reduction of the photosynthetic chain and consequent production of oxygen reactive species. Further, this situation does not sustain the ability to grow in autotrophic conditions.

Finally, $\Delta\textit{psaD}$ was transformed with the library as described in section 3.1 and final *Synechocystis* transconjugants selected on BG-11 plates incubated in NL conditions. After two weeks of incubation, three out of five rounds of complementation with the *Arabidopsis* cDNA library displayed colonies on selection plates (27, 23, 7 colonies respectively). All the transconjugants which were able to grow on selection plates were screened by PCR using primers that amplify a short amplicon inside *AtpsaD* (primers 23-24, Table 2.3). In two out of three positive rounds of complementation, one transconjugant was found positive for the presence of *AtpsaD*.

Hence, the described method to construct an *Arabidopsis* cDNA library was successfully used to complement *Synechocystis* $\Delta\textit{psaD}$ strain.

Interestingly, some positive transconjugants harboured different cDNA inserts than *AtpsaD*. As control, for each round of complementation, *Syne-*

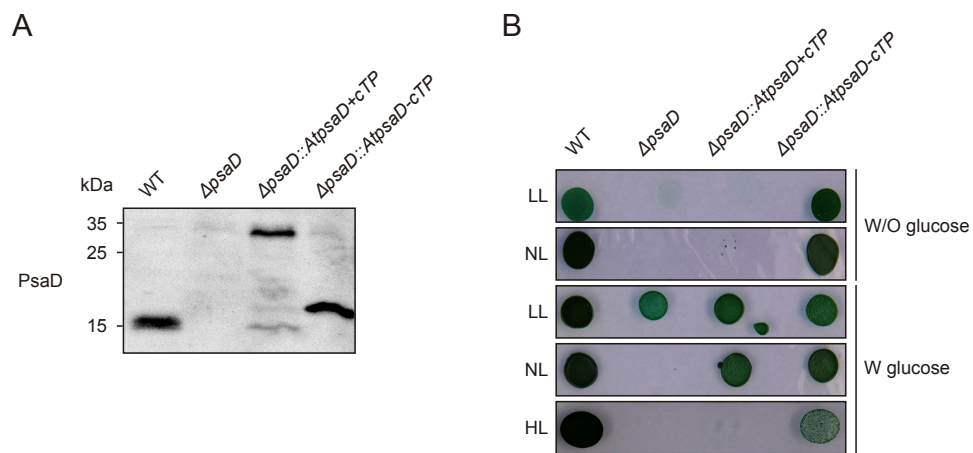


Figure 3.7: Immunoblot analysis and phenotypic characterization of *Synechocystis* $\Delta ps a D$ expressing *AtPsaD+cTP* and *AtPsaD-cTP*. **A.** Total proteins from *Synechocystis* WT, $\Delta ps a D$, $\Delta ps a D::Atps a D+cTP$ and $\Delta ps a D::Atps a D-cTP$ were loaded on SDS-PAGE and transferred on nitrocellulose membrane. The antibody raised against *AtPsaD* was used to detect the presence of the protein in the different *Synechocystis* strains. The antibody cross-reacts also with *PsaD* from *Synechocystis*, confirming the absence of the protein in all the $\Delta ps a D$ strains. **B.** Drop-test to identify the best screening conditions to isolate complemented mutants with a cDNA library. The strains were cultivated in liquid cultures to exponential phase, adjusted to 0.2 OD_{750} and spotted on BG-11 agar plates (with or without glucose, and in different light intensities).

chocystis Δ *psaD* (not transformed with the cDNA library) was plated and grown in the screening conditions. On the control plates, between 1 and 5 clones were counted, but all proven to be negative for the WT *psaD* gene (data not shown). These clones are probably pseudorevertants. The ability of *Synechocystis* to easily generate pseudorevertants of *Synechocystis* mutants has been extensively exploited to find novel proteins or regulatory pathways [121] [122] [123] [124] [125], functionally characterize protein domains [126] or find new aspects in promoter sequences [127].

Therefore, the presence of Δ *psaD* clones harbouring cDNA fragments different from *AtpsaD* could be seemingly due to i) pseudorevertants of Δ *psaD* which functional complementation is independent from the expression of the cDNA sequence ii) the cDNA expression which could help overcoming the physiological constraints of *Synechocystis* Δ *psaD* in the screening condition. In Table 3.3 some sequences retrieved are listed, which were from the isolated Δ *psaD* complemented clones. Although interesting, the putative involvement of these proteins in the recovery of Δ *psaD* mutant was not further investigated.

3.1.5 Complementation of other *Synechocystis* mutants

In order to assess the potential of the cDNA library, different *Synechocystis* photosynthetic mutants were selected for functional complementation:

Δ *ycf48* : YCF48 is a luminal protein involved in assembly and repair of PSII [129], it is homologous to the *Arabidopsis* protein HCF136;

Δ *PratA* : *PratA* is involved in the pre-loading of D1 (core protein of PSII) with Mn [88] and does not have clear plant homologues;

Δ *CurT* : *CurT* is a small thylakoid membrane protein involved in the bending of membranes both in *Synechocystis* [130] and in *Arabidopsis* [131] where it has 4 homologues;

Δ *Pitt* : *Pitt* is a protein involved in the early steps of photosynthetic pigment/protein complex formation [132] and does not have clear *Arabidopsis* homologues;

Δ *SynPAM71* : *SynPAM71* is a membrane-embedded cation transporter involved in Mn homeostasis (see section 3.3), homologous to a family of 5 proteins in *Arabidopsis* [89].

The growth of each mutant was tested in various conditions in order to find a suitable selective screening.

Δ *YCF48*, Δ *PratA*, Δ *CurT*, Δ *Pitt* were tested for growth in high light (up to 1000 $\mu\text{mol photons m}^{-2} \text{s}^{-1}$), high temperature (35°C), salinity (NaCl up

Table 3.3: List of some cDNAs retrieved from complemented $\Delta psdD$. Note that *psbM* and *psaB* are chloroplastic genes (for an explanation see section 3.1.3). Informations on the locus were gathered from TAIR database [128]. No., number of isolated clones bearing that particular sequence.

Gene locus	Protein Name	Function	No.
ATCG00340	PsaB	Core protein of PSI	1
AT5G47320	RPS19	Nuclear encoded 5' UTR of mitochondrial ribosomal subunits	1
AT1G31580	ECS1	Cell wall protein, maybe involved in light reactions of photosynthesis	1
AT1G69510	cAMP-regulated phosphoprotein 19-related protein	-	1
AT3G61470	LHCA2	PSI Light Harvesting Complex antennas, gene 1	1
AT2G07707	ATPase, F0 subunit	ATP synthesis	1
AT1G20340	PETE2, Plastocyanin	Copper homeostasis, redox-oxidation processes	2
AT3G49870	ARLA1C	Cell division, chromosome segregation, defense in response to viruses	1
ATCG00220	PsbM	Low-molecular-weight protein of PSII	2
AT5G42530	-	Uncharacterized	1
AT3G54890	LHCA1	PSI Light Harvesting Complex antennas, gene 2	1
AT1G42970	GAPB	Chloroplast localized Glyceraldehyde-3-phosphate dehydrogenase	1

to 3%), 680 nm light (PSII absorption wavelength). Unfortunately, none of the above mutants showed drastic impairments compared to WT in any of the conditions tested.

The only exception was $\Delta CurT$ which displays sensitivity towards salt addition. Although $\Delta CurT$ showed a strong tendency to generate pseudorevertants, in the order of tens, it has been decided to try the complementation with the library. Out of three rounds of complementation, positive transconjugants were screened by PCR using primers to amplify inside the coding sequences of all the four *Curt* genes of *Arabidopsis* [131]. However, none of the screened clones resulted positive for the presence of any of the *Curt* genes from *Arabidopsis*.

$\Delta SynPAM71$ was found to be sensitive to Mn addition: 10-fold Mn in the growth medium compared to the normal growth medium is a lethal condition for the mutant. The generation of pseudorevertants was absent. Therefore, $\Delta SynPAM71$ was subjected to two rounds of complementation with the *Arabidopsis* cDNA library. However, the only clone retrieved from the screening was found to be a contaminant that still contained the *SynPAM71* wild-type gene.

3.2 Expression and stabilization of functional LHCII in *Synechocystis*

Two strategies have been pursued in order to introduce LHCs into *Synechocystis*. In the first strategy, it was attempted to introduce an operon (hereafter LHC operon) containing *cpSRP43*, *cpSRP54*, *cpFtsY*, *Alb3* and *Lhcb1* genes, under the strong promoter P_{psbA2} , into the genome of *Synechocystis*. In the second strategy, a gene cluster (hereafter LHCgc) containing the same genes but divided in three transcriptional units, was designed, synthesized, cloned into a replicative plasmid and introduced into *Synechocystis*.

3.2.1 First strategy: introducing the LHC operon into the genome of *Synechocystis*

The first attempt to introduce LHCs into *Synechocystis*, employed the insertion of the LHC operon into the *Synechocystis* genome. Two suicide vectors (vector that can not replicate in the host) have been assembled for this purpose, each harbouring half of the final LHC operon (Fig. 3.8). The genes constituting the LHC operon were divided on two suicide vectors according to the type-II restriction enzymes that are used during the Golden-Gate assembly (see section 2.3.2). The *cpSRP43*, *Alb3* and *Lhcb1* genes were

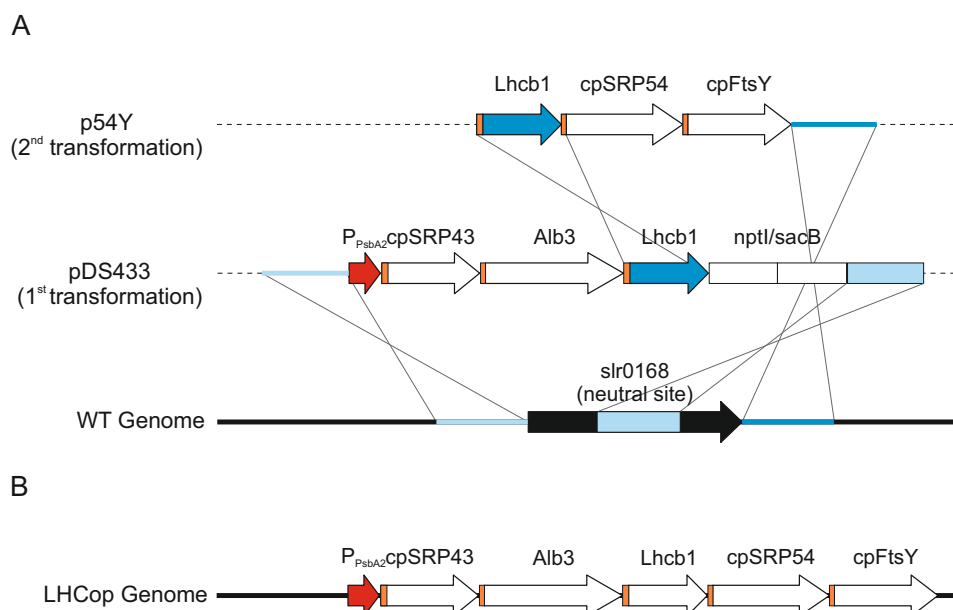


Figure 3.8: Scheme for the introduction of the LHC operon into the genome of *Synechocystis*. **A.** Scheme for the planned two-step transformation with the suicide vectors pDS433 and p54Y. The first transformation with the p433 vector replaced part of the neutral site with the *cpSRP43*, *Alb3* and *Lhcb1* genes under the endogenous strong promoter P_{PsbA2} , followed by the *nptI/sacB* double selection cassette conferring kanamycin resistance and sucrose sensitivity. The second transformation replace the remaining neutral site and the double selection cassette with the *cpSRP54* and *cpFtsY* genes, resulting in a marker-less strain (sucrose resistant and kanamycin sensitive) harbouring the LHC operon. Thick black line: *Synechocystis* genome; broken line: plasmid backbones; Light and dark blue: regions used for homologous recombination during the first (light) and the second (dark) transformation; orange boxes: ribosomal binding sites (RBS). **B.** Map of the neutral site region of the genome of the final LHCop *Synechocystis* strain. Note that the last gene, *cpFtsY*, is followed by the natural terminator of *slr0168*.

assembled with *Bsa*I restriction enzyme in the final plasmid pDS433, while the *cpSRP54* and *cpFtsY* genes, containing many *Bsa*I restriction sites in their CDS, were assembled in the vector p54Y using the type-II restriction enzyme *Bsm*BI.

The plasmid pDS433 was used to transform *Synechocystis* WT strain. The plasmid pDS433 replaced the genomic neutral site *slr0168* with the genes *cpSRP43*, *Alb3* and *Lhcb1*, placed downstream the promoter P_{PsbA2} , together with the *nptI/sacB* double selection cassette (Fig. 3.8). The resulting *Synechocystis* strain was named DS433. The introduced *nptI/sacB* double selection cassette contains the gene for kanamycin resistance (*nptI*), used for the positive selection of transformants, and the levansucrase gene

(*sacB*) is used for negative selection. The presence of the levansucrase enzyme cause lethality to bacteria when they are grown in the presence of 5% sucrose [102].

To obtain a homozygous mutant, *Synechocystis* DS433 was subjected to increasing kanamycin concentrations in order to raise the selective pressure. Since heterozygosity should not influence the expression of proteins, the heterozygous mutant was subjected to preliminary investigation.

Immunoblot analysis of *Synechocystis* DS433 failed the detection of *Lhcb1* (data not shown). Next, the presence of transcripts was investigated. RNA was extracted from WT and DS433 *Synechocystis* strains, and treated with dsDNase to avoid genomic contamination of the samples. The RNA was then retro-transcribed to cDNA, and the synthesized single-stranded cDNA was analyzed for the presence of *cpSRP43*, *Alb3* and *Lhcb1* transcripts. However, the pDS433-specific transcripts were not clearly detected in the mutant (data not shown).

These results, together with some issues encountered in the assembly of the plasmid p54Y, drove me to find a faster and more reliable way to introduce the whole LHC operon into *Synechocystis*.

3.2.2 Second strategy: generation of a *Synechocystis* strain harbouring a synthetic gene cluster for LHC reconstitution

A gene cluster containing *Arabidopsis lhcb1*, *cpSRP43*, *cpSRP54*, *cpFtsY* and *Alb3* was designed as depicted in Fig. 3.9A to be artificially synthesized.

The designed gene cluster (hereafter referred as LHCgc) was divided in three independent transcriptional units in order to better identify the position of a possible failure in transcription or translation.

The first transcriptional unit was defined by the *cpSRP43* and *cpSRP54* genes, expressed from the promoter P_{cpc} . The second transcriptional unit carried the *Lhcb1* and *cpFtsY* genes under the promoter P_{rbcl} , and, at last, *Alb3* was expressed by the promoter P_{PsbA2} . Care was taken that each gene sequence would have been introduced by a ribosome binding site (RBS), and that the viral transcription terminator OOP [93] terminated each transcriptional unit. Each coding sequence was gathered from *Arabidopsis* mature mRNAs sequences (see section 2.3.7 for accession numbers), from which the N-terminal cTP (as predicted from the software ChloroP [133]) was removed. Each CDS was optimized by GeneScript correcting codon usage, GC content, mRNA secondary structures, internal ribosomal binding sites and RNA instability motifs.

The promoters employed in the gene cluster are well characterized *Synechocystis* endogenous constitutive promoters that drive highly expressed genes: P_{cpc} drives the expression of phycocyanin subunits and

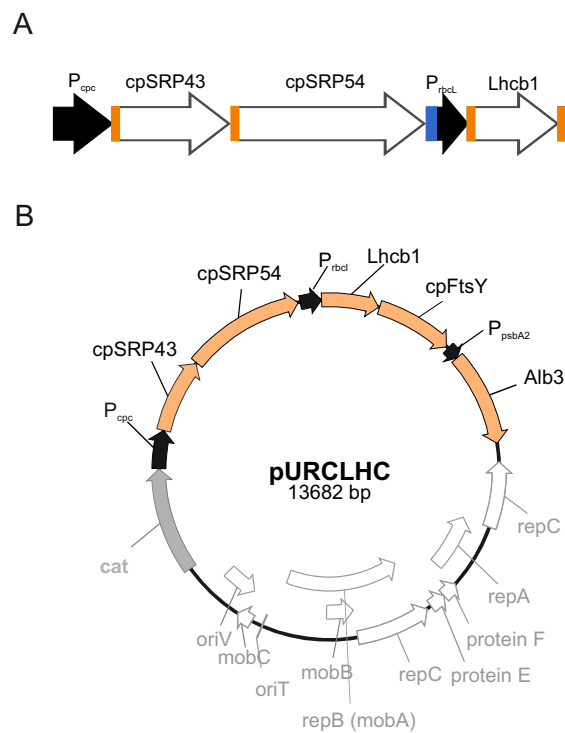


Figure 3.9: Maps of the synthetic LHC gene cluster and the final vector pURCLHC. **A.** Scheme of the LHC gene cluster (LHCgc). Black arrows: promoters; white arrows: CDSs; orange boxes: RBSs; blue boxes: transcription terminators. **B.** Map of the final replicative vector pURCLHCgc.

linker polypeptides of phycobilisomes, P_{rbcl} drives the expression of the large subunit of the Ribulose-1,5-bisphosphate carboxylase/oxygenase (Ru-BisCo) and P_{PsbA2} drives the expression of the PSII core subunit PsbA (D1) [134] [34]. The promoter sequences used in the operon were the same as reported in [20].

The designed LHCgc sequence (reported in section A) was synthesized by Genescript. All the CDS were optimized for gene expression in *Synechocystis*, as described in section 2.3.3.

The LHCgc was cloned into a pUC backbone. Hence, the LHCgc was cut with *KpnI* and *BamHI* restriction sites, which were flanking the LHCgc sequence, and cloned into pURC, to give the final plasmid pURCLHC (vector map shown in Fig. 3.9B). pURC is a replicative vector based on pUR2LC (see Table 2.4) in which the spectinomycin and kanamycin resistance cassettes were substituted by a chloramphenicol resistance cassette (chloramphenicol acetyl transferase, CAT). The protein product of the *CAT* gene allow the transformation of all *Synechocystis* strains of interest, which were resistant to either kanamycin or spectinomycin (e.g. in the *Synechocystis* strain SynLut that produce lutein, or Δ APC which lacks phycobilisomes), with pURCLHC.

The plasmid pURCLHC was introduced in *Synechocystis* WT, SynLUT, and Δ APC strains. Since the initial characterization of the LHCgc harbouring strains confirmed the absence of the Lhcb1 protein by immunoblot analysis (data not shown), further investigations were performed only on the WT strain harbouring pURCLHC, hereafter referred to as WT_LHCgc.

3.2.3 Analysis of *Synechocystis* strains harbouring the synthetic gene cluster for LHC reconstitution

First, the presence of the whole LHCgc was confirmed by PCR from two independent WT_LHCgc strains (Fig. 3.10A).

The WT_LHCgc strains were further investigated for the accumulation of the heterologous proteins (Fig. 3.10A). In *Arabidopsis*, functional cp-SRP43 and cpSRP54 proteins were detected in the stroma [57], Lhcb1 and Alb3 were found in thylakoids, while cpFtsY was detected in both stroma and thylakoids fractions of chloroplasts [65]. Hence, in order to examine both the accumulation and subcellular localization of the heterologous expressed proteins, the crude protein extracts from *Synechocystis* WT and WT_LHCgc#1 and #2 were further divided between soluble and insoluble fractions, separated by SDS-PAGE and subjected to immunoblot analysis (Fig3.10B).

The immunoblot analysis confirmed the absence of the Lhcb1 protein, together with the absence of the co-transcribed cpFtsY. Both the cpSRP43

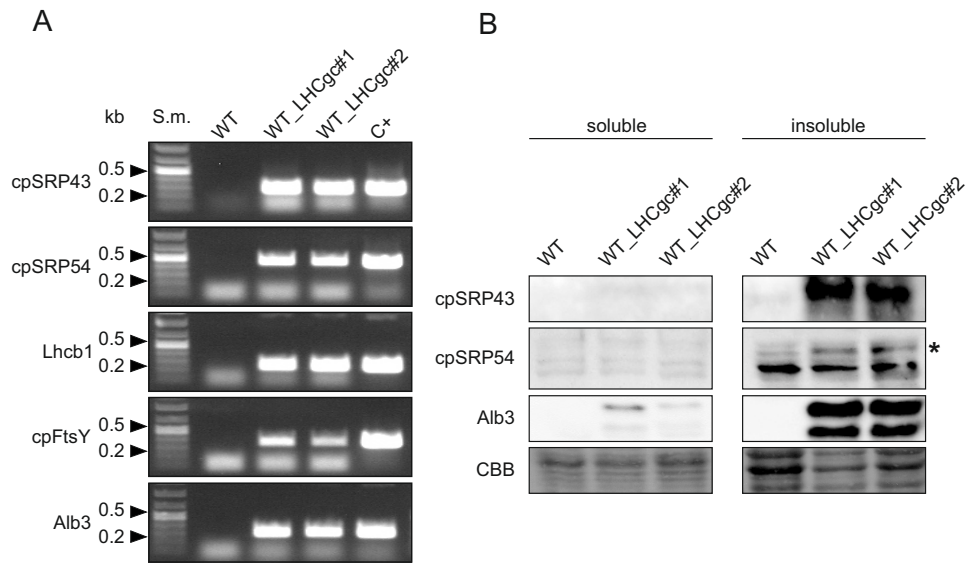


Figure 3.10: Genotyping and immunoblot analysis of the heterologous proteins expressed from LHCgc in two WT_LHC strains. **A.** Two independent clones of *Synechocystis* WT_LHCgc (# 1 and # 2) were tested by PCR for the presence of each gene of the cluster. Primers used are numbers 19 to 24 listed in Table 2.7, amplicon sizes: cpSRP43 273 bp , cpSRP54 477 bp, Lhcb1 477 bp , cpFtsY 349 bp , Alb3 291 bp. S.m.: size marker, C: positive control. **B.** Immunoblot analysis of heterologous protein expression in two WT_LHC strains. Crude extract was separated in soluble and insoluble fractions, and 30 μ g of protein for each genotype was loaded and fractionated on SDS-PAGE. Signals were detected for cpSRP43, cpSRP54 and Alb3 only in the insoluble fraction, while signals from Lhcb1 and cpFtsY were not detected (data not shown). CBB: gel stained with Coomassie Brilliant Blue shown as loading control.

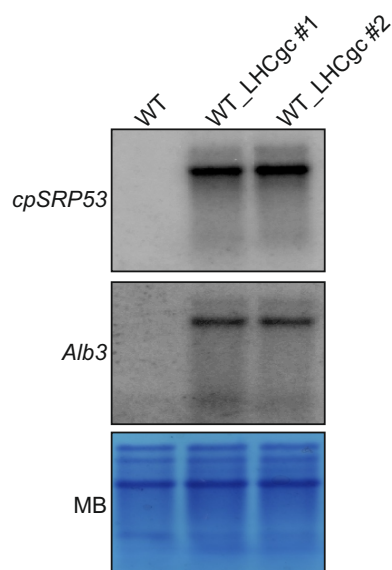


Figure 3.11: pURCLHCgc transcripts analysis of *Synechocystis* WT and two WT_LHC strains. RNA was extracted from the indicated *Synechocystis* strains, run in formaldehyde gel (20 μ g each lane) and blotted into a nitrocellulose membrane. The presence of transcripts from *cpSRP43*, *Alb3* and *Lhcb1* was investigated with radioactive probes as described in section 2.3.6. *Lhcb1* probe resulted in no detectable signal (data not shown), while signals from *cpSRP43* and *Alb3* were detected. MB: methylene blue staining indicative for equal RNA loading.

and cpSRP54 proteins were detected in the mutants, albeit only in the insoluble fraction. The accumulation of the proteins in the insoluble fraction could be due to a failure of reconstituting the functional soluble cpSRP complex into the cytoplasm of *Synechocystis*, which should be stable even in the absence of Lhc proteins [135]. A possible explanation could be that the proteins fail to fold properly and accumulate in an unfolded insoluble state, although not in such amount to be seen as inclusion bodies. Finally, *Alb3* properly accumulates in the insoluble fraction of the mutants, but whether *Alb3* is properly inserted in the thylakoids or it accumulates as an insoluble non-functional protein has to be further elucidated.

To investigate the cause of the absence of *Lhcb1* and cpFtsY proteins, transcript analysis by northern blot was performed. RNA was extracted from WT and WT_LHCgc strains, loaded on formaldehyde gels, blotted on nitrocellulose membrane and hybridized with radioactive probes for *Lhcb1* and, as positive controls, membranes were also hybridized with probes for *cpSRP43* and *Alb3* transcripts (Fig. 3.11). While *cpSRP43* and *Alb3* transcripts were detected, no signal for *Lhcb1* was observed (Fig. 3.11). The latter result suggested a problem in mRNA synthesis and/or stabilization of the second transcriptional unit of the LHCgc.

Different causes can be ascribed for inefficient mRNA synthesis or stabilization. To exclude that the problem was due to the chosen bacterial chassis (*Synechocystis*), the transcript abundance was also analyzed in the *E. coli* strain harbouring pURCLHC (hereafter referred to as *E. coli* LHCgc).

RNA was extracted from *E. coli* DH5 α and LHCgc strains and processed as described above. Radioactive probes for cpSRP54, cpFtsY and *Alb3* were

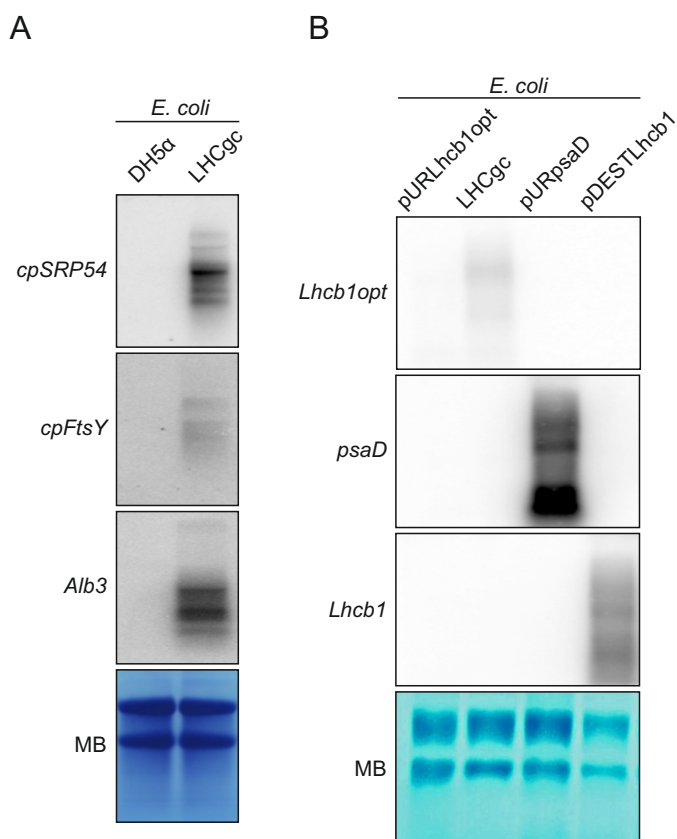


Figure 3.12: Transcripts analysis of LHCgc genes in different *E. coli* strains. **A.** Transcripts analysis from of *E. coli* DH5 α and LHCgc strains. **B.** Transcript analysis of the codon optimized and wild-type *Lhcb1* sequences in different genetic contexts. Upper blot: accumulation of codon optimized *Lhcb1* transcripts under P_{rbcl} (strong, from pURCLHC) and P_{Petj} (weak, from pURLhcb1opt) promoters; middle blot: positive control showing transcript accumulation of the *psaD* gene under the weak promoter P_{Petj} (from pURpsaD); Lower blot: accumulation of *Lhcb1* wild-type sequence transcript under the P_{PsbA2} promoter (from pDESTLhcb1). MB: methylene blue staining is indicative of RNA loading. Each lane was loaded with 30 μ g of RNA instead of 20 μ g as for the *Synechocystis* blot of Fig. 3.11. All transcripts were detected with radioactive probes as described in section 2.3.6, the signals of each panel were recorded exposing the blots simultaneously.

used to visualize the accumulation of transcripts from the first, second and third transcriptional units of the LHCgc, respectively (Fig. 3.12A). As been already observed in *Synechocystis* (Fig. 3.11), the signal for the transcripts from the second transcriptional unit was hardly detectable (Fig. 3.12A).

To investigate whether the optimization of the coding sequence of *Lhcb1* was responsible for the undetected level of transcript, the optimized *Lhcb1* was cloned downstream the promoter P_{petJ} , into the replicative vector pUR. The expression level of *Lhcb1* was compared to the expression level of the gene *psaD*, cloned in pUR under the same P_{petJ} promoter. As shown in Fig. 3.12B, the expression of the optimized *Lhcb1* is barely detectable compared to the strong *psaD* signal. In addition, the expression of the *Arabidopsis* wild-type *Lhcb1* under the control of the promoter $P_{P_{sabA2}}$ was tested (plasmid pDESTLhcb1, Fig. 3.12B). In this condition, the expression from *Lhcb1* was enhanced. These results suggested that the expression of the LHCgc second transcriptional unit could be hampered by the sequence optimization of *Lhcb1*.

3.3 The transporter SynPAM71 is required to maintain Mn homeostasis in *Synechocystis*

3.3.1 Identification of SynPAM71 and construction of *Synechocystis* Δ SynPAM71

It was recently shown that the protein PAM71 is involved in manganese uptake at the thylakoid membrane in *Arabidopsis* [89]. Based on phylogenetic analysis [136] and sequence alignments (Fig. 3.13), a single PAM71 homolog was identified in *Synechocystis* (SynPAM71), encoded by the gene *sll0615*. SynPAM71, as PAM71, belongs to the UPF0016 family of membrane proteins. Some of its plant, yeast and human homologs have already been characterized, and they exhibit the ability to transport Ca^{2+} and/or Mn^{2+} ions across membranes [91] [92] [89] [90]. SynPAM71 contains six putative transmembrane (TM) domains, including two highly conserved motifs ExGD(KT)(RT) (Fig. 3.13), which are thought to be responsible for cation binding and transport [91].

To investigate the function of SynPAM71, a knock-out mutant for *sll0615* was generated via homologous recombination, substituting a kanamycin resistance cassette for the wild-type gene (Fig. 3.14A). Complete segregation of the mutant was obtained under LAHG (light-activated heterotrophic growth) conditions (Anderson and McIntosh, 1991), and the genotype was confirmed by PCR (Fig. 3.14B).

Δ SynPAM71 cells exhibited a significantly slower growth rate than WT

```

SynPAM71 -----mkltslsknanstatavtvssiqklpflslsetlpcpkssrkptflpckcrrrpkdlldw 60
AtPAM71HL -----mkltslsknanstatavtvssiqklpflslsetlpcpkssrkptflpckcrrrpkdlldw 60
AtPAM71 -----mkslnlslsrripfqnrppksdfsstsspsssrrrcvsaypipigfsvrnqyfsrcltqlrrnesqql 70

SynPAM71 -----
AtPAM71HL gkfrvrASDAGVSGSGSYSGGEEDGSQSSSLDQSPATSS-ESLKPRGPPFPYLSLIALVLLSCGLVFSLITF 129
AtPAM71 gfrCFQRNDAACYLEKAESEEHDRNLDVLVESSIAHSRREIQRVLMFLAVSGSVALLGTDPAFAASSIPN 140

SynPAM71 -----MLTAFIAQLLITVSELGDKTFFIAMLLAMRYPRRWLVGVVCGSLAAMTILSVLMG 56
AtPAM71HL VKGGPSSVLAAV--AKSGRTAFSLITVSELGDKTFFIAALLAMQYEKTIIVLLGSMGALSLMTILSVVIG 197
AtPAM71 VTQSLVTSFGDLGDISGASFLITVSELGDKTFFIAALLAARNSAATVRFVGVVCGALGIMTILSVVIG 210

SynPAM71 -----YAEWALFLLFGTKLWDARRIKATAN-----LEEMEDAEKAIASG 108
AtPAM71HL KIFQSVP AQFQTTL-----PIGEYAAIALLMFFGLKSLKDAWDLPPVEAKNGEETGIELGEYSAEELVK 262
AtPAM71 RTFHYVDEVLPFRFGGTDLPIDDIAAWCLLVYFCVSTLLDAVSDGKKADE-----EQKE--AEPLAVSEL 272

SynPAM71 -----
AtPAM71HL EKKLKIPRGWIVVESGALTEVAEWGDRITQIATIALAASNNAWGVSAALDCHTICAVIIVMGGKFLVAG 178
AtPAM71HL EKASKKLTNPLEILWKSLSLVEFAEWGDRSMLATVALGAAQSPLGVASGALAGHLVATVIAIMCGAFLAN 332
AtPAM71 SGNAGVVAANTLISSTALVEFAEWGDKSFFSTIALAASSPLGVIAGALAGHGAATLLIIVLGGSLLEN 342

SynPAM71 -----
AtPAM71HL RISEKTVTLICGLLEFLVFAVVSWWTKIA 206
AtPAM71HL YISEKLVGYVGCALFLVFAAAFFGVF- 359
AtPAM71 FLSEKALAYVGGVLEFLVFAVIVVAEIVT 370

```

Figure 3.13: Sequence alignment of SynPAM71 with its (predicted) chloroplast-localized homologs from *A. thaliana*, AtPAM71 and AtPAM71HL. Similarity/identity of amino acids in at least 50% of the sequences is highlighted in gray/black shading, respectively. Chloroplast target peptides predicted by ChloroP [133] are indicated in lower case letters, the predictions for transmembrane (TM) domains and the soluble central loop (as predicted by TMHMM [137]) are indicated above the sequences. The two highly conserved E-x-G-D-(KR)(TS) motifs are boxed.

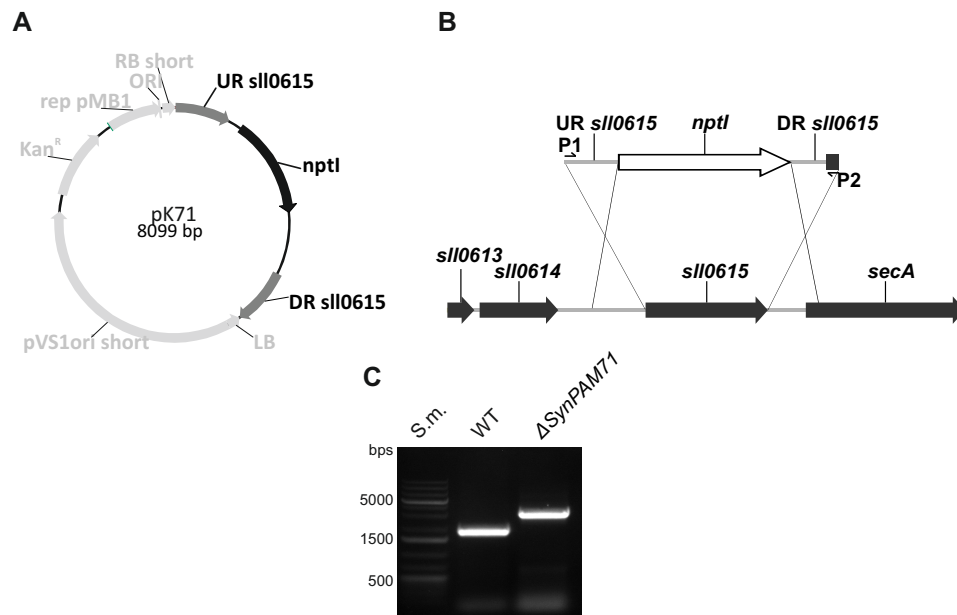


Figure 3.14: Generation of the Δ SynPAM71 strain. **A.** Suicide vector pK71 used to knock-out *sll0615*. UR, upstream region of *sll0615* (600 bp); DR, downstream region of *sll0615* (600 bp); nptI, kanamycin resistance. **B.** Schematic diagram of the generation of Δ SynPAM71 by homologous recombination. The *sll0615* gene, which codes for SynPAM71, was knocked out with an nptI cassette coding for kanamycin resistance. **C.** Genotyping of Δ SynPAM71. P1 (UR0615FW) and P2 (UR0615RV) primers (annealing positions depicted in A) were used to confirm the *sll0615* knock-out. Amplicon sizes: WT 1899 bp; Δ SynPAM71 3271 bp. S.m.: size marker

under the standard growth conditions used (Table 3.4). Their yellow-green color suggested an imbalance in the chlorophyll a (Chl a) to carotenoid ratio, and indeed levels of light absorbance by whole cells at 480-500 nm (indicative for carotenoids) were similar in WT and mutant, while the absorbance in the interval indicative for Chl a and phycocyanin was lower in the mutant (Fig. 3.15A). Subsequent analysis by methanol extraction confirmed that carotenoids accumulated to almost 90% of WT levels, whereas the amount of Chl a was reduced to about 60% relative to WT (Table 3.4). Pigment analysis was normalized on optical density, therefore the correlation between OD $_{750}$ and cell number in the two genotypes was verified with Thoma cell counting chamber (around 1.8×10^5 cells/mL, OD $_{750}$ 0.1).

Furthermore, Δ SynPAM71 cells showed a five times slower growth rate than WT under high light intensities (Fig. 3.15B), suggesting an impairment of photoprotective mechanisms.

3.3.2 Δ SynPAM71 is sensitive to increased Mn $^{2+}$ concentrations

Based on its homology to PAM71 (Fig. 3.13), we speculated that SynPAM71 could be involved in metal transport. Therefore, the effect of different divalent metals on the viability of the mutant was investigated. Δ SynPAM71 was grown on BG-11 medium supplemented with 10-, 20- or 50-fold more Ca $^{2+}$, Zn $^{2+}$, Cu $^{2+}$, Mn $^{2+}$, Fe $^{2+}$, or Mg $^{2+}$ than is present in standard growth medium. Δ SynPAM71 proved to be extremely sensitive to Mn $^{2+}$ supplementation to the growth medium: cell death was observed even at 10-fold increased Mn $^{2+}$ concentrations (Fig. 3.15C). Sensitivity to particular ions could be alleviated with the incubation in media limiting for the particular ion. Therefore, WT and mutant were grown in Mn limiting conditions (Fig. 3.15C, right panel). However, both WT and mutant maintained their growth phenotype when incubated for 5 days in Mn limiting conditions (Fig. 3.15C). WT growth is presumably sustained by the storage of Mn in the periplasmic place [80]. Mn starvation in *Synechocystis* is indeed observed only after six rounds of cell division when incubated in Mn-limiting conditions (corresponding to around 5 days in our growth conditions, see Table 3.4) [80]. The impaired growth of the mutant was also retained in Mn-limiting condition, presumably because of the inability of the mutant to re-allocate a possible detrimental Mn accumulation inside the cell in the growth medium. The inability to expel Mn from cells was already observed by Keren and coworkers [80].

Furthermore, the mutant was also slightly sensitive to Cu $^{2+}$ supplementation when compared to WT (Fig. 3.15c). It has previously been shown that Mn uptake into the cell is stimulated in the presence of Cu [84], which in turn suggests that the externally added Cu could amplify the sensitivity

Table 3.4: Growth rates and pigment analysis of WT and Δ SynPAM71. The values are means of three independent experiments (\pm SD). Cells were cultured under heterotrophic conditions at 22°C and illuminated with 50 μ mol photons $\text{m}^{-2} \text{s}^{-1}$. Pigments were extracted from 1 mL of culture at OD₇₅₀ 0.5 corresponding to equal cells number (data not shown) and to around 60 μ g protein for both genotypes. Values (\pm SD) are means of three experiments, each including three replicates. Asterisks indicate statistical significance (t test, *** P < 0.001, ** P < 0.01) of difference between WT and mutant. Chla: chlorophyll a.

Strain	Duplication time (h)	Chla ($\mu\text{g mL}^{-1}$)	Carotenoids ($\mu\text{g mL}^{-1}$)	Chla /carotenoids
WT	21.68 \pm 0.4	4.08 \pm 0.2	0.95 \pm 0.1	4.28
Δ SynPAM71	43.57 \pm 1.4***	2.41 \pm 0.1***	0.84 \pm 0.01**	2.25

of Δ SynPAM71 towards Mn.

3.3.3 Accumulation of photosynthetic supercomplexes is reduced in the mutant

To further characterize the phenotype of Δ SynPAM71, the steady-state levels of photosynthesis-related proteins were examined by SDS-PAGE and immunoblot analysis (Fig. 3.16). Equal amounts of total proteins were analyzed for each genotype, and PSI subunits (PsaB and PsaD) were found to be reduced to about 65% of WT levels. The amount of the PSII core subunits D1, CP47 and D2 was also reduced compared to WT level, while the accumulation of CP43 and PsbO was not altered in the mutant (Fig. 3.16). Interestingly, amounts of CyanoP increased by up to 4.5-fold relative to the WT level (Fig. 3.16). Accumulation of allophycocyanin (APC) – a component of phycobilisomes, the light-harvesting proteins of cyanobacteria – was also reduced in the mutant, in accordance with the absorbance spectrum profile (Fig. 3.16, 3.15A).

To investigate the formation of thylakoid protein complexes in Δ SynPAM71, thylakoids were isolated and solubilized, and an equal amount of thylakoid proteins were separated by BN-PAGE (Fig. 3.17A). The BN-PAGE profile of the mutant showed an overall decrease in protein complexes (Fig. 3.17A), confirming the results of the immunoblot analysis (see Fig. 3.16). Due to their inherently low abundance, altered steady-state levels of PSII supercomplexes could not be easily inferred from BN-PAGE profiles. Therefore, protein complexes first separated by BN-PAGE were further fractionated on a denaturing SDS-PAGE gel (2nd dimension) and subjected to immunoblot analysis for PSII subunits (Fig. 3.17B). The analysis of CP47 and D2 in thylakoid membranes of the mutant confirmed the decreases noted above

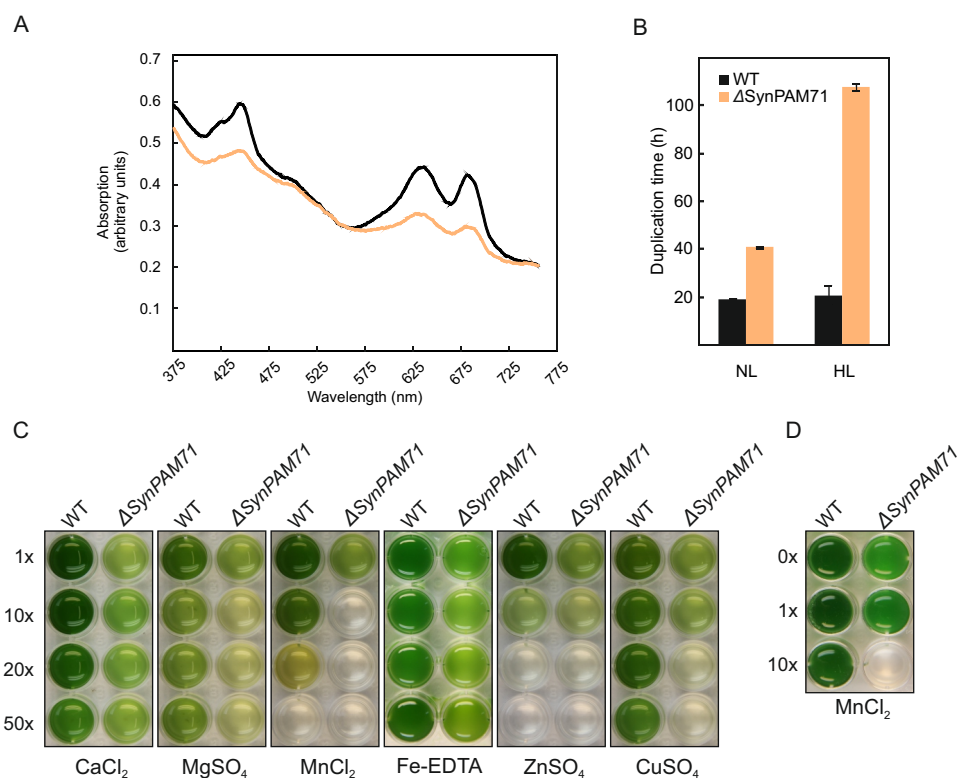


Figure 3.15: Initial characterization of $\Delta SynPAM71$. **A.** WT (black) and mutant (orange) absorbance spectra profiles were recorded from cell suspensions at OD_{750} 0.25. The spectra are means of three independent measurements, normalized with respect to the value at 750 nm. Absorbance peaks at 440 nm and 675 nm correspond to chlorophyll *a*, at 480-500 nm to carotenoids and at 625 nm to phycocyanin. **B.** WT (black) and mutant cells (orange) were grown in normal and high light conditions (NL and HL, 50 and 200 $\mu\text{mol photons m}^{-2} \text{s}^{-1}$ respectively). The calculated duplication time is the average of at least three independent experiments. Bars represent mean values \pm SD. **C.** $\Delta SynPAM71$ cells are sensitive to Mn and are not rescued by Mn depletion. (left panel) WT and mutant strains were grown in 24-well plates in the presence of increasing concentrations (10, 20 and 50 times that found in standard BG-11 medium, as indicated) of different divalent cations. The cultures were inoculated at OD_{750} 0.05 and let grown for a week. (right panel) WT and mutant were grown as in left panel in the presence of 0x, 1x and 10x Mn^{2+} .

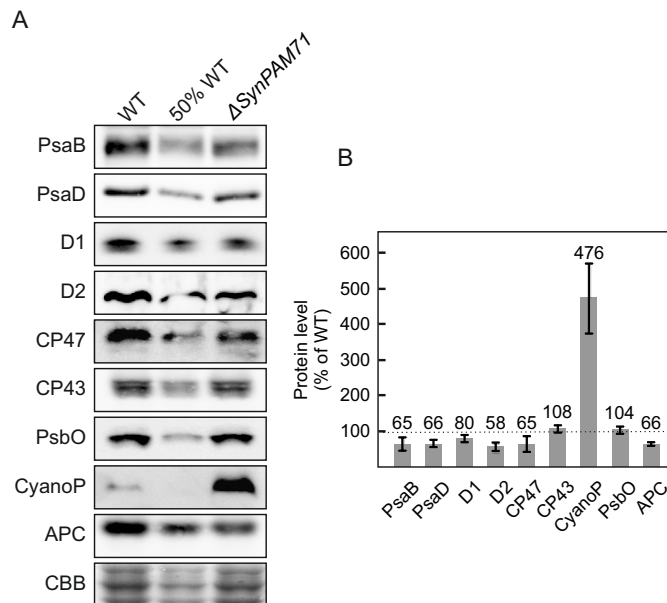


Figure 3.16: **A.** Immunodetection of proteins from WT and the mutant strain using different antibodies directed against individual subunits of PSI (PsaB, PsaD), PSII (D1, D2, CP47, CP43, PsaO, CyanobP) and allophycocyanin (APC). Samples equivalent to 30 μg of total protein were loaded in each lane, except for those marked "50% WT", where half as much was loaded. As a loading control, Rubisco was visualized by staining with Coomassie Brilliant Blue (CBB). **B.** Quantification of steady-state levels of photosynthesis-related proteins of which representatives immunoblots are shown in A. Bars represent mean values (\pm SD) of at least three technical replicates. Mean values (%) are indicated. Steady-state levels of $\Delta\text{SynPAM71}$ proteins are shown in percentage to steady-state levels of WT (100%).

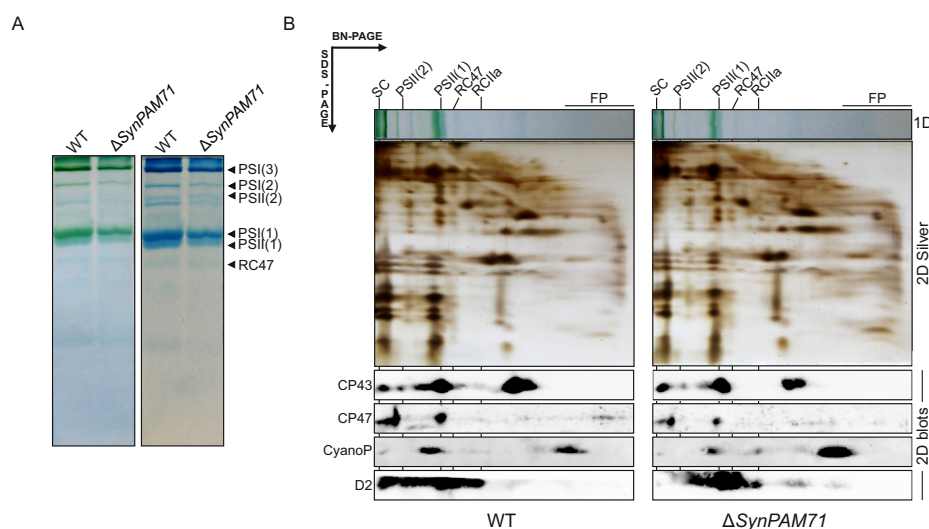


Figure 3.17: A. Separation of thylakoid membrane complexes obtained from WT and Δ SynPAM71 cells. Thylakoid membranes were solubilized with 2% β -DM, and protein complexes were fractionated by Blue-Native gel electrophoresis (50 μ g of protein were loaded in each lane) (left panel) and then stained with Coomassie (right panel). The positions of protein complexes (PSI(3)/(2)/(1) = tri/di/monomeric PSI complexes, respectively, RC47 = CP43-free PSII complexes, PSII(2)/(1) = PSII di/monomers complexes, respectively), are indicated, and were verified by immunoblot analysis (Fig. 3.20B). Please note, the PSII(2) is not visible due to low abundance, the ATP Synthase complex is more abundant and runs at similar size (Fig. 3.20A) [138]. **B.** Thylakoid protein supercomplexes separated by BN-PAGE (1D) were further analyzed on a denaturing SDS-PAGE gel, followed by silver staining (2D silver). Immunodetection of PSII proteins was performed using antibodies against CP47, CP43, CyanoP and D2 (2D blot). Exposure times for WT and Δ SynPAM71 immunoblots were identical. FP: free proteins.

(Fig. 3.17B). The two-dimensional BN/SDS-PAGE analyses also confirmed that CyanoP over-accumulates in Δ SynPAM71, mostly as free protein. The distribution of PSII protein complexes differs slightly between WT and mutant. Whereas CP43 and CP47 behave similarly in WT and Δ SynPAM71, in the latter CyanoP accumulates together with D2 in a small PSII subcomplex, which might correspond to the recently characterized CyanoP-containing RCIIa subcomplex [76].

3.3.4 Lack of SynPAM71 affects PSII photochemistry

The results described above indicate that Δ SynPAM71 is highly sensitive to Mn^{2+} and impaired with respect to the accumulation of thylakoid membrane protein complexes. Since Mn is of pivotal importance for PSII, the consequences of the loss of SynPAM71 function on PSII photochemistry

were measured by analyzing the rate of oxygen evolution using a Clark-type electrode. In the absence of an artificial electron acceptor, Δ SynPAM71 showed a 50% decrease in oxygen evolution compared to WT (Table 3.5). To investigate whether the diminished capability to evolve oxygen is due to the decrease in PSI levels or to a specific defect in PSII photochemistry, the analysis was performed in the presence of the artificial acceptors DMBQ and ferricyanide. DMBQ can accept electrons from the Q_A/Q_B site of PSII, thereby revealing defects on the PSII donor side, while ferricyanide keeps quinones in the oxidized form. Indeed, when DMBQ and ferricyanide were added, the rate of oxygen evolution for Δ SynPAM71 significantly dropped to only 30% compared to the WT strain (Table 3.5).

To further exclude the possibility that the decreased amounts of PSI might account for the observed drop in PSII activity, the rate of oxygen evolution was determined for a PsaA knock-out strain ($psaA^{prim}$, [7]) as control. Although the $psaA^{prim}$ mutant was markedly affected in its overall photosynthetic efficiency, its specific PSII activity (in the presence of the two artificial acceptors) was even higher when compared to WT (Table 3.5). PSII activity in $psaA^{prim}$ is uncoupled from the reduction in PSI abundance, therefore for $psaA^{prim}$ an acceptor side limitation of PSII occurs, as described before [139].

In addition, to test whether the effects of Mn toxicity and lack of SynPAM71 are comparable, the WT strain was grown in a medium containing 20-fold additional Mn compared to normal medium (hereafter WT 20xMn). As shown in Fig. 3.15C, the growth in 20xMn indeed triggers, in WT cells, growth impairments and change in pigmentation. As in the case of Δ SynPAM71, the reduced photosynthetic efficiency observed in WT 20xMn cells could be attributed to a specific defect in PSII photochemistry (20% compared to WT, Table 3.5). Moreover, WT 20xMn cells displayed Δ SynPAM71-like reductions in the accumulation of photosynthetic proteins and complexes (Fig. 3.18). Thus, it seems that the exposure of WT cells to excessive levels of Mn in the medium results in the same physiological defects, including PSI reduction, accumulation of CyanoP (albeit to a lesser extent) and impairment of PSII activity, as lack of SynPAM71 in the mutant cells. Thus, interestingly, the exposure of WT cells to excessive levels of Mn in the medium results in the same physiological defects, including PSI reduction, accumulation of CyanoP (albeit to a lesser extent) and impairment of PSII activity, as the lack of SynPAM71 in mutant cells.

Therefore, taking the reduced amount of PSII core subunits into account (Fig. 3.16, 3.17), the specific activity of PSII is even more decreased in Δ SynPAM71 (Table 3.5), revealing an additional defect on the donor side of PSII.

Table 3.5: Rates of oxygen evolution in WT, $\Delta SynPAM71$ and $psaA^{prim}$ strains, and WT cells grown in 20-fold Mn (WT 20xMn). Each strain was harvested in late exponential phase and concentrated to OD_{750} 5. Rates of oxygen evolution are means of at least three independent cultures (\pm SD) and are expressed in $nmolO_2 mL^{-1}$ (i.e., effectively on the basis of cell number). ¹Electron transport between PSII and ferredoxin was measured without acceptors. ²Electron transport between the donor (OEC) and acceptor (Q_A/Q_B) sides of PSII was measured in the presence of DCBQ/FeCN as electron acceptors. Values (\pm SD) are means of three replicates. Asterisks indicate statistical significance (t test, *** $P < 0.001$) of difference between WT and mutant strains or between WT and WT 20xMn.

	WT	$\Delta SynPAM71$	$psaA^{prim}$	WT 20xMn
PSII to Fd ¹	33.2 ± 1.1	$16.1 \pm 1^{***}$	$8.2 \pm 0.9^{***}$	$0.95 \pm 0.1^{***}$
PSII to DCBQ ²	52.3 ± 2.3	$15.8 \pm 0.8^{***}$	$70.8 \pm 4^{***}$	10.7^{***}

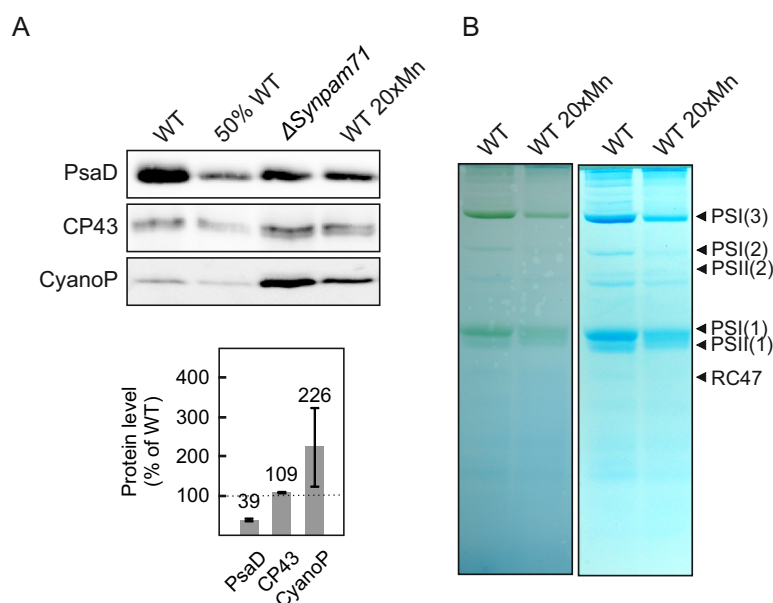


Figure 3.18: Analysis of protein complexes accumulation in *Synechocystis* WT cells grown in toxic amounts of Mn. **A.** Immunodetection of proteins from WT and $\Delta SynPAM71$ cells cultured in standard growth medium, and from WT grown in 20xMn medium. Each lane was loaded with 30 μg of total protein extract, except those marked 50% WT, which contained 15 μg of protein. **B.** BN-PAGE profile of WT cells grown in standard and in 20xMn medium.

3.3.5 Δ SynPAM71 cytoplasm, thylakoids and PSII protein complexes are enriched in Mn

In order to examine how and to what extent the absence of SynPAM71 affects the subcellular allocation of Mn and other metals, the concentration of Mn, Mg, Ca, Fe, Cu, and Zn in whole cells and isolated membrane fractions from Δ SynPAM71 and WT were determined by ICP-MS (Fig. 3.19A, and Tables B.1, B.2, B.3, B.4 in appendix B). Prior to the measurements, collected cells were carefully washed with EDTA-containing buffer to remove the Mn-rich pool present in the outer membrane and periplasmic space [80]. Whole cells (comprising cytoplasm, plasma membrane and thylakoids) and isolated membrane fractions (plasma membrane and thylakoids) were normalized based on protein concentrations, digested, and subsequently analyzed by ICP-MS for total element concentrations (Fig. 3.19A, and Tables B.1, B.2 in appendix B). The amount of Mn was significantly increased in Δ SynPAM71, in both whole cells and in the isolated membrane fractions, whereas the concentrations of the remaining analyzed elements were similar to WT levels, beside a small increase in Ca. For better visual interpretation of the results, the ratio between mutant and WT for each element is displayed in Fig. 3.19B. In whole cells of Δ SynPAM71, the Mn levels were significantly increased up to 2.5-fold and by 2-fold in the isolated membrane fraction, compared to WT (Fig. 3.19B, Table B.3, B.4).

To investigate Mn binding in PSII and the integrity of the inorganic Mn cluster, solubilized thylakoids from Δ SynPAM71 and WT were first fractionated using size-exclusion chromatography (SEC) and then ion intensities for $^{48}\text{SO}^+$, $^{55}\text{Mn}^+$, $^{72}\text{FeO}^+$ and $^{24}\text{Mg}^+$ were analyzed by ICP-QQQ-MS [140](Fig. 3.19C). SEC-ICP-QQQ-MS analysis has previously been successfully employed for the quantification of Mn- and Fe-containing super- and subcomplexes in barley and *Arabidopsis* thylakoids [140] [89]. Because the $^{55}\text{Mn}^+$ and $^{72}\text{FeO}^+$ SEC-profiles from *Synechocystis* differed from the previously analyzed $^{55}\text{Mn}^+$ and $^{72}\text{FeO}^+$ profiles for higher plants, individual fractions corresponding to the Mn and Fe main peaks (annotated as Mn₁, Mn₂, Fe₁ and Fe₂ in Fig. 3.19C) were collected and loaded onto a BN-PAGE gel for protein complex identification (Fig. 3.20). The *Synechocystis* $^{55}\text{Mn}^+$ chromatogram revealed two major peaks, Mn₁ and Mn₂ (Fig. 3.19C). The Mn₁ peak co-eluted with a minor sulfur peak (proxy for proteins), did not co-elute with any Mg peak (proxy for chlorophyll bound to protein complexes) (Fig. 3.19C) and further overlapped with the phosphate P1 peak (proxy for membrane phospholipids) (Fig. 3.21). Hence, the Mn₁ peak could not be ascribed to PSII supercomplexes, but could instead represent Mn bound to the thylakoid membrane or membrane fragments. The second eluting Mn peak (Mn₂) included both PSII monomers and dimers (Fig.).

The Mn₁ and Mn₂ peaks were both found to be increased in Δ *SynPAM71* compared to WT (Fig. 3.19C), suggesting that accumulation of Mn occurs in membrane fractions and in PSII protein complexes.

While thylakoid Mn is bound solely to PSII, Fe is enriched in PSI (12 Fe atoms per monomer), PSII (3 atoms), cytochrome *b₆f* (6 atoms) and NDH-1 protein complexes (12 atoms) [141] [142]. However, PSI is the most abundant chlorophyll-containing protein complex in *Synechocystis* thylakoids; therefore, the largest Mg- and Fe-containing fractions are here considered as proxy for PSI complexes. The ⁷²FeO⁺ size-exclusion profile of *Synechocystis* revealed two major peaks, Fe₁ and Fe₂ (Fig. 3.19C). The Fe₁ fraction was enriched in PSI supercomplexes, trimers and dimers, while the Fe₂ fraction was enriched in PSI monomer complexes (Fig. 3.20A). The first Fe-eluting fraction Fe₁ of Δ *SynPAM71* was strongly reduced compared to WT, whereas the decrease in the Fe₂ fraction was less pronounced (Fig. 3.19C). The total Fe peak area in the SEC profile of Δ *SynPAM71* is decreased to about 70% of WT which is in good agreement with the observed reduction in the amount of PSI subunits and complexes (Fig. 3.16, 3.17). Likewise, the total peak area of the Mg profile of Δ *SynPAM71* showed a decrease to around 70% compared to WT (Fig. 3.19C), which nicely supports the measured reductions in Chl*a* content of the mutant (Table 3.4).

Taken together, the results demonstrate that Mn accumulates within Δ *SynPAM71* cells, and in particular in the thylakoid membranes. Moreover, the Mg and Fe profiles support the reduction in PSI amounts as also deduced from protein analysis (Fig. 3.16, 3.17).

3.3.6 *SynPAM71* is predominantly located in the plasma membrane of *Synechocystis*

Synechocystis possesses an outer membrane, an inner (or plasma) membrane and thylakoid membranes. In order to identify the subcellular localization of *SynPAM71*, a tagged version of *SynPAM71* (FLAG:*SynPAM71*:6xHis, hereafter F*SynPAM71*H) under control of the cytochrome *c₆* promoter (P_{petj}) was generated and introduced into Δ *SynPAM71* to generate the strain F*SynPAM71*H. Strikingly, F*SynPAM71*H not only complemented Δ *SynPAM71*, it also conferred a higher degree of resistance to Mn toxicity than that exhibited by WT cells (Fig. 3.22A). Indeed, F*SynPAM71*H was able to survive in growth medium containing 100-fold Mn²⁺, while the WT could not tolerate manganese concentrations above 20-fold (Fig. 3.22A). This suggests that F*SynPAM71*H is functional and its increased activity might be due to the enhanced efficiency of the P_{petj} promoter used to drive F*SynPAM71*H expression. In *Synechocystis* the P_{petj} promoter drives the expression of cytochrome *c₆*, which replaces plastocyanin under conditions

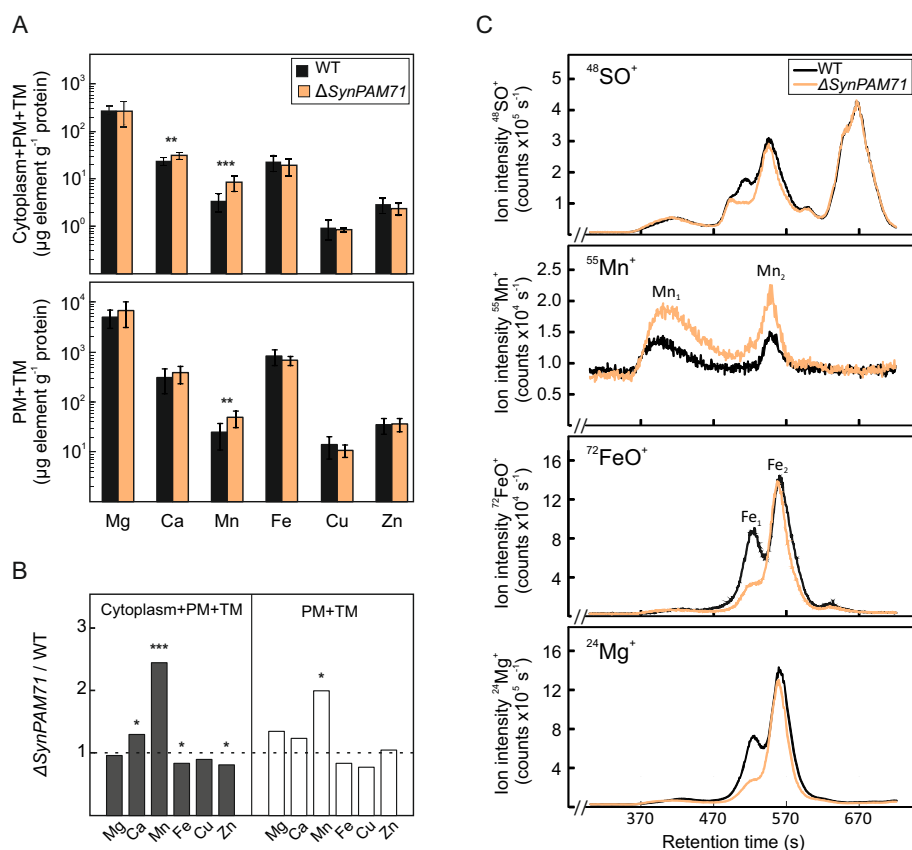


Figure 3.19: A. Analysis of total element concentrations in WT and $\Delta\text{SynPAM71}$ whole cells (comprising cytoplasm, plasma membrane and thylakoids) (upper panel) and isolated membrane fractions (plasma membrane and thylakoids) (lower panel). Bars represent mean values (\pm SD) of two experiments, including six and three replicates. Asterisks indicate statistical significance (t test, *** $P < 0.001$, ** $P < 0.01$) of difference between WT and mutant. Numerical values are given in Table B.1, B.2. TM: thylakoid membranes; PM: plasma membranes. **B.** Columns represent the ratio of $\Delta\text{SynPAM71}$ to WT for the indicated element. Values were calculated from Table B.1, B.2. Asterisks indicate significant differences to a ratio of one (two-way ANOVA, *** $P < 0.001$, * $P < 0.05$, Table B.3, B.4). TM: thylakoid membranes; PM: plasma membranes. **C.** SEC-ICP-QQQ-MS profiles for WT and $\Delta\text{SynPAM71}$. Thylakoids were solubilized with 2% β -DM, loaded onto a SEC column and the metal-binding profiles of the eluting separated protein complexes were analyzed by ICP-QQQ-MS. Size-exclusion profiles were recorded for $^{48}\text{SO}^+$, $^{24}\text{Mg}^+$, $^{55}\text{Mn}^+$ and $^{72}\text{FeO}^+$ ions for WT (black lines) and $\Delta\text{SynPAM71}$ (orange lines) and expressed as ion intensities (counts s^{-1}). Individual Mn and Fe peaks (Mn_1 , Mn_2 , Fe_1 , Fe_2) were annotated using BN-PAGE for identification (Fig. 3.20). Mn_1 : thylakoid membrane fraction; Mn_2 : PSII(2) and PSII(1); Fe_1 : PSI supercomplexes, PSI(3) and PSI(2); Fe_2 : primarily PSI(1). The profile of the $^{48}\text{SO}^+$ signal verifies equal loading of solubilized proteins.

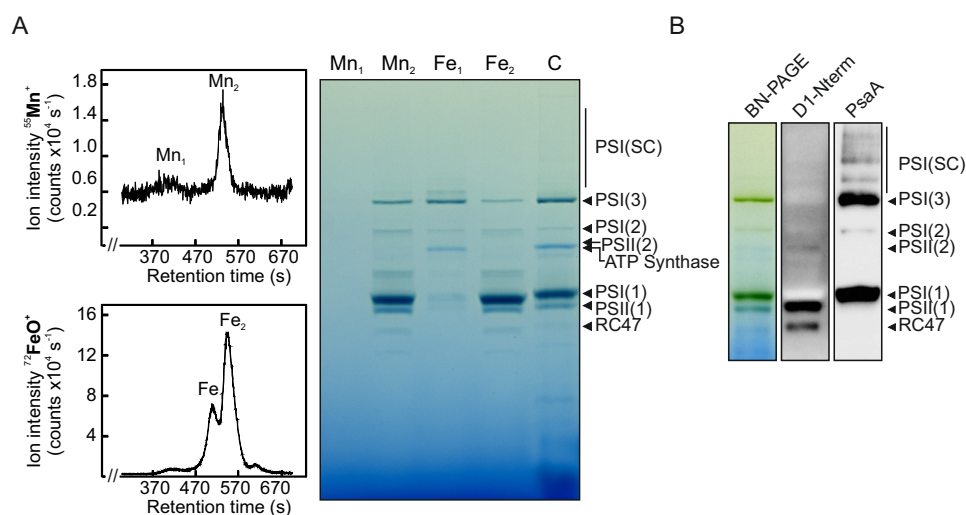


Figure 3.20: Assignment of Mn and Fe peaks in SEC-ICP-MS profiles to thylakoid complexes and other fractions. **A.** Enrichment of Mn and Fe in photosystem complexes. Left panel: Size-exclusion chromatography (SEC) profiles for a WT sample recorded for $^{55}\text{Mn}^+$ and $^{72}\text{Fe}^+$. Middle panel: BN-PAGE gel of the individual Mn and Fe subfractions. Right panel: BN-PAGE followed by immunoblot analysis using antibodies against D1 and PsaA in order to discriminate between PSI and PSII supercomplexes. Subfractions from SEC were collected (Mn_1 , Mn_2 , Fe_1 and Fe_2 as indicated in the chromatograms), concentrated on 100K spin-filters and loaded (15 \AA tg protein per sample) onto a BN-PAGE gel for protein complex identification. No visual protein bands for the Mn_1 peak were observed. Since the Mn_1 peak does not overlap with any Mg peak (Fig. 5) but does overlap with the P peak (Fig. 3.21), Mn_1 cannot be derived from any PSII supercomplex. Instead, it could represent the membrane fraction. Mn_2 is the major Mn-containing fraction, and is enriched in both PSII dimers and monomers. The Fe_1 subfraction is enriched in PSI trimers and dimers, whereas the Fe_2 is primarily enriched in PSI monomers. Please note, that PSII(2) is not visible due to low abundance, the ATP Synthase complex is more abundant and runs at similar size as indicated next to the control lane (C).

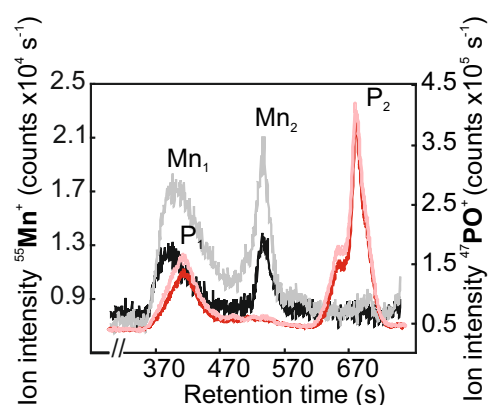


Figure 3.21: Mn₁ peak overlays with a P peak. Mn size-exclusion profiles from WT (black) and mutant (gray) were overlaid with the corresponding ⁴⁷PO⁺ size-exclusion profiles (red for WT and pink for Δ SynPAM71) in order to highlight the similarity in retention times between peaks Mn₁ and P₁. Data shown are from one representative experiment (of a total of three).

of copper deficiency in cyanobacteria, and this gene is activated in growth medium devoid of copper. However, its basal expression (as in the normal BG-11 medium used in our study) has been shown to be sufficient for the complementation of null mutants [118]. The protein SynPAM71 has so far been elusive in proteomic studies on membranes of *Synechocystis* [143] [144]. Only recently it was detected in small amounts in thylakoids membranes in an extensive proteomic study on membrane fractions from *Synechocystis* [145], suggesting that SynPAM71 is present only in low concentrations in vivo. Therefore, despite the relatively weak promoter employed to drive the FSynPAM71H expression (in normal BG-11 medium), the actual protein accumulation in FsynPAM71H strain might be higher compared to WT, enhancing its resistance to Mn toxicity.

In order to clarify the membrane localization of SynPAM71, membranes of FSynPAM71H were separated on a sucrose step gradient as described previously [146] (Fig. 3.22). Solubilized proteins corresponding to plasma membrane and thylakoid membrane fractions were normalized to protein concentration, subjected to SDS-PAGE and blotted onto a nitrocellulose membrane, which was then probed with antibodies raised against D2, SbtA, Prata and His-tag. The D2 and SbtA signals confirmed the purity of thylakoid and plasma membrane fractions, respectively, while the Prata antibody was used to identify the fraction enriched in thylakoids biogenesis centers [147]. Based on the His-tag signal, FSynPAM71H was found primarily in the plasma membrane fraction, although a minor portion of the protein was detected in the thylakoid membrane fraction (Fig. 3.22B), indicating that FSynPAM71H is present in both membrane systems.

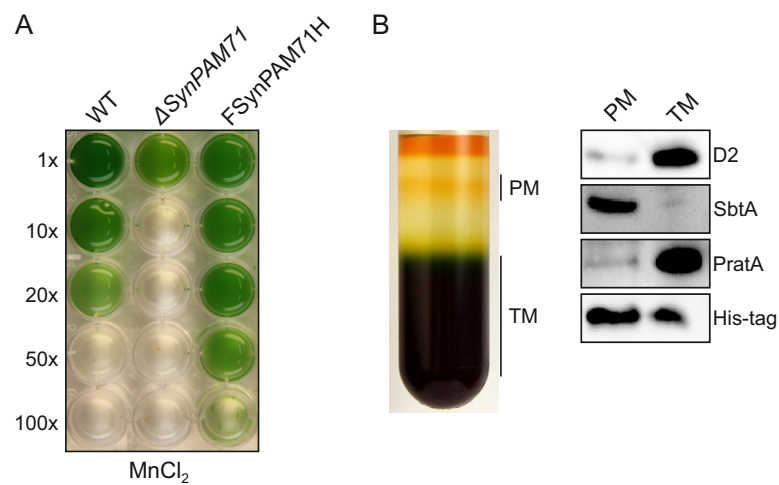


Figure 3.22: SynPAM71 is enriched in plasma membranes. (a) WT, Δ SynPAM71 and FSynPAM71H were grown in the presence of increasing concentrations of Mn, as indicated. Note that only FSynPAM71H can grow in 100xMn. (b) Membrane fractions from *Synechocystis* were separated on a sucrose gradient as described [146] (left panel). Plasma (PM) and thylakoid (TM) membrane fractions were collected. Solubilized proteins (4 μ g per lane) of PM and TM were fractionated by SDS-PAGE and immunoblotted with antibodies raised against D2 (marker for thylakoid membrane proteins), SbtA (marker for plasma membrane proteins), PratA (marker for thylakoids biogenesis center proteins) and the His-tag (to identify the FSynPAM71H protein) (right panel).

Chapter 4

Discussion

4.1 Shotgun functional complementation of *Synechocystis* photosynthetic mutants with a cDNA library from *Arabidopsis*

A method to construct and express a cDNA library in the model cyanobacterium *Synechocystis* is described in this work. A tailored replicative vector, named pUR2L, was constructed for the expression of cDNA libraries in *Synechocystis*. The cDNA cloning strategy involved the conjugative transfer of an *Arabidopsis* cDNA library from an *E. coli* donor strain into the final *Synechocystis* host. Exploiting the efficiency of conjugation was indeed possible to transform a sufficient number of *Synechocystis* cells to obtain a representative cDNA library from *Arabidopsis*.

So far, a successful complementation was observed only for the *Synechocystis* Δ *psaD* mutant, and only from two out of five rounds of complementation. Albeit Δ *SynPAM71* was a promising candidate to isolate complemented transconjugants due to its robust and selective screening, it was not possible, to date, to isolate a complemented clone.

Taken all together, these results suggest that the described method to obtain a cDNA library to complement *Synechocystis* still lacks the quality necessary to isolate complemented clones of low transcribed genes, such as genes encoding for regulatory factors. *PsaD* is indeed a small, highly transcribed gene encoding for a structural subunit of PSI. The robustness of the cDNA library is pivotal when the goal is to isolate genes taking part in assembly or regulatory pathways, since these genes are indeed much lower expressed than genes encoding structural proteins [148]. Nevertheless, various improvements could still be addressed to better achieve the required cDNA library quality.

First, the high throughput of the library preparation was hampered by

the laborious plasmid preparation and handling during the cloning procedures (see section 2.2.2). Library trials have indeed frequently failed due to the low quality of plasmid preparation (e.g. the aversion to subsequent *SfiI* restriction [42]). Putative targets for plasmid processing improvements are i) increasing the copy number and ii) decreasing the size of the pUR2LT vector. The copy number of pUR2LT is dictated by the origin of replication *oriV* (and its trans-acting *rep* genes), which are required for the broad-host range replication of the plasmid and therefore restricted from further modification. The backbone of pUR2LT could be shortened by around 3.5 kb. Theoretically, if a replicative plasmid has to be mobilized, it must contain the origin of transfer *oriT* and mobilization proteins that recognise this site, given that the *oriT* differs from the *oriT* of the helper plasmid. Hence, if the *oriT* of the mobilizable plasmid is identical to the one from the helper plasmid, the mobilizable plasmid can undergo conjugation without requiring additional *mob* genes. The *oriT* from pUR2LT comes from RSF1010 and requires *mob* genes to be trans-conjugated by RP4 (helper plasmid). Hence, exchanging the RSF1010 *oriT* with the *oriT* from RP4 would allow the removal of the *mob* genes from the pUR2LT backbone. Together with the reduction to one antibiotic resistance cassette, this deletion would shrink the backbone to around 6.5 kb, improving the processing of the plasmid together with releasing the bacterial cells from additional metabolic burdens.

Second, the cDNA expression could be improved, as well as its transcript stability. The P_{PetJ} promoter, initially chosen for its inducible properties, could be exchanged with the strong P_{PsbA2} and the transcript stability could be enhanced through the introduction of a hairpin structure at the 5' of the transcript, in order to prevent its degradation [149].

Furthermore, increasing the relative presence of rare transcripts could be achieved by library normalization [150] [151]. Otherwise, commercially kits are available for the the construction of *Arabidopsis* normalized cDNA libraries which are suitable for Gateway cloning (e.g. Thermo Fischer Scientific # 19625011). To employ the latter approach, the *SfiI* restriction sites of the pUR vector would be substituted by Gateway recombination sites and the LR recombinase reaction would be performed in the place of the ligation reaction. Another way to increase the presence of certain cDNA sequences in the library, could be achieved inducing the production of the specific mRNA of interest directly from the source of RNA (in this case, *Arabidopsis*). For example, to induce the production of Mn transporters mRNAs, the RNA pool would be extracted from plants grown in Mn-toxic or Mn-deficient conditions in order to induce the transcription of transporters involved in Mn homeostasis.

Lastly, the isolation *Synechocystis* strains which are able to reconstitute whole plant-like photosynthetic machineries would probably require many rounds of complementation since more than one unknown plant-specific accessory factor is missing. To identify assembly intermediates that increase but still do not completely recover the viability of *Synechocystis* photosynthetic mutants, bimolecular fluorescence complementation (BiFC) [51] could be employed.

4.2 Expression and stabilization of functional LHCII in *Synechocystis*

The genes for *Lhcb1* and the SRP pathway constituents (*cpSRP43*, *cpSRP54*, *Alb3* and *cpFtsY*) from *Arabidopsis* have been introduced into *Synechocystis*.

Initially, the genes were introduced into *Synechocystis* genome by a two-step transformation (Fig.3.8). However, the completion of this strategy was prevented by i) the successful construction of the second vector p54Y and ii) the transcript instability of the genes from the first cloned construct (pDS433, see Fig.3.8).

Hence, a tailored gene cluster containing *Lhcb1* and the genes from the SRP pathway (LHCgc) was designed to be synthesized and introduced into *Synechocystis* with a replicative vector (pURCLHC, Fig.3.9). The LHCgc was divided in three independent transcriptional units in order to help identifying the position of a possible failure in transcription or translation within LHCgc. Furthermore, the sequence for each gene was optimized for protein production in *Synechocystis*. Analysis of *Synechocystis* LHCs strain revealed that protein and transcripts accumulate from the first (*cpSRP43*, *cpSRP54*) and last transcriptional unit (*Alb3*), while protein and transcripts from the second transcriptional unit (*Lhcb1*, *cpFtsY*) were not detected in *Synechocystis* WT_LHCgc strains (see Figs.3.10 and 3.11).

Interestingly, the expression profile of WT_LHCgc mirrored the expression profile of the *E. coli* LHCgc strain (containing pURCLHC Fig.3.12A), suggesting that the *Synechocystis* chassis could be excluded as the cause of the absence of transcript, or, at least, the transcript reduction could be due to molecular mechanisms contained by both *Synechocystis* and *E. coli*. Given the faster time in duplication, further analysis were performed on *E. coli* strains. The expression of the *Lhcb1* gene was investigated in different genetic contexts, and the results suggested that the sequence optimization of *Lhcb1* could be ascribed for the transcript accumulation impairment (Fig. 3.12B).

The accumulation of a transcript is influenced by the rates of synthesis and degradation. Transcripts synthesis rate is decided by transcription

initiation and elongation mechanisms, which involved the nature of promoter sequences and therefore the binding of RNA-polymerase, which are additionally regulated by *trans*- or *cis*-acting factors (such as regulators, transcript secondary structure and metabolites). Transcript degradation is instead influenced by the action of ribonucleases (RNases) which can be either endoribonucleases, that cleave internally the RNA chain, or exoribonucleases, that degrade the RNA from either the 5' end or the 3' end. The susceptibility of a transcript to degradation depends on the accessibility of sites at which RNases can act (influenced by the RNA structure). Transcript degradation is also coupled to efficient translation, since mRNA that are most efficiently transcribed (and therefore densely covered with ribosomes) are more stable than transcripts that are not efficiently translated.

Synthesis of *Lhcb1* transcript could be excluded as the cause for the loss in *Lhcb1* transcript accumulation. Indeed, as shown in Fig. 3.12B, the promoter P_{petJ} induced the expression of the *psaD* gene, while the optimized sequence of *Lhcb1*, cloned downstream the same promoter, still remained unexpressed. The expression level of *Lhcb1* from the P_{petJ} promoter resulted lower when compared to the expression produced by the P_{rbcl} promoter (from the pURCLHC vector, in the *E. coli* LHCgc strain, Fig. 3.12B, upper panel). The difference could be ascribed to the dissimilar promoter strength (P_{rbcl} is a strong promoter while P_{petJ} is a weak promoter).

The accumulation of the *Lhcb1* transcript was probably prevented by its degradation. Indeed, when a non-optimized version of the *Lhcb1* gene was cloned downstream the P_{psbA2} promoter (having a comparable strength to the P_{rbcl} promoter) the transcript accumulation was observed (Fig. 3.12B, lower panel). This result suggested that the optimized sequence of *Lhcb1* could expose cryptic RNA sequences recognised by RNases.

Notably, the detection of *Lhcb1* by immunoblot analysis from the *E. coli* pDEST*Lhcb1* strain resulted unsuccessful (data not shown). Although this finding is in line with what was previously observed in *Synechocystis* [36], it is in contrast with the reported expression of *Lhcb1* in *E. coli* [67], where the *Lhcb1* protein was shown to accumulate up to 20% of the total protein pool, as inclusion bodies [67]. This latter discrepancy could be again due to the different promoters used to drive the *Lhcb1* expression. Previously, *Lhcb1* was expressed by the strong promoter P_{N25} (derived from the T5 bacteriophage) [67] while the expression from pDEST*Lhcb1* *Lhcb1* was driven by the P_{psbA2} promoter, which is orders of magnitude weaker than the P_{N25} promoter. Possibly, since *Lhcb1* would be an insoluble and futile protein for the cellular functions of *E. coli*, *Lhcb1* is sequestered in inclusion bodies when it is expressed by the P_{N25} promoter, whereas the slower expression driven by P_{psbA2} allows the *Lhcb1* degradation by cellular

proteases.

The prediction of the transcriptional outcome for a combination of promoter, 5' untranslated region (UTR) and CDS in a chassis is not an easy task. An ideal promoter (and its 5' UTR) would drive a certain level of transcription, independently on the CDS it express. However, promoters are rarely well defined, and this lead to unpredictable effects on the stability of certain mRNA species. The interaction between the promoter, the 5' UTR and the CDS could lead to the formation of a ribosome-blocking secondary structure [152] [153]. Indeed, a combinatorial study in which different promoters and 5' UTRs were used to drive the expression of reporter genes, found the junction between translation initiation elements and CDSs as the major source of irregular gene expression [154]. An approach that prevents the cross-talk between genetic parts in prokaryotes could exploit the bicistronic system that Mutalik and co-workers had established for *E. coli* [154]. Another way to decouple 5'-UTR and CDS would be the introduction of a self-cleaving ribozyme to the RBS that would cleave the mRNA from the 5'-UTR [155]. Otherwise, a method to enhance the transcript stability would be the introduction of a hairpin structure at the 5' of the transcript, to hamper its degradation [149].

In general, improving the prediction of how the combination of genetic parts (promoters and CDSs) behave in *Synechocystis* would be important to implement future SynBio approaches in this chassis. However, predictions are intrinsically biased by the degree of knowledge of a bacterial chassis. Indeed, bacterial chassis behave mostly as black-boxes, in which even the best-thought genetic constructs could fail in giving the expected output. The *in vivo* testing of complex genetic constructs scales poorly, and although large-scale successes have been accomplished, significant time cost is due to the *in vivo* testing. For instance, the industrial production of artemisin has costed 150 person-years of work, of which much time has been spent on genetic construct testing (developing or refining genetic parts and testing their expression) [156]. Recently, to overcome this problem, a procedure for the assembly and testing of complex genetic constructs in a *E. coli* S30-based transcription-translation system (TX-TL) has been successfully established [157]. This cell-free expression system is designed to behave as a "biomolecular breadboard", mirroring the *E. coli in vivo* state while preserving protein production molecular mechanisms [157] [158]. Prototyping of genetic constructs in TX-TL systems could decrease the testing time (down to 8h [157]) and therefore increase iteration speed for complex genetic constructs of which predictions behave poorly.

4.3 The transporter SynPAM71 is required to maintain Mn homeostasis in *Synechocystis*

The various impairments observed in Δ *SynPAM71* can all be attributed to Mn toxicity. Δ *SynPAM71* is very sensitive to Mn supplementation to the growth medium (Fig. 3.15C). This finding is in sharp contrast to the *Arabidopsis* mutant *pam71*, whose growth and development is boosted by added Mn [89].

Δ *SynPAM71* is also characterized by a lower chlorophyll content (Table 3.4) and a decrease in PSI complex accumulation (Fig. 3.16,3.17). Both symptoms have previously been associated with Mn toxicity in plants [159] [160] [161]. However, the effects of Mn vary greatly among plant cultivars [162] [163] [161] [164] [165]. Chlorophyll and PSI deficiencies have furthermore been linked to Mn-induced Fe starvation, in which Mn could compete with Fe for protein binding. The correlation between Mn and Fe homeostasis has been demonstrated in several organisms [166] [167] [168] [169]. Indeed, in various plant species, Mn and Fe toxicity can be corrected by addition of Fe or Mn, respectively [166] and in *Synechocystis* an increased Mn-to-Fe ratio reveals symptoms of iron starvation [169]. The ICP-MS analysis showed that Δ *SynPAM71* accumulated 2 - 2.5 times more Mn than WT, in both whole cells and in isolated membrane fractions (Fig. 3.19A,B). Concomitantly, Fe accumulation was decreased (Fig. 3.19A,B), confirming that Mn-induced Fe starvation indeed ensues in the mutant.

The observed sensitivity of Δ *SynPAM71* cells to high light (Fig. 3.15B) can also be explained by Mn toxicity. It has been demonstrated that Mn toxicity increases susceptibility to photodamage in plants [162], [161] [164] and in *Synechocystis* [170]. In particular, *Synechocystis* ManSR mutants exhibit stable overexpression of the *mntCAB* operon under normal growth conditions. The resulting continuous uptake of Mn from the periplasm into the cytoplasm eventually triggers symptoms of Mn toxicity in the cell [170] and these mutants display reduced resistance to high light. Interestingly, concomitantly with the overexpression of the *mntCAB* operon, the ManSR mutant also overexpresses D1 and D2 transcripts, suggesting a correlation between Mn toxicity and PSII core turnover [170].

PSII is the primary sink for Mn in oxygenic photosynthetic organisms. Taking the reduced amount of PSII core subunits into account (Fig. 3.16,3.17), the specific activity of PSII is even more decreased in the Δ *SynPAM71* (Table 3.5), revealing an additional defect on the donor side of PSII.

Determination of Mn extracted from chromatographically size-fractionated membrane protein complexes showed that in Δ *SynPAM71* cells more Mn is

associated with the membrane fraction overall (Fig. 3.19C, Mn₁ peak) and specifically with PSII monomers, dimers and subcomplexes (Fig. 3.19C, Mn₂ peak). How might the additional Mn be bound to PSII, and can this Mn pool account for the observed decrease in PSII photochemistry? There is normally little, if any, free Mn²⁺ inside the cell [80]. It is therefore unlikely that the accumulation of Mn observed in PSII complexes and in the membrane fraction in Δ SynPAM71 (Fig. 5c) is derived from unbound Mn²⁺. Most of the extra Mn should be bound to protein, most probably to metallochaperones. Indeed, it is conceivable that, during membrane fractionation, Mn bound to metallochaperones might have been released and then trapped by the negative charges of phospholipids, which could (in part) account for the prominent Mn₁ peak (Fig. 3.19C). One candidate for such a metallochaperone is CyanoP, which was found to be overexpressed both in Δ SynPAM71 and WT 20xMn (although to a lesser extent) (Fig. 3.16,3.14) and it resides in the thylakoid lumen presumably attached to the membrane [171]. Δ SynPAM71 cells accumulate over four times as much CyanoP as WT (Fig. 3.16). When the macro-organization of photosynthetic complexes was analyzed by two-dimensional BN/SDS-PAGE separation gel (Fig. 3.17), most of the excess CyanoP was found as the free protein, while the rest was found in a PSII subcomplex together with D2, which accumulates in Δ SynPAM71 (Fig. 3.17). However, if CyanoP could accumulate as free protein in vivo has to be further elucidated since it was reported that CyanoP could be readily solubilized from protein complexes during detergent treatments [172]. The molecular role of CyanoP has been debated, but evidence has been presented for its involvement in the early stages of PSII assembly [76]. Specifically, CyanoP was found in a PSII subcomplex named RCIIa, which contained D2, D1 and PsbO subunits, besides other assembly factors (Knoppova et al., 2016). The current model proposes that CyanoP binds to the luminal side of D2 and CP43, and remains bound to PSII subcomplexes until PsbO takes its place in order to form the final OEC (Cormann et al., 2014; Knoppova et al., 2016). CyanoP is the ancestral form from which the PsbP family of proteins in land plants evolved (Bricker et al., 2013). Notably, it was recently demonstrated that purified PsbP from *Spinacia oleracea* contains two specific Mn²⁺ binding sites in its structure, with one site having a relatively low affinity for Mn²⁺, which would make it a suitable chaperone for Mn donation (Cao et al., 2015). A putative role for PsbP as a metallochaperone for Mn²⁺ storage and subsequent delivery to the newly assembled OEC was therefore suggested (Cao et al., 2015; Schmidt et al., 2016). CyanoP has five potential binding sites for divalent metals (Michoux et al., 2010) making it a promising candidate as a Mn chelator/chaperone.

On the basis of the subcellular localization of SynPAM71 and the phenotype of Δ SynPAM71, a working model can be developed for Mn homeostasis in *Synechocystis*, depicted in Fig.4.1. In this model, SynPAM71 serves to balance the otherwise harmful effects of Mn accumulation in the cytoplasm. It was previously reported that under Mn-sufficient conditions *Synechocystis* stores as much of the Mn as possible in the periplasmic space [80]. The stored Mn is then gradually delivered to cellular sinks for Mn (foremost PSII) and diluted when the cells divide [80]. Therefore, once the cells have established a store of Mn in the periplasmic space, it must be properly delivered to the thylakoid lumen, retained and recycled. Considering that PSII is the major sink for Mn in photosynthetic organisms, Mn homeostasis and PSII assembly and repair (turnover) must be tightly coordinated and regulated. Although still debatable, multiple lines of evidence support the idea that PSII assembly in cyanobacteria is distributed between plasma membrane and thylakoid centers, while PSII repair processes occur primarily in thylakoid membranes [130] [173] [174] [175] [176]. Very little is known about how Mn is delivered, allocated and recycled during these processes. Part of the Mn used in the Mn cluster is delivered to D1 by PratA in thylakoid centers [147]. Whether this is the only mode of delivery of Mn to newly assembled PSII and how the Mn is inserted into the final OEC remains an open question. Furthermore, during repair of photodamaged D1, the core of PSII is partially disassembled together with the OEC, which means dismantling the Mn cluster. How this Mn is sequestered and possibly recycled into a new OEC remains unknown. Considering the data presented in this work, two ways of handling the Mn released from the OEC can be envisioned: 1) It is exported to the cytoplasm and returned to the periplasmic storage pool by SynPAM71, and/or 2) the released Mn²⁺ is bound and neutralized by a Mn chelator/chaperone, perhaps CyanoP, which could possibly sequester it for subsequent reassembly of the OEC during PSII repair. In the absence of SynPAM71, Mn released from PSII accumulates in the cytoplasm and in thylakoids, inducing symptoms of Mn toxicity, which are exacerbated in high-light conditions.

Taken together, the data suggest that SynPAM71 plays a crucial role in Mn homeostasis in *Synechocystis*, most probably involved in the export of Mn²⁺ from the cytoplasm into the periplasmic space, thus mitigating the noxious effects induced by an accumulation of Mn. Intriguingly, a novel role for CyanoP in Mn homeostasis in *Synechocystis* is emerging, which might involve buffering of surplus Mn ions inside the thylakoid lumen.

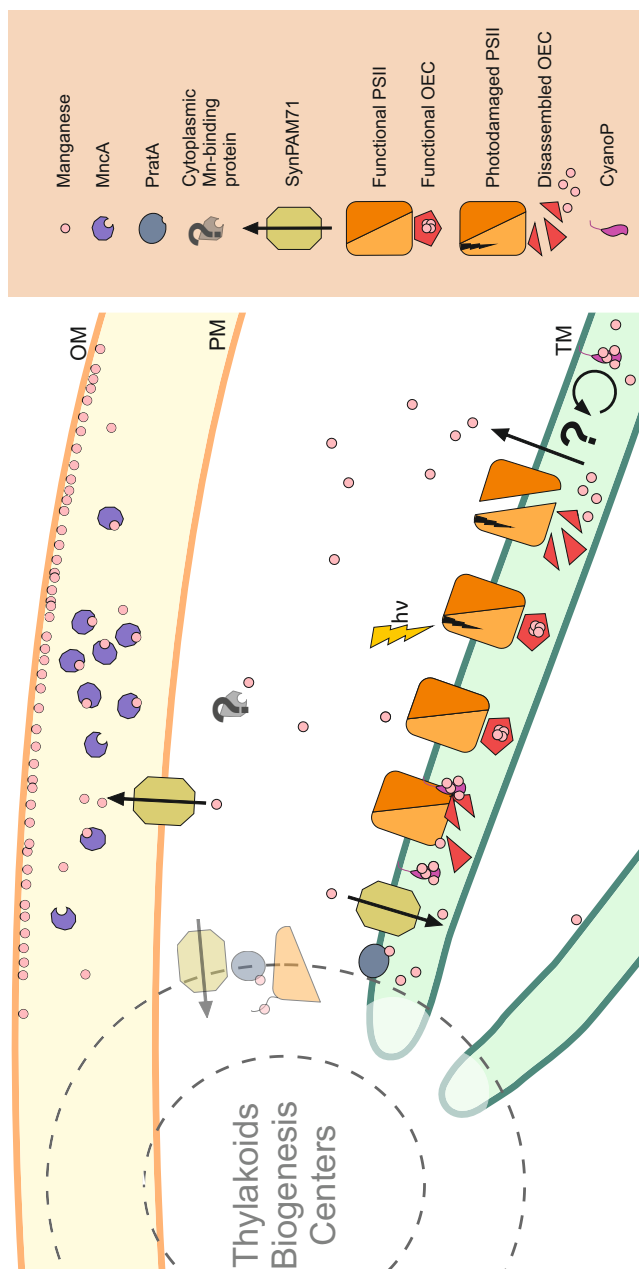


Figure 4.1: Schematic view of Mn homeostasis in *Synechocystis* grown in Mn-sufficient conditions. Mn is stored in the periplasmic space either bound to the outer membrane or to specialized Mn-binding proteins, such as MncA [80]. Mn is delivered to the newly assembled OEC of PSII, which is located in the thylakoid lumen, with the help of PrtA, that pre-load Mn to the D1 precursor (pD1) in the thylakoid biogenesis centers [88]. The final assembly of the OEC Mn cluster occurs into proper thylakoids [177]. CyanoP is known to interact with D2, and remains associate with the new assembled PSII complex until PsbO take its place in the OEC [77] [76]. In this scheme, CyanoP is depicted binding Mn. During repair, the OEC and its Mn cluster are dismantled. The Mn could be recycled inside the thylakoid lumen and/or released into the cytoplasm. SynPAM71 helps preventing the accumulation of Mn into the cytoplasm, delivering Mn back to the periplasmic space or into the lumen. If this process could be mediated by a cytoplasmic Mn-binding protein, as happen for *Atx1* and *Cu²⁺* ions [178], remains to be investigated.

Chapter 5

Conclusion

In the work presented here, in line with the previous works of Viola [37] and Vamvaka [38], *Synechocystis* has been exploited as a synthetic biology chassis to study plant photosynthesis.

Tailor-made vectors and improved transformation efficiency made *Synechocystis* suitable to be used as the final host for heterologous functional complementation with cDNA libraries from *Arabidopsis*. Although further improvements can be pursued, the availability of this method offer an invaluable tool for the isolation of unknown accessory factors involved in the regulation of the plant photosynthetic apparatus. Furthermore, *Synechocystis* $\Delta PsaD$ mutant could be rescued by the *Arabidopsis* homologous protein PsaD. This functional complementation adds another example of the high degree of similarity existing between the photosynthetic machineries of cyanobacteria and plants.

The reconstitution of LHCII from *Arabidopsis* in *Synechocystis* has been attempted by the introduction of an operon carrying the *Arabidopsis* SRP pathway. The ease in handling of the *Synechocystis* chassis allowed the investigation two approaches to integrate the operon in *Synechocystis*. However, the reconstitution of LHCII in *Synechocystis* was unsuccessful. The issue was identified in the partial transcript instability of the operon, probably due to the codon optimization of the Lhcb1 gene. The introduction of a Lhcb1 wild-type DNA sequence which, in contrast with the optimized Lhcb1 sequence, was successfully transcribed in *E. coli*, would be the next step to investigate the LHCII reconstitution in *Synechocystis*. The outcome of complex genetic constructs is difficult to predict. The implementation of new methods for the high-throughput screening of complex genetic constructs (e.g. the *in vitro* transcription-translation cell-free systems in combination with microfluidic devices) would be particularly beneficial to identify the best combination of genetic modules to be subsequently tested *in vivo*.

Last, the characterization of a *Synechocystis* mutant for SynPAM71, a cation transporter involved in Mn homeostasis, highlighted the differences between *Synechocystis* and *Arabidopsis* in Mn transport. A family of five proteins homolog to SynPAM71 has been found in *Arabidopsis*, two of which (PAM71 and PAM71-HL) possess a N-terminal chloroplast target peptide [179]. *Arabidopsis* PAM71, the only protein of this family that has so far been characterized in *Arabidopsis*, is a thylakoid integral membrane protein responsible for the Mn uptake in the lumen. Whether the remaining chloroplast-localized SynPAM71 homolog, PAM71-HL, catalyzes the export of Mn^{2+} from the chloroplast stroma, completing the functions that SynPAM71 alone fulfill in *Synechocystis*, remains to be investigated.

To keep up with the increasing complexity of the biological processes that remain to be investigated of plant photosynthesis, plant scientist must develop new research tools. Despite the challenge, the methods described and discussed here suggested that *Synechocystis* is a valuable chassis to implement SynBio approaches to study plant photosynthesis.

Appendix A

Complete sequence of the synthetic construct used for LHC reconstitution in *Synechocystis*

Names of genes and promoters appearing in the DNA sequence are indicated on the page margins. The CDSs are delimited by yellow highlighted **Start and stop codons**. The RBSs present in the promoters and in front of the genes are underlined. The viral **terminators OOP** are shown in bold. Introduced unique *restriction sites* (*KpnI* at the 5' and *BamHI* at the 3' end of the sequence) are shown in bold and italics.

P_{cpc} **GGTACC**TGGTTCCCTAGGCAACAGTCTTCCCTACCCCACTGGAAACTAAAAAACGA
GAAAAGTTCGCACCGAACATCAATTGCATAATTTTAGCCCTAAACATAAGCTGAACGAA
ACTGGTTGTCTTCCCTTCCCAATCCAGGACAATCTGAGAATCCCCTGCAACATTACTTAA
CAAAAAAGCAGGAATAAAATTAACAAGATGTAACAGACATAAGTCCCATCACCGTTGTAT
AAAGTAACTGTGGGATTGCAAAAGCATTCAAGCCTAGGCGCTGAGCTGTTTGAGCATCC
CGGTGGCCCTTGTCGCTGCCTCCGTGTTTCTCCCTGGATTTATTTAGGTAATATCTCTC
ATAAATCCCCGGGTAGTTAACGAAAGTTAATGGAGATCAGTAACAATAACTCTAGGGTC
ATTACTTTGGACTCCCTCAGTTTATCCGGGGGAATTGTGTTTAAGAAAATCCCAACTCAT
cpSRP43 AAAGTCAAGTAGGAGATTAATTCA**ATG**GCCGCCGTGCAGCGCAATTACGAAGAAACCACC
AGTAGCGTTGAAGAAGCCGAAGAAGACGACGAAAGCAGTTCCTCCTATGGAGAAGTGAAT
AAAATTATTGGCTCCCGGACCGCTGGTGAAGGTGCTATGGAATACTTGATTGAATGGAAA
GATGGTCATTCCCCAGTTGGGTGCCCTCCAGTTATATTGCCGCCGATGTGGTGTCCGAA
TATGAAACTCCCTGGTGGACCGCTGCTCGTAAAGCTGATGAACAAGCCTTAAGTCAATTG
TTAGAAGATCGGGATGTGGATGCCGTGGATGAAAATGGCCGCACCGCCTTGTTATTTGTG
GCCGGCTTGGGTAGTGATAAATGTGTGCGCTTGTTAGCCGAAGCCGGGGCCGATTTAGAT
CATCGTGATATGCGGGGCGGTTTGACCGCCTTACATATGGCCGCCGGCTATGTGCGTCC

CGAAGTGGTGGGAAGCCTTGGTGGGAATTAGGGGCCGATATTGAAGTGGGAAGATGAACGCG
 GCTTGACCGCCTTGGGAATTAGCCCGTGAAATTTTAAAAACCACTCCCAAAGGTAATCCC
 ATGCAATTTGGCCGTCGGATTGGTTTTGGAAAAAGTGATTAACGTGTTGGAAGGGCAAGTG
 TTTGAATATGCCGAAGTGGATGAAATTGTGGAAAAACGTGGGAAAGGCAAAGATGTGGAA
 TATTTGGTGCCTGGAAAGATGGGGGCGATTGTGAATGGGTGAAAGGTGTGCATGTGGCC
 GAAGATGTGGCCAAAGATTATGAAGATGGTTTTGGAATATGCCGTGGCCGAATCCGTGATT
 GGGAAACGTGTGGGTGATGATGGGAAAACCATTGAATACTTGGTGAATGGACCGATATG
 AGTGATGCCACCTGGGAACCCCAAGACAATGTGGATAGCACCTTAGTTCTGTTATACCAG
 CAGCAGCAGCCCATGAATGAA **TAAAGGAGATTAATTC** **ATG** *cpSRP54*
 GTAAAACCGTGGTGGGGCATGGTCGTTATCGGCGTAGTCAAGTGCCTGCTGAAATGTTT
 GGCAGTTGACCGGCGGTTTTAGAAGCCGCCTGGTCCAAATTGAAAGGCGAAGAAGTGTTAA
 CCAAAGATAATATTGCCGAACCCATGCGTGATATTTCGTCGGGCCTTGTTAGAAGCCGATG
 TTAGTTTGGCCGTGGTGCCTCGGTTTTGTGCAATCCGTGAGTGATCAAGCCGTGGGGATGG
 GCGTGATTCGGGGTGTGAAACCCGATCAACAATTTGGTGAATTTGTGCATGATGAATTG
 GTGAAATTTGATGGGCGGCGAAGTGTCCGAATTTGCAATTTGCCAAAAGTGGGCCACCGTG
 ATTTTGTAGCCGGCTTACAAGGTGTGGGAAAACCACCGTGTGTGCCAAATTGGCCTGT
 TACTTGAAAAAACAGGGTAAATCCTGTATGTTGATTGCCGGGGATGTGTATCGCCCCGCC
 GCCATTGATCAATTTGGTGATTTTAGGGGAACAAGTGGGCGTGCCTGTATACCGCTGG
 CACCGATGTGAAACCCGCCGATATTGCCAAACAAGTTTTGAAAGAAGCCAAGAAAAATAA
 TGTGGATGTGGTGATTATGGATACCGCCGTCGTTTTACAAATTGATAAAGGGATGATGGA
 TGAATTGAAAGATGTGAAAAAATTTTTGAATCCCACCGAAGTGTGTTAGTGGTGGATGC
 CATGACCGGCCAAGAAGCCGCCGCTTGGTGACCACCTTTAATGTGGAATTTGGCATTAC
 CGGTGCCATTTTGACCAAATTAGATGGTGATAGTCGGGGTGGGGCCGCCTTATCCGTGAA
 AGAAGTGAGTGGGAAACCCATTAAATTTGGTGGGCCGCGGTGAACGTATGGAAGATTTAGA
 ACCCTTTTATCCCGATCGGATGGCCGGCCGATTTTGGGGATGGGCGATGTGTTATCCTT
 TGTGGAAAAAGCCACCGAAGTGTGCGGCAAGAAGATGCTGAAGATTTGCAAAAAGAAAAT
 TATGAGTGCCAAATTTGATTTTAACGATTTTCTGAAACAAACCCGCGCCGTGGCCAAAAT
 GGGCTCCATGACCCGTGTGTTGGGTATGATTCCCGGTATGGGAAAGTGAGTCCCGCCC
 AAATTCGCGAAGCCGAAAAGAATTTGTTGGTGATGGAAGCCATGATTGAAGTGTGACTC
 CCGAAGAACGTGAACGGCCCGAATTGTTAGCCGAATCCCCGAACCGCGTAAACGGATTG
 CCAAAGATTCCGGGAAAACCGAACAACAAGTGAGTGCCTTGGTGGCCCAAATTTTTCAAA
 TGCGCGTGAAAATGAAAATTTAATGGGCGTGATGGAAGGCGGTTCCATTCCCGCCTTGA
 GTGGCTTAGAAGATGCCTTAAAAGCCGAACAAAAAGCCCCCTCCCGGCACCGCTCGTCGG
 AAACGTAAAGCCGATAGTCGGAAAAAATTTGTGGAATCTGCTTCTTCTAAACCCGGACCC
 CGTGGCTTTGGGAGTGGAAC **TAA** **CAACGCTCGGTTGCCGCCGGGCGTTTTT** *P_{rbc1}*
 TGGACAAAACATCAGGAATTCCTAATTAGAAAAGTCCAAAAATTGTAATTTAAAAAACAGTC
 AATGGAGAGCATTGCCATAAGTAAAGGCATCCCTGCGTGATAAGATTACCTTCAGAAAA
 CAGATAGTTGCTGGGTTATCGCAGATTTTCTCGCAACCAAATAACTGTAATAATAAAC
 TGTCTCTGGGGCGACGGTAGGCTTTATATTGCCAAATTTCCGCCGTGGGAGAAAGCTAGG
 CTATTCAATGTTTATGGAGGACTGACCTAG **ATG** *Lhcb1*
 GTGACTATGCGTAAAACCTGTGGCTAAACCCAAAGGTCCCTCTGGCTCCCCCTGGTATGG

CTCCGATCGGGTGAATATTTAGGCCCTTTAGTGGTGAATCCCCAGTTATTTGACCG
GGGAATTTCCCGGGGATTATGGCTGGGATACCGCCGGCTTATCCGCCGATCCCGAAACC
TTTGCCCGGAATCGCGAATTGGAAGTGATTTCATAGTCGTTGGGCCATGTTGGGTGCCTTA
GGGTGTGTGTTTTCCCGAATTGTTAGCCCCGAATGGGGTGAATTTGGCGAAGCCGTGTG
GTTTAAAGCCGGTTCCCAAATTTTTAGTGATGGCGGTTTGGATTATTTAGGGAATCCCTC
CTTAGTGCATGCCCAAAGTATTTTGGCCATTTGGGCCACCCAAGTGATTTTAATGGGTG
CTGTGGAAGGTTATCGGGTGGCTGGTAATGGGCCCTTGGGCGAAGCCGAAGATTTGTTAT
ATCCCGGGGGCTCCTTTGATCCCTTGGGTTTAGCCACCGATCCCGAAGCCTTTGCCGAAT
TGAAAGTGAAAGAATTGAAAAATGGCCGTTTGGCCATGTTTAGTATGTTTGGCTTTTTCG
TGCAAGCCATTGTGACCGGCAAAGTCCCATTGAAAATTTGGCCGATCATTTAGCCGACC
CCGTGAATAATAATGCCTGGGCTTTTGCCTAACTTTGTTCCCGTAAATAAATGGCC
TCTGAAGTGTTAGGAAGCGGGCGTGTGACTATGCGTAAAACGTGGCTAAACCCAAAGGT
CCCTCTGGCTCCCCCTGGTATGGCTCCGATCGGGTGAATATTTAGGCCCTTTAGTGG
TGAATCCCCCAGTTATTTGACCGGGGAATTTCCCGGGGATTATGGCTGGGATACCGCCGG
CTTATCCGCCGATCCCGAAACCTTTGCCCGGAATCGCGAATTGGAAGTGATTTCATAGTC
GTTGGGCCATGTTGGGTGCCTTAGGGTGTGTGTTTTCCCGAATTGTTAGCCCCGAATGGG
GTGAAATTTGGCGAAGCCGTGTGGTTTAAAGCCGGTTCCCAAATTTTTAGTGATGGCGG
TTTGGATTATTTAGGGAATCCCTCCTTAGTGCATGCCCAAAGTATTTTGGCCATTTGGGC
CACCCAAGTGATTTAATGGGTGCTGTGGAAGGTTATCGGGTGGCTGGTAATGGGCCCTT
GGGCGAAGCCGAAGATTTGTTATATCCCGGGGGCTCCTTTGATCCCTTGGGTTTAGCCAC
CGATCCCGAAGCCTTTGCCGAATTGAAAGTGAAAGAATTGAAAAATGGCCGTTTGGCCAT
GTTTAGTATGTTTGGCTTTTTCTGTCGAAGCCATTGTGACCGGCAAAGGTCCCATTGAAAA
TTTGGCCGATCATTTAGCCGACCCCGTGAATAATAATGCCTGGGCTTTTGCCTAACTT
TGTTCCCGGTAAATAAAGGACTGACCTAGATGTGCTCCGCTGGTCCCTCTGGGTTCTTTA
CTCGGTTGGGTTCGGTTGATTAAGAAAAAGCCAAATCTGATGTTGAAAAAGTGTTTTCC
GGTTTTAGTAAAACCCGGGAAAACCTTGGCCGTGATTGATGAATTGTTGTTGTTTTGGAAC
TTGGCCGAAACCGATCGCGTGTAGATGAATTGGAAGAAGCCTTATTGGTGTCCGATTTT
GGCCCCAAAATTACCGTGCAGATTGTGGAACGGTTACGCGAAGATATTATGAGTGGTAAA
TTGAAATCCGGGAGTGAAATTAAGATGCCTTAAAGAATCCGTGTTGGAATGTTGGCC
AAGAAAAATAGTAAAACCGAATTGCAATTGGGGTTTTCGCAAACCCGCCGTGATTATGATT
GTGGGCGTGAATGGCGGTGGGAAAACCACCAGTTGGATAGTGGCTTTTGTTTTTCCGG
TAAATTAGCCCATCGTTTAAAAACGAAGGCACCAAAGTGTTGATGGCTGCTGGTGATAC
CTTTCGTGCTGCTGCCAGTGATCAATTGGAATTTGGGCCGAACGGACCGGCTGTGAAAT
TGTGGTGGCCGAAGGTGATAAAGCCAAAGCCGCCACCGTGTATCCAAAGCCGTGAAACG
CGGAAAGAAGAAGGCTATGATGTGGTGTATGTGATACCAGTGGCCGTTTGCATACCAA
CTACAGTTTGGATGGAAGAATTGATTGCCTGTAAGAAAGCCGTGGGGAAAATTGTGAGTG
GCGCCCCAACGAAATTTTGTGGTGTGGATGGTAACACCGGGTTAAATATGTTGCC
CAAGCCCGTGAATTTAATGAAGTGGTGGCATTACCGGTTAATTTTGACCAAATTGGAT
GGTAGTGCTCGGGGCGGTTGTGTGGTGTGAGTGTGGTGGGAAGAATTGGGGATTCCCGTGA
TTTATTGGGGTGGGCGAAGCCGTGGAAGACTTACAGCCCTTTGACCCCGAAGCCTTTGTG
AACGCTATTTTTAGTAAACAACGCTCGGTTGCCGCCGGGCGTTTTTCCCATGGAAAAAAC

cpFtsY

P_{psbA2}

GACAATTACAAGAAAGTAAAACCTTATGTCATCTATAAGCTTCGTGTATATTAACCTCCTG
TTACAAAGCTTTACAAAACCTCTCATTAAATCCTTTAGACTAAGTTTAGTCAGTTCCAATCT
GAACATCGACAAATACATAAGGAATTATAACCAAATGTTTAGTCTGAACGAAATTCCGCC *Alb3*
CTTTCACGGGTTAGATAGCAGTGTGGACATTGGTGCCATTTTTACTCGGGCTGAATCCTT
ATTGTATACCATTGCCGATGCCGCCGTGGTGGGCGCCGATAGTGTGGTGACCACCGATAG
TTCCGCCGTGCAAAAATCCGGCGGTTGGTTGGCTTTATTTCCGATGCCATGGAATTGGT
GTTGAAAATTTTTGAAAGATGGCTTGAGTGCCGTGCATGTGCCCTATGCCTATGGGTTTG
CCATTATTTGTAAACCATTATTGTGAAAGCCGCCACCTATCCCTTGACCAAACAACAAG
TGGAATCCACCTTAGCCATGCAAAAATTTGCAACCCAAAATTAAGCCATTCAACAACGGT
ATGCCGGTAATCAAGAACGGATTCAATTGGAACCCAGTCGGTTATATAACAAGCCGGGG
TGAATCCCTTAGCCGGCTGTTTACCCACCTTGGCCACCATTCCCCTGTGGATTGGCTTAT
ATCAAGCCTTGTCCAATGTGGCCAATGAAGGCTTGTTTACCGAAGGCTTTTTCTGGATT
CCTCCTTGGGTGGGCCACCAGTATTGCCGCCCGCAAAGTGGTCCGGTATTTCTGG
TTATTTCCCTTTGTGGATGGTCATCCCCGTTAGGCTGGTATGATACCGTGGCCTATTTG
GTGTTACCCGTGTTATTGATTGCCTCCCAATATGTGTCCATGGAAATTATGAAACCGCC
CCAAACCGATGATCCCGCCAAAAGAATACCTTATTGGTGTTTAAATTTTTACCCTTGAT
GATTGGGTATTTGCCTTGAGTGTGCCCTCCGGTTTATCCATTTATTGGTTGACCAATAA
TGTGTTGTCCACCGCCCAACAAGTGTATTTACGCAAATTGGGTGGCGCCAAACCCAATAT
GGATGAAAATGCCTCCAAAATTATTTCCGCCGGTCGTGCCAAACGGAGTATTGCCCAACC
CGATGATGCCGGCGAACGCTTTCCGGCAATTGAAAGAACAAGAAAAACGGTCCAAAAGAA
TAAAGCCGTGGCCAAAGATACCGTGAATTGGTGAAGAATCCCAAAGTGAATCCGAAGA
AGGGTCCGATGATGAAGAAGAAGAAGCCCGGAAGGTGCCTTAGCCTCCAGTACCACCAG
TAAACCCCTGCCGAAGTGGGTGAGCGGCGGTCTAAACGGAGCAAACGGAAACGGACTGT
GTAA**CAACGCTCGGTTGCCGCCGGGCGTTTTTGGATCC**

Appendix B

Raw data for element analysis in WT and Δ *SynPAM71* *Synechocystis* strains

In the following pages are reported the raw data for element analysis in whole cells and isolated membrane of *Synechocystis* WT and Δ *SynPAM71* mutant and the two-way ANOVA analysis calculated for element ratios of WT and Δ *SynPAM71* *Synechocystis* strains.

Table B.1: Raw data for element analysis in whole cell samples of *Synechocystis* WT and Δ *SynPAM71* mutant. Analysis of total elements in WT and Δ *SynPAM71* whole cells comprising cytoplasm, plasma membrane and thylakoids. Element concentrations are given in μg element g^{-1} protein. The two datasets (#1 and #2) were derived from independent grown cultures of WT and Δ *SynPAM71*. Mean values (\pm SD) were calculated and are highlighted in bold.

Strain	Mg	Ca	Mn	Fe	Cu	Zn
WT #1	286.5	19.3	5.5	17.0	0.8	2.9
	252.2	24.3	1.9	17.1	0.6	2.3
	186.1	21.6	4.2	16.4	0.9	2.0
	252.6	27.0	1.9	18.1	0.6	2.2
	238.6	21.2	4.5	19.0	0.8	2.4
	239.8	23.6	5.0	18.0	0.8	2.2
WT #2	308.5	27.0	2.9	35.3	1.1	3.3
	373.5	19.8	2.3	30.8	1.9	4.8
	330.7	29.2	2.7	34.8	1.0	4.0
WT	274.27 \pm 56.50	23.65 \pm 3.50	3.44 \pm 1.39	22.94 \pm 8.13	0.94 \pm 0.4	2.92 \pm 0.95
Δ <i>SynPAM71</i> #1	220.5	24.5	10.5	21.5	1.0	2.5
	147.6	31.7	4.8	13.4	0.8	1.8
	171.9	33.0	4.3	10.2	0.8	1.8
	180.6	26.6	6.8	11.5	0.7	1.7
	165.1	33.6	5.6	13.3	0.8	1.9
	188.0	28.7	9.9	19.0	0.8	2.0
Δ <i>SynPAM71</i> #2	447.1	33.3	11.0	29.4	0.9	3.5
	405.0	27.9	11.6	24.8	0.9	2.9
	439.0	37.7	11.2	28.5	1.0	3.1
Δ <i>SynPAM71</i>	262.77 \pm 127.71	30.78 \pm 4.15	8.42 \pm 3.00	19.08 \pm 7.37	0.85 \pm 0.09	2.37 \pm 0.68

Table B.2: Raw data for element analysis in isolated membrane fractions of *Synechocystis* WT and Δ SynPAM71 mutant. Analysis of total elements in WT and Δ SynPAM71 membrane fractions comprising plasma membrane and thylakoids. Element concentrations are given in μg element g^{-1} protein. The two datasets (#1 and #2) were derived from independent grown cultures of WT and Δ SynPAM71. Mean values (\pm SD) were calculated and are highlighted in bold.

Strain	Mg	Ca	Mn	Fe	Cu	Zn
WT #1	3458.7	252.9	25.7	421.8	11.0	28.7
	3907.1	203.8	21.1	1262.7	9.0	60.8
	3968.2	630.9	48.1	911.2	23.8	34.5
	2355.5	245.4	14.3	364.8	6.5	19.7
	5324.1	447.2	42.5	733.7	19.2	39.3
	4858.9	314.3	27.3	781.8	16.0	32.7
WT #2	5327.9	121.6	13.6	914.1	9.3	25.3
	6890.1	378.7	10.3	955.8	21.8	41.5
	9124.0	161.9	15.4	1051.8	7.7	27.9
WT	5023.84 \pm 2013.58	306.29 \pm 159.14	24.26 \pm 13.26	821.96 \pm 287.24	13.81 \pm 6.52	34.48 \pm 11.99
Δ SynPAM71 #1	5731.2	642.5	71.7	669.0	12.2	30.3
	4851.2	393.0	41.9	622.5	9.8	48.0
	4713.3	291.8	35.4	524.7	9.4	37.2
	4221.4	311.9	37.2	472.3	7.0	34.2
	6126.7	444.8	58.5	709.0	16.8	50.1
	4532.8	475.0	59.9	977.5	12.6	48.6
Δ SynPAM71 #2	9654.8	241.1	31.9	755.4	9.2	28.0
	5804.1	148.9	25.1	646.5	8.1	20.2
	15415.2	459.7	74.3	750.5	10.6	28.5
Δ SynPAM71	6783.41 \pm 3621.09	378.74 \pm 147.37	48.43 \pm 18.02	680.82 \pm 146.54	10.64 \pm 2.94	36.12 \pm 10.63

Table B.3: ANOVA *P*-values calculated for element ratios in whole cell samples of WT and Δ *SynPAM71* *Synechocystis* strains. Two-way ANOVA analysis is based on data derived from element measurements in whole cells comprising cytoplasm, plasma membrane and thylakoids (Table B.1). Significant differences to a ratio of 'one' of the Δ *SynPAM71* to WT ratios are indicated in bold. SS, sum of squares; MS, mean square.

Element	Source of Variation	SS	df	MS	F	<i>P</i> -value	F crit
Mg	Sampling	553018.44	1	553018.44	103.02	0.00	5.32
	Genotypes	612.35	1	612.35	0.52	0.63	5.32
	Interaction	46051.36	1	46051.36	16.73	0.04	5.32
	Within	72534.66	8	9066.83			
	Total	672216.81	11				
Ca	Sampling	26.45	1	26.45	1.47	0.30	5.32
	Genotypes	161.64	1	161.64	9.65	0.02	5.32
	Interaction	3.25	1	3.25	0.20	0.74	5.32
	Within	138.53	8	17.32			
	Total	329.87	11				
Mn	Sampling	9.49	1	9.49	7.29	0.21	5.32
	Genotypes	104.01	1	104.01	54.82	0.0003	5.32
	Interaction	23.59	1	23.59	14.23	0.02	5.32
	Within	18.75	8	2.34			
	Total	155.85	11				
Fe	Sampling	628.71	1	628.71	93.75	0.00	5.32
	Genotypes	62.88	1	62.88	10.32	0.04	5.32
	Interaction	9.36	1	9.36	1.02	0.44	5.32
	Within	65.25	8	8.16			
	Total	766.20	11				
Cu	Sampling	0.35	1	0.35	4.97	0.06	5.32
	Genotypes	0.11	1	0.11	1.52	0.26	5.32
	Interaction	0.20	1	0.20	2.83	0.14	5.32
	Within	0.56	8	0.07			
	Total	1.20	11				
Zn	Sampling	6.56	1	6.56	34.52	0.00	5.32
	Genotypes	1.18	1	1.18	6.09	0.04	5.32
	Interaction	0.15	1	0.15	0.77	0.42	5.32
	Within	1.59	8	0.20			
	Total	9.49	11				

Table B.4: ANOVA *P*-values calculated for element ratios in isolated membrane fractions of WT and Δ SynPAM71 *Synechocystis* strains. Two-way ANOVA analysis is based on data derived from element measurements in isolated membrane fractions comprising plasma membrane and thylakoids (Table B.2). Significant differences to a ratio of 'one' of the Δ SynPAM71 to WT ratios are indicated in bold. SS, sum of squares; MS, mean square.

Element	Source of Variation	SS	df	MS	F	<i>P</i> -value	F crit
Mg	Sampling	53205060.94	1	53205060.94	7.40	0.03	5.32
	Genotypes	13456552.12	1	13456552.12	1.87	0.21	5.32
	Interaction	3538144.18	1	3538144.18	0.49	0.51	5.32
	Within	57587624.11	8	7198453.01			
	Total	127787381.35	11				
Ca	Sampling	59060.80	1	59060.80	2.70	0.17	5.32
	Genotypes	19505.13	1	19505.13	1.06	0.50	5.32
	Interaction	6652.93	1	6652.93	0.33	0.65	5.32
	Within	176911.17	8	22113.90			
	Total	262130.03	11				
Mn	Sampling	468.39	1	468.39	1.74	0.29	5.32
	Genotypes	1991.21	1	1991.21	7.39	0.04	5.32
	Interaction	125.10	1	125.10	0.45	0.62	5.32
	Within	2213.97	8	276.75			
	Total	4798.67	11				
Fe	Sampling	83167.50	1	83167.50	3.01	0.31	5.32
	Genotypes	103683.62	1	103683.62	3.08	0.22	5.32
	Interaction	38735.22	1	38735.22	1.56	0.46	5.32
	Within	291458.68	8	36432.34			
	Total	517045.02	11				
Cu	Sampling	18.50	1	18.50	0.70	0.56	5.32
	Genotypes	38.22	1	38.22	1.27	0.35	5.32
	Interaction	4.64	1	4.64	0.18	0.72	5.32
	Within	236.95	8	29.62			
	Total	298.31	11				
Zn	Sampling	349.90	1	349.90	4.14	0.16	5.32
	Genotypes	14.59	1	14.59	0.18	0.74	5.32
	Interaction	115.49	1	115.49	1.83	0.33	5.32
	Within	707.41	8	88.43			
	Total	1187.39	11				

Bibliography

- [1] Woodward W Fischer, James Hemp, and Jena E Johnson. Evolution of oxygenic photosynthesis. *Annual Review of Earth and Planetary Sciences*, 44:647–683, 2016.
- [2] John F Allen, Wilson BM de Paula, Sujith Puthiyaveetil, and Jon Nield. A structural phylogenetic map for chloroplast photosynthesis. *Trends in plant science*, 16(12):645–655, 2011.
- [3] Christopher J Howe, Adrian C Barbrook, V Lila Koumandou, R Ellen R Nisbet, Hamish A Symington, and Tom F Wightman. Evolution of the chloroplast genome. *Philosophical Transactions of the Royal Society of London B: Biological Sciences*, 358(1429):99–107, 2003.
- [4] S Blair Hedges, Jaime E Blair, Maria L Venturi, and Jason L Shoe. A molecular timescale of eukaryote evolution and the rise of complex multicellular life. *BMC evolutionary biology*, 4(1):2, 2004.
- [5] Javier A Gimpel, Hussam H Nour-Eldin, Melissa A Scranton, Daphne Li, and Stephen P Mayfield. Refactoring the six-gene photosystem ii core in the chloroplast of the green algae *chlamydomonas reinhardtii*. *ACS synthetic biology*, 5(7):589–596, 2015.
- [6] Peter J Nixon, Matthias Rögner, and Bruce A Diner. Expression of a higher plant *psbA* gene in *Synechocystis* 6803 yields a functional hybrid photosystem ii reaction center complex. *The Plant Cell*, 3(4):383–395, 1991.
- [7] Stefania Viola, Thilo Rühle, and Dario Leister. A single vector-based strategy for marker-less gene replacement in *synechocystis* sp. pcc 6803. *Microbial cell factories*, 13(1):1, 2014.
- [8] Robert E Blankenship. *Molecular mechanisms of photosynthesis*. John Wiley & Sons, 2013.
- [9] J’org Nickelsen and Rengstl Birgit. Photosystem ii assembly: from cyanobacteria to plants. *Annual review of plant biology*, 64:609–635, 2013.
- [10] Poul Erik Jensen and Dario Leister. Cyanobacteria as an experimental platform for modifying bacterial and plant photosynthesis. *Frontiers in bioengineering and biotechnology*, 2:7, 2014.
- [11] Thilo Rühle and Dario Leister. Photosystem ii assembly from scratch. *Frontiers in plant science*, 6, 2015.
- [12] Josef Komenda, Roman Sobotka, and Peter J Nixon. Assembling and maintaining the photosystem ii complex in chloroplasts and cyanobacteria. *Current opinion in plant biology*, 15(3):245–251, 2012.
- [13] Stephen P Long, Amy Marshall-Colon, and Xin-Guang Zhu. Meeting the global food demand of the future by engineering crop photosynthesis and yield potential. *Cell*, 161(1):56–66, 2015.

- [14] Donald R Ort, Sabeeha S Merchant, Jean Alric, Alice Barkan, Robert E Blankenship, Ralph Bock, Roberta Croce, Maureen R Hanson, Julian M Hibberd, Stephen P Long, et al. Redesigning photosynthesis to sustainably meet global food and bioenergy demand. *Proceedings of the National Academy of Sciences*, 112(28):8529–8536, 2015.
- [15] Xin-Guang Zhu, Stephen P Long, and Donald R Ort. What is the maximum efficiency with which photosynthesis can convert solar energy into biomass? *Current opinion in biotechnology*, 19(2):153–159, 2008.
- [16] Xin-Guang Zhu, Stephen P Long, and Donald R Ort. Improving photosynthetic efficiency for greater yield. *Annual review of plant biology*, 61:235–261, 2010.
- [17] Richard G Miller and Steven R Sorrell. The future of oil supply. *Annual review of plant biology*, 2014.
- [18] Parveen Kumar, Diane M Barrett, Michael J Delwiche, and Pieter Stroeve. Methods for pretreatment of lignocellulosic biomass for efficient hydrolysis and biofuel production. *Industrial & engineering chemistry research*, 48(8):3713–3729, 2009.
- [19] Turgay Cakmak, Pinar Angun, Yunus Emre Demiray, Alper Devrim Ozkan, Zeynep Elibol, and Turgay Tekinay. Differential effects of nitrogen and sulfur deprivation on growth and biodiesel feedstock production of *chlamydomonas reinhardtii*. *Biotechnology and bioengineering*, 109(8):1947–1957, 2012.
- [20] Xinyao Liu, Jie Sheng, and Roy Curtiss III. Fatty acid production in genetically modified cyanobacteria. *Proceedings of the National Academy of Sciences*, 108(17):6899–6904, 2011.
- [21] Anjana Srivastava and Ram Prasad. Triglycerides-based diesel fuels. *Renewable and sustainable energy reviews*, 4(2):111–133, 2000.
- [22] Paolo Bombelli, Thomas Müller, Therese W Herling, Christopher J Howe, and Thomas PJ Knowles. A high power-density, mediator-free, microfluidic biophotovoltaic device for cyanobacterial cells. *Advanced energy materials*, 5(2), 2015.
- [23] Kamrul Hasan, Yusuf Dilgin, Sinan Cem Emek, Mojtaba Tavahodi, Hans-Erik Åkerlund, Per-Åke Albertsson, and Lo Gorton. Photoelectrochemical communication between thylakoid membranes and gold electrodes through different quinone derivatives. *ChemElectroChem*, 1(1):131–139, 2014.
- [24] Andreas Mershin, Kazuya Matsumoto, Liselotte Kaiser, Daoyong Yu, Michael Vaughn, Md K Nazeeruddin, Barry D Bruce, Michael Graetzel, and Shuguang Zhang. Self-assembled photosystem-i biophotovoltaics on nanostructured tio₂ and zno. *Scientific reports*, 2, 2012.
- [25] Omer Yehezkeli, Ran Tel-Vered, Julian Wasserman, Alexander Trifonov, Dorit Michaeli, Rachel Nechushtai, and Itamar Willner. Integrated photosystem ii-based photo-bioelectrochemical cells. *Nature communications*, 3:742, 2012.
- [26] Michelle Rasmussen and Shelley D Minteer. Photobioelectrochemistry: solar energy conversion and biofuel production with photosynthetic catalysts. *Journal of The Electrochemical Society*, 161(10):H647–H655, 2014.
- [27] Zhengyan Feng, Botao Zhang, Wona Ding, Xiaodong Liu, Dong-Lei Yang, Pengliang Wei, Fengqiu Cao, Shihua Zhu, Feng Zhang, Yanfei Mao, et al. Efficient genome editing in plants using a crispr/cas system. *Cell research*, 23(10):1229, 2013.
- [28] Michelle Christian, Yiping Qi, Yong Zhang, and Daniel F Voytas. Targeted mutagenesis of *arabidopsis thaliana* using engineered tal effector nucleases. *G3: Genes | Genomes | Genetics*, 3(10):1697–1705, 2013.

- [29] Sylvia De Pater, Leon W Neuteboom, Johan E Pinas, Paul JJ Hooykaas, and Bert J Van Der Zaal. Zfn-induced mutagenesis and gene-targeting in arabidopsis through agrobacterium-mediated floral dip transformation. *Plant biotechnology journal*, 7(8):821–835, 2009.
- [30] Karolin Zerulla, Katharina Ludt, and Jörg Soppa. The ploidy level of *synechocystis* sp. pcc 6803 is highly variable and is influenced by growth phase and by chemical and physical external parameters. *Microbiology*, 162(5):730–739, 2016.
- [31] John GK Williams. [85] construction of specific mutations in photosystem ii photosynthetic reaction center by genetic engineering methods in *synechocystis* 6803. *Methods in enzymology*, 167:766–778, 1988.
- [32] Shawn L Anderson and Lee McIntosh. Light-activated heterotrophic growth of the cyanobacterium *synechocystis* sp. strain pcc 6803: a blue-light-requiring process. *Journal of bacteriology*, 173(9):2761–2767, 1991.
- [33] Hsin-Ho Huang, Daniel Camsund, Peter Lindblad, and Thorsten Heidorn. Design and characterization of molecular tools for a synthetic biology approach towards developing cyanobacterial biotechnology. *Nucleic acids research*, 38(8):2577–2593, 2010.
- [34] Thorsten Heidorn, Daniel Camsund, Hsin-Ho Huang, Pia Lindberg, Paulo Oliveira, Karin Stensjö, and Peter Lindblad. Synthetic biology in cyanobacteria engineering and analyzing novel functions. *Methods in enzymology*, 497:539–579, 2010.
- [35] Hong Xu, Dmitrii Vavilin, and Wim Vermaas. Chlorophyll b can serve as the major pigment in functional photosystem ii complexes of cyanobacteria. *Proceedings of the National Academy of Sciences*, 98(24):14168–14173, 2001.
- [36] Qingfang He, Thomas Schlich, Harald Paulsen, and Wim Vermaas. Expression of a higher plant light-harvesting chlorophyll a/b-binding protein in *synechocystis* sp. pcc 6803. *The FEBS Journal*, 263(2):561–570, 1999.
- [37] Stefania Viola. *Expression of higher plant photosynthetic proteins in the cyanobacterium Synechocystis sp. PCC 6803*. PhD thesis, lmu, 2014.
- [38] Evgenia Vamvaka. *Metabolic engineering of Synechocystis sp. PCC6803 for plant type pigment production, and identification of new splicing factors in Arabidopsis thaliana*. PhD thesis, LMU, 2016.
- [39] Kevin Struhl, John R Cameron, and Ronald W Davis. Functional genetic expression of eukaryotic dna in *escherichia coli*. *Proceedings of the National Academy of Sciences*, 73(5):1471–1475, 1976.
- [40] Stanley N Cohen, Annie CY Chang, Herbert W Boyer, and Robert B Helling. Construction of biologically functional bacterial plasmids in vitro. *Proceedings of the National Academy of Sciences*, 70(11):3240–3244, 1973.
- [41] FRANCTOIS Rougeon and Bernard Mach. Stepwise biosynthesis in vitro of globin genes from globin mrna by dna polymerase of avian myeloblastosis virus. *Proceedings of the National Academy of Sciences*, 73(10):3418–3422, 1976.
- [42] Tom Maniatis, Sim Gek Kee, Argiris Efstratiadis, and Fotis C Kafatos. Amplification and characterization of a β -globin gene synthesized in vitro. *Cell*, 8(2):163–182, 1976.
- [43] TH Rabbitts. Bacterial cloning of plasmids carrying copies of rabbit globin messenger rna. *Nature*, 260:221–225, 1976.
- [44] Ueli Gubler and Beth J Hoffman. A simple and very efficient method for generating cDNA libraries. *Gene*, 25(2):263–269, 1983.

- [45] Peter D Ennis, Jacqueline Zemmour, Russell D Salter, and Peter Parham. Rapid cloning of hla-a, b cDNA by using the polymerase chain reaction: frequency and nature of errors produced in amplification. *Proceedings of the National Academy of Sciences*, 87(7):2833–2837, 1990.
- [46] Piero Carninci, Catrine Kvam, Akiko Kitamura, Tomoya Ohsumi, Yasushi Okazaki, Mitsuteru Itoh, Mamoru Kamiya, Kazuhiro Shibata, Nobuya Sasaki, Masaki Izawa, et al. High-efficiency full-length cDNA cloning by biotinylated cap trapper. *Genomics*, 37(3):327–336, 1996.
- [47] Yutaka Suzuki, Kiyomi Yoshitomo-Nakagawa, Kazuo Maruyama, Akira Suyama, and Sumio Sugano. Construction and characterization of a full length-enriched and a 5′-end-enriched cDNA library. *Gene*, 200(1):149–156, 1997.
- [48] YY Zhu, EM Machleder, A Chenchik, R Li, and PD Siebert. Reverse transcriptase template switching: A SMART approach for full-length cDNA library construction. *Biotechniques*, 30(4):892–897, 2001.
- [49] Joseph Sambrook, Edward F Fritsch, Tom Maniatis, et al. *Molecular cloning*, volume 2. Cold Spring Harbor Laboratory Press New York, 1989.
- [50] Stephen J Elledge, John T Mulligan, Sandra W Ramer, Matthew Spottswood, and Ronald W Davis. Lambda yes: a multifunctional cDNA expression vector for the isolation of genes by complementation of yeast and *Escherichia coli* mutations. *Proceedings of the National Academy of Sciences*, 88(5):1731–1735, 1991.
- [51] Lan-Ying Lee, Fu-Hui Wu, Chen-Tran Hsu, Shu-Chen Shen, Hsuan-Yu Yeh, De-Chih Liao, Mei-Jane Fang, Nien-Tze Liu, Yu-Chen Yen, Ladislav Dokládál, et al. Screening a cDNA library for protein–protein interactions directly in planta. *The Plant Cell*, 24(5):1746–1759, 2012.
- [52] Fu-Hui Wu, Shu-Chen Shen, Lan-Ying Lee, Shu-Hong Lee, Ming-Tsar Chan, and Choun-Sea Lin. Tape-arabidopsis sandwich—a simpler arabidopsis protoplast isolation method. *Plant methods*, 5(1):16, 2009.
- [53] Dariusz M Niedzwiedzki and Robert E Blankenship. Singlet and triplet excited state properties of natural chlorophylls and bacteriochlorophylls. *Photosynthesis research*, 106(3):227–238, 2010.
- [54] Stefan Jansson. The light-harvesting chlorophyll a/b-binding proteins. *Biochimica et Biophysica Acta (BBA)-Bioenergetics*, 1184(1):1–19, 1994.
- [55] Grzegorz Jackowski, Karol Kacprzak, and Stefan Jansson. Identification of lhcb1/lhcb2/lhcb3 heterotrimers of the main light-harvesting chlorophyll a/b-protein complex of photosystem II (LHC II). *Biochimica et Biophysica Acta (BBA)-Bioenergetics*, 1504(2):340–345, 2001.
- [56] Ralph L Henry. Srp: adapting to life in the chloroplast. *Nature structural & molecular biology*, 17(6):676–677, 2010.
- [57] Danja Schuenemann, Shalini Gupta, Fabienne Persello-Cartieaux, Victor I Klimyuk, Jonathan DG Jones, Laurent Nussaume, and Neil E Hoffman. A novel signal recognition particle targets light-harvesting proteins to the thylakoid membranes. *Proceedings of the National Academy of Sciences*, 95(17):10312–10316, 1998.
- [58] Christiane Reinbothe, Sandra Bartsch, Laura L Eggink, J Kenneth Hooper, Judy Bruslan, Ricardo Andrade-Paz, Julie Monnet, and Steffen Reinbothe. A role for chlorophyllide a oxygenase in the regulated import and stabilization of light-harvesting chlorophyll a/b proteins. *Proceedings of the National Academy of Sciences of the United States of America*, 103(12):4777–4782, 2006.

- [59] Victor I Klimyuk, Fabienne Persello-Cartieaux, Michel Havaux, Pascale Contard-David, Danja Schuenemann, Karin Meierhoff, Patrice Gouet, Jonathan DG Jones, Neil E Hoffman, and Laurent Nussaume. A chromodomain protein encoded by the arabidopsis *cao* gene is a plant-specific component of the chloroplast signal recognition particle pathway that is involved in lhcp targeting. *The Plant Cell*, 11(1):87–99, 1999.
- [60] Annemarie Horn, Janosch Hennig, Yasar L Ahmed, Gunter Stier, Klemens Wild, Michael Sattler, and Irmgard Sinning. Structural basis for *cpsrp43* chromodomain selectivity and dynamics in *alb3* insertase interaction. *Nature communications*, 6:8875–8875, 2014.
- [61] Min Ouyang, Xiaoyi Li, Jinfang Ma, Wei Chi, Jianwei Xiao, Meijuan Zou, Fan Chen, Congming Lu, and Lixin Zhang. *Ltd* is a protein required for sorting light-harvesting chlorophyll-binding proteins to the chloroplast *srp* pathway. *Nature communications*, 2:277, 2011.
- [62] Sebastian Falk, Stephanie Ravaud, Joachim Koch, and Irmgard Sinning. The c terminus of the *alb3* membrane insertase recruits *cpsrp43* to the thylakoid membrane. *Journal of Biological Chemistry*, 285(8):5954–5962, 2010.
- [63] Peera Jaru-Ampornpan, Kuang Shen, Vinh Q Lam, Mona Ali, Sebastian Doniach, Tony Z Jia, and Shu-ou Shan. Atp-independent reversal of a membrane protein aggregate by a chloroplast *srp* subunit. *Nature structural & molecular biology*, 17(6):696–702, 2010.
- [64] Katharina F Stengel, Iris Holdermann, Peter Cain, Colin Robinson, Klemens Wild, and Irmgard Sinning. Structural basis for specific substrate recognition by the chloroplast signal recognition particle protein *cpsrp43*. *Science*, 321(5886):253–256, 2008.
- [65] Chao-Jung Tu, Danja Schuenemann, and Neil E Hoffman. Chloroplast *fts*, chloroplast signal recognition particle, and *gtp* are required to reconstitute the soluble phase of light-harvesting chlorophyll protein transport into thylakoid membranes. *Journal of Biological Chemistry*, 274(38):27219–27224, 1999.
- [66] Zhenfeng Liu, Hanchi Yan, Kebin Wang, Tingyun Kuang, Jiping Zhang, Lulu Gui, Xiaomin An, and Wenrui Chang. Crystal structure of spinach major light-harvesting complex at 2.72 Å resolution. *Nature*, 428(6980):287–292, 2004.
- [67] H Paulsen, U Rüdiger, and W Rüdiger. Reconstitution of pigment-containing complexes from light-harvesting chlorophyll a/b-binding protein overexpressed in *escherichia coli*. *Planta*, 181(2):204–211, 1990.
- [68] Ruth Horn and Harald Paulsen. Early steps in the assembly of light-harvesting chlorophyll a/b complex time-resolved fluorescence measurements. *Journal of Biological Chemistry*, 279(43):44400–44406, 2004.
- [69] Cromwell E Espineda, Alicia S Linford, Domenica Devine, and Judy A Brusslan. The *atca* gene, encoding chlorophyll a oxygenase, is required for chlorophyll b synthesis in arabidopsis thaliana. *Proceedings of the National Academy of Sciences*, 96(18):10507–10511, 1999.
- [70] Luca Dall’Osto, Mauro Bressan, and Roberto Bassi. Biogenesis of light harvesting proteins. *Biochimica et Biophysica Acta (BBA)-Bioenergetics*, 1847(9):861–871, 2015.
- [71] Sabine Steiger, Lutz Schäfer, and Gerhard Sandmann. High-light-dependent up-regulation of carotenoids and their antioxidative properties in the cyanobacterium *synechocystis pcc 6803*. *Journal of Photochemistry and Photobiology B: Biology*, 52(1):14–18, 1999.

- [72] Soichirou Satoh, Masahiko Ikeuchi, Mamoru Mimuro, and Ayumi Tanaka. Chlorophyll b expressed in cyanobacteria functions as a light-harvesting antenna in photosystem i through flexibility of the proteins. *Journal of Biological Chemistry*, 276(6):4293–4297, 2001.
- [73] Luca Dall’Osto, Chiara Lico, Jean Alric, Giovanni Giuliano, Michel Havaux, and Roberto Bassi. Lutein is needed for efficient chlorophyll triplet quenching in the major Lhci antenna complex of higher plants and effective photoprotection in vivo under strong light. *BMC Plant Biology*, 6(1):32, 2006.
- [74] Kentaro Ifuku and Takumi Noguchi. Structural coupling of extrinsic proteins with the oxygen-evolving center in photosystem ii. *Frontiers in plant science*, 7, 2016.
- [75] Yasufumi Umena, Keisuke Kawakami, Jian-Ren Shen, and Nobuo Kamiya. Crystal structure of oxygen-evolving photosystem ii at a resolution of 1.9 Å. *Nature*, 473(7345):55–60, 2011.
- [76] Jana Knoppová, Jianfeng Yu, Peter Konik, Peter J Nixon, and Josef Komenda. Cyanop is involved in the early steps of photosystem ii assembly in the cyanobacterium *synechocystis* sp. pcc 6803. *Plant and Cell Physiology*, 57(9):1921–1931, 2016.
- [77] Kai U Cormann, Maik Bartsch, Matthias Rögner, and Marc M Nowaczyk. Localization of the cyanop binding site on photosystem ii by surface plasmon resonance spectroscopy. *Frontiers in plant science*, 5:595, 2014.
- [78] Johnna L Roose, Yasuhiro Kashino, and Himadri B Pakrasi. The psbq protein defines cyanobacterial photosystem ii complexes with highest activity and stability. *Proceedings of the National Academy of Sciences*, 104(7):2548–2553, 2007.
- [79] Leeann E Thornton, Hiroshi Ohkawa, Johnna L Roose, Yasuhiro Kashino, Nir Keren, and Himadri B Pakrasi. Homologs of plant psbp and psbq proteins are necessary for regulation of photosystem ii activity in the cyanobacterium *synechocystis* 6803. *The Plant Cell*, 16(8):2164–2175, 2004.
- [80] Nir Keren, Matthew J Kidd, James E Penner-Hahn, and Himadri B Pakrasi. A light-dependent mechanism for massive accumulation of manganese in the photosynthetic bacterium *synechocystis* sp. pcc 6803. *Biochemistry*, 41(50):15085–15092, 2002.
- [81] Andrew W Foster, Deenah Osman, and Nigel J Robinson. Metal preferences and metallation. *Journal of biological chemistry*, 289(41):28095–28103, 2014.
- [82] Steve Tottey, Kevin J Waldron, Susan J Firbank, Brian Reale, Conrad Bessant, Katsuko Sato, Timothy R Cheek, Joe Gray, Mark J Banfield, Christopher Dennison, et al. Protein-folding location can regulate manganese-binding versus copper-or zinc-binding. *Nature*, 455(7216):1138–1142, 2008.
- [83] Victor V Bartsevich and HB Pakrasi. Molecular identification of an abc transporter complex for manganese: analysis of a cyanobacterial mutant strain impaired in the photosynthetic oxygen evolution process. *The EMBO journal*, 14(9):1845, 1995.
- [84] Victor V Bartsevich and Himadri B Pakrasi. Manganese transport in the cyanobacterium *synechocystis* sp. pcc 6803. *Journal of Biological Chemistry*, 271(42):26057–26061, 1996.
- [85] Katsushi Yamaguchi, Iwane Suzuki, Hiroshi Yamamoto, Alexander Lyukevich, Irina Bodrova, Dmitry A Los, Irina Piven, Vladislav Zinchenko, Minoru Kanehisa, and Norio Murata. A two-component mn²⁺-sensing system negatively regulates expression of the mntcab operon in *synechocystis*. *The Plant Cell*, 14(11):2901–2913, 2002.
- [86] Teruo Ogawa, Ding Hui Bao, Hirokazu Katoh, Mari Shibata, Himadri B Pakrasi, and Maitrayee Bhattacharyya-Pakrasi. A two-component signal transduction pathway

- regulates manganese homeostasis in *synechocystis* 6803, a photosynthetic organism. *Journal of Biological Chemistry*, 277(32):28981–28986, 2002.
- [87] Leeann E Chandler, Victor V Bartsevich, and Himadri B Pakrasi. Regulation of manganese uptake in *synechocystis* 6803 by *rfra*, a member of a novel family of proteins containing a repeated five-residues domain. *Biochemistry*, 42(18):5508–5514, 2003.
- [88] Anna Stengel, Irene L Gügel, Daniel Hilger, Birgit Rengstl, Heinrich Jung, and Jörg Nickelsen. Initial steps of photosystem ii de novo assembly and preloading with manganese take place in biogenesis centers in *synechocystis*. *The Plant Cell*, 24(2):660–675, 2012.
- [89] Anja Schneider, Iris Steinberger, Andrei Herdean, Chiara Gandini, Marion Eisenhut, Samantha Kurz, Anna Morper, Natalie Hoecker, Thilo Rühle, Ulf Ingo Flügge, et al. The evolutionarily conserved protein photosynthesis affected mutant71 is required for efficient manganese uptake at the thylakoid membrane in *arabidopsis*. *The Plant Cell*, pages tpc-00812, 2016.
- [90] Chao Wang, Weitao Xu, Honglei Jin, Taijie Zhang, Jianbin Lai, Xuan Zhou, Shengchun Zhang, Shengjie Liu, Xuewu Duan, Hongbin Wang, et al. A putative chloroplast-localized ca^{2+}/h^{+} antiporter *ccha1* is involved in calcium and ph homeostasis and required for *psii* function in *arabidopsis*. *Molecular Plant*, 9(8):1183–1196, 2016.
- [91] Didier Demaegd, François Foulquier, Anne-Sophie Colinet, Louis Gremillon, Dominique Legrand, Pascal Mariot, Edgar Peiter, Emile Van Schaftingen, Gert Matthijs, and Pierre Morsomme. Newly characterized golgi-localized family of proteins is involved in calcium and ph homeostasis in yeast and human cells. *Proceedings of the National Academy of Sciences*, 110(17):6859–6864, 2013.
- [92] Sven Potelle, Willy Morelle, Eudoxie Dulary, Sandrine Duvet, Dorothée Vicogne, Corentin Spriet, Marie-Ange Krzewinski-Recchi, Pierre Morsomme, Jaak Jaeken, Gert Matthijs, et al. Glycosylation abnormalities in *gdt1p/tmem165* deficient cells result from a defect in golgi manganese homeostasis. *Human molecular genetics*, page ddw026, 2016.
- [93] Anika Wiegard, Anja K Dörrich, Hans-Tobias Deinzer, Christian Beck, Annegret Wilde, Julia Holtzendorff, and Ilka M Axmann. Biochemical analysis of three putative kaic clock proteins from *synechocystis* sp. pcc 6803 suggests their functional divergence. *Microbiology*, 159(5):948–958, 2013.
- [94] Werner Pansegrau, Erich Lanka, Peter T Barth, David H Figurski, Donald G Guiney, Dieter Haas, Donald R Helinski, Helmut Schwab, Vilma A Stanisich, and Christopher M Thomas. Complete nucleotide sequence of birmingham *incpα* plasmids: compilation and comparative analysis. *Journal of molecular biology*, 239(5):623–663, 1994.
- [95] David Swarbreck, Christopher Wilks, Philippe Lamesch, Tanya Z Berardini, Margarita Garcia-Hernandez, Hartmut Foerster, Donghui Li, Tom Meyer, Robert Muller, Larry Ploetz, et al. The *arabidopsis* information resource (*tair*): gene structure and function annotation. *Nucleic acids research*, 36(suppl 1):D1009–D1014, 2008.
- [96] Joseph C Kamalay and Robert B Goldberg. Regulation of structural gene expression in tobacco. *Cell*, 19(4):935–946, 1980.
- [97] Eric H Davidson and Roy J Britten. Regulation of gene expression: possible role of repetitive sequences. *Science*, 204(4397):1052–1059, 1979.

- [98] Piero Carninci, Yuko Shibata, Norihito Hayatsu, Yuichi Sugahara, Kazuhiro Shibata, Masayoshi Itoh, Hideaki Konno, Yasushi Okazaki, Masami Muramatsu, and Yoshihide Hayashizaki. Normalization and subtraction of cap-trapper-selected cdnas to prepare full-length cdna libraries for rapid discovery of new genes. *Genome Research*, 10(10):1617–1630, 2000.
- [99] Rosmarie Rippka, Josette Deruelles, John B Waterbury, Michael Herdman, and Roger Y Stanier. Generic assignments, strain histories and properties of pure cultures of cyanobacteria. *Microbiology*, 111(1):1–61, 1979.
- [100] Daniel Tillett and Brett A Neilan. Xanthogenate nucleic acid isolation from cultured and environmental cyanobacteria. *Journal of Phycology*, 36(1):251–258, 2000.
- [101] Carola Engler, Ramona Gruetzner, Romy Kandzia, and Sylvestre Marillonnet. Golden gate shuffling: a one-pot dna shuffling method based on type iis restriction enzymes. *PLoS one*, 4(5):e5553, 2009.
- [102] YP Cai and C PETER Wolk. Use of a conditionally lethal gene in anabaena sp. strain pcc 7120 to select for double recombinants and to entrap insertion sequences. *Journal of Bacteriology*, 172(6):3138–3145, 1990.
- [103] VV Zinchenko, IV Piven, VA Melnik, and SV Shestakov. Vectors for the complementation analysis of cyanobacterial mutants. *RUSSIAN JOURNAL OF GENETICS C/C OF GENETIKA*, 35:228–232, 1999.
- [104] Tomáš Zavřel, Maria A Sinetova, Jan Červený, et al. Measurement of chlorophyll a and carotenoids concentration in cyanobacteria. *Bio-protocol*, 5:e1467, 2015.
- [105] Alan R Wellburn. The spectral determination of chlorophylls a and b, as well as total carotenoids, using various solvents with spectrophotometers of different resolution. *Journal of plant physiology*, 144(3):307–313, 1994.
- [106] Carl R Merrill, David Goldman, and Margaret L Van Keuren. [17] silver staining methods for polyacrylamide gel electrophoresis. *Methods in enzymology*, 96:230–239, 1983.
- [107] Thomas Hesselhøj Hansen, Thomas Christian de Bang, Kristian Holst Laursen, Paj Pedas, Søren Husted, and Jan Kofod Schjørring. Multielement plant tissue analysis using icp spectrometry. *Plant Mineral Nutrients: Methods and Protocols*, pages 121–141, 2013.
- [108] John M Grange, KR Fox, and Neil L Morgan. *Genetic manipulation: techniques and applications*. John Wiley & Sons, 2009.
- [109] Ronald D Porter. Transformation in cyanobacteria. *CRC Critical reviews in microbiology*, 13(2):111–132, 1986.
- [110] F Chauvat, P Rouet, H Bottin, and A Boussac. Mutagenesis by random cloning of an escherichia coli kanamycin resistance gene into the genome of the cyanobacterium synechocystis pcc 6803: selection of mutants defective in photosynthesis. *Molecular and General Genetics MGG*, 216(1):51–59, 1989.
- [111] Galyna I Kufryk, Monika Sachet, Georg Schmetterer, and Wim FJ Vermaas. Transformation of the cyanobacterium synechocystis sp. pcc 6803 as a tool for genetic mapping: optimization of efficiency. *FEMS microbiology letters*, 206(2):215–219, 2002.
- [112] Larry Snyder, Joseph E Peters, Tina M Henkin, and Wendy Champness. *Molecular genetics of bacteria*. American Society of Microbiology, 2013.
- [113] Keith M Derbyshire, Graham Hatfull, and Neil Willetts. Mobilization of the non-conjugative plasmid rsf1010: a genetic and dna sequence analysis of the mobilization region. *Molecular and General Genetics MGG*, 206(1):161–168, 1987.

- [114] MegaX DH10 T1R Electrocompetent Cells Thermo Fisher Scientific.
- [115] Richard J Reece. *Analysis of genes and genomes*. John Wiley & Sons Hoboken, NJ, 2004.
- [116] Sabine Kreps, Fabrice Ferino, Christine Mosrin, Jozef Gerits, Max Mergeay, and Pierre Thuriaux. Conjugative transfer and autonomous replication of a promiscuous incq plasmid in the cyanobacterium *synechocystis* pcc 6803. *Molecular and General Genetics MGG*, 221(1):129–133, 1990.
- [117] Honda Yoichi, Sakai Hiroshi, and Komano Tohru. Two single-strand dna initiation signals located in the oriv region of plasmid rsf1010. *Gene*, 68(2):221–228, 1988.
- [118] Enrico Peter, Annabel Salinas, Thomas Wallner, Danny Jeske, Dennis Dienst, Anegret Wilde, and Bernhard Grimm. Differential requirement of two homologous proteins encoded by *sll1214* and *sll1874* for the reaction of mg protoporphyrin monomethylester oxidative cyclase under aerobic and micro-oxic growth conditions. *Biochimica et Biophysica Acta (BBA)-Bioenergetics*, 1787(12):1458–1467, 2009.
- [119] Irena Lisitsky, Petra Klaff, and Gadi Schuster. Addition of destabilizing poly (a)-rich sequences to endonuclease cleavage sites during the degradation of chloroplast mrna. *Proceedings of the National Academy of Sciences*, 93(23):13398–13403, 1996.
- [120] Parag R Chitnis, Patricia A Reilly, and Nathan Nelson. Insertional inactivation of the gene encoding subunit ii of photosystem i from the cyanobacterium *synechocystis* sp. pcc 6803. *Journal of Biological Chemistry*, 264(31):18381–18385, 1989.
- [121] Svetlana Ermakova-Gerdes and Wim Vermaas. Inactivation of the open reading frame *slr0399* in *synechocystis* sp. pcc 6803 functionally complements mutations near the *qa* niche of photosystem ii a possible role of *slr0399* as a chaperone for quinone binding. *Journal of Biological Chemistry*, 274(43):30540–30549, 1999.
- [122] Galyna I Kufryk and Wim FJ Vermaas. *Sll1717* affects the redox state of the plastoquinone pool by modulating quinol oxidase activity in thylakoids. *Journal of bacteriology*, 188(4):1286–1294, 2006.
- [123] Galyna I Kufryk and Wim FJ Vermaas. *Slr2013* is a novel protein regulating functional assembly of photosystem ii in *synechocystis* sp. strain pcc 6803. *Journal of bacteriology*, 185(22):6615–6623, 2003.
- [124] Galyna I Kufryk and Wim FJ Vermaas. A novel protein involved in the functional assembly of the oxygen-evolving complex of photosystem ii in *synechocystis* sp. pcc 6803. *Biochemistry*, 40(31):9247–9255, 2001.
- [125] Tina C Summerfield, Julian J Eaton-Rye, and Louis A Sherman. Global gene expression of a δ psbo: δ psbu mutant and a spontaneous revertant in the cyanobacterium *synechocystis* sp. strain pcc 6803. *Photosynthesis research*, 94(2-3):265–274, 2007.
- [126] Hadar Kless and Wim Vermaas. Tandem sequence duplications functionally complement deletions in the *d1* protein of photosystem ii. *Journal of Biological Chemistry*, 270(28):16536–16541, 1995.
- [127] Takafumi Midorikawa, Rei Narikawa, and Masahiko Ikeuchi. A deletion mutation in the spacing within the *psaa* core promoter enhances transcription in a cyanobacterium *synechocystis* sp. pcc 6803. *Plant and Cell Physiology*, 53(1):164–172, 2012.
- [128] Tanya Z Berardini, Leonore Reiser, Donghui Li, Yarik Mezheritsky, Robert Muller, Emily Strait, and Eva Huala. The arabidopsis information resource: making and mining the gold standard annotated reference plant genome. *genesis*, 53(8):474–485, 2015.

- [129] Josef Komenda, Jörg Nickelsen, Martin Tichý, Ondřej Prášil, Lutz A Eichacker, and Peter J Nixon. The cyanobacterial homologue of hcf136/ycf48 is a component of an early photosystem ii assembly complex and is important for both the efficient assembly and repair of photosystem ii in *synechocystis* sp. pcc 6803. *Journal of Biological Chemistry*, 283(33):22390–22399, 2008.
- [130] Steffen Heinz, Anna Rast, Lin Shao, Andrian Gutu, Irene L Gügel, Eiri Heyno, Birgit Rengstl, Stefania Viola, Marc M Nowaczyk, Dario Leister, et al. Thylakoid membrane architecture in *synechocystis* depends on curt, a homolog of the granal curvature thylakoid1 proteins. *The Plant Cell*, pages tpc-00491, 2016.
- [131] Ute Armbruster, Mathias Pribil, Stefania Viola, Wenteng Xu, Michael Scharfenberg, Alexander P Hertle, Ulrike Rojahn, Poul Erik Jensen, Fabrice Rappaport, Pierre Joliot, et al. Arabidopsis curvature thylakoid1 proteins modify thylakoid architecture by inducing membrane curvature. *The Plant Cell*, 25(7):2661–2678, 2013.
- [132] Marco Schottkowski, Janina Ratke, Ulrike Oster, Marc Nowaczyk, and Jörg Nickelsen. Pitt, a novel tetratricopeptide repeat protein involved in light-dependent chlorophyll biosynthesis and thylakoid membrane biogenesis in *synechocystis* sp. pcc 6803. *Molecular plant*, 2(6):1289–1297, 2009.
- [133] ChloroP 1.1 Server. <http://www.cbs.dtu.dk/services/ChloroP/>. Accessed: 2017-02-15.
- [134] Bo Wang, Jiangxin Wang, Weiwen Zhang, and Deirdre R Meldrum. Application of synthetic biology in cyanobacteria and algae. *Front Microbiol*, 3(344):344, 2012.
- [135] Matthew R Groves, Alexandra Mant, Audrey Kuhn, Joachim Koch, Stefan Dübel, Colin Robinson, and Irmgard Sinning. Functional characterization of recombinant chloroplast signal recognition particle. *Journal of Biological Chemistry*, 276(30):27778–27786, 2001.
- [136] Didier Demaegd, Anne-Sophie Colinet, Antoine Deschamps, and Pierre Morsomme. Molecular evolution of a novel family of putative calcium transporters. *PloS one*, 9(6):e100851, 2014.
- [137] TMHMM Server v. 2.0. <http://www.cbs.dtu.dk/services/TMHMM/>. Accessed: 2017-02-15.
- [138] Mirkka Herranen, Natalia Battchikova, Pengpeng Zhang, Alexander Graf, Sari Sirpiö, Virpi Paakkarinen, and Eva-Mari Aro. Towards functional proteomics of membrane protein complexes in *synechocystis* sp. pcc 6803. *Plant Physiology*, 134(1):470–481, 2004.
- [139] Lawrence B Smart, SL Anderson, and L McIntosh. Targeted genetic inactivation of the photosystem i reaction center in the cyanobacterium *synechocystis* sp. pcc 6803. *The EMBO journal*, 10(11):3289, 1991.
- [140] Sidsel Birkelund Schmidt, Daniel Pergament Persson, Marta Powikrowska, Jens Frydenvang, Jan K Schjoerring, Poul Erik Jensen, and Søren Husted. Metal binding in photosystem ii super-and subcomplexes from barley thylakoids. *Plant physiology*, 168(4):1490–1502, 2015.
- [141] John A Raven, Michael CW Evans, and Rebecca E Korb. The role of trace metals in photosynthetic electron transport in o₂-evolving organisms. *Photosynthesis Research*, 60(2-3):111–150, 1999.
- [142] Natalia Battchikova, Marion Eisenhut, and Eva-Mari Aro. Cyanobacterial ndh-1 complexes: novel insights and remaining puzzles. *Biochimica et Biophysica Acta (BBA)-Bioenergetics*, 1807(8):935–944, 2011.

- [143] Fang Huang, Ingela Parmryd, Fredrik Nilsson, Annika L Persson, Himadri B Pakrasi, Bertil Andersson, and Birgitta Norling. Proteomics of *synechocystis* sp. strain pcc 6803 identification of plasma membrane proteins. *Molecular & Cellular Proteomics*, 1(12):956–966, 2002.
- [144] Tatiana Pisareva, Joseph Kwon, Jihyun Oh, Soohyun Kim, Changrong Ge, Åke Wieslander, Jong-Soon Choi, and Birgitta Norling. Model for membrane organization and protein sorting in the cyanobacterium *synechocystis* sp. pcc 6803 inferred from proteomics and multivariate sequence analyses. *Journal of proteome research*, 10(8):3617–3631, 2011.
- [145] Michelle Liberton, Rajib Saha, Jon M Jacobs, Amelia Y Nguyen, Marina A Gritsenko, Richard D Smith, David W Koppelaar, and Himadri B Pakrasi. Global proteomic analysis reveals an exclusive role of thylakoid membranes in bioenergetics of a model cyanobacterium. *Molecular & Cellular Proteomics*, 15(6):2021–2032, 2016.
- [146] Tatsuo Omata and Norio Murata. Electron-transport reactions in cytoplasmic and thylakoid membranes prepared from the cyanobacteria (blue-green algae) *anacystis nidulans* and *synechocystis* pcc 6714. *Biochimica et Biophysica Acta (BBA)-Bioenergetics*, 810(3):354–361, 1985.
- [147] Birgit Rengstl, Ulrike Oster, Anna Stengel, and Jörg Nickelsen. An intermediate membrane subfraction in cyanobacteria is involved in an assembly network for photosystem ii biogenesis. *Journal of Biological Chemistry*, 286(24):21944–21951, 2011.
- [148] Prakitchai Chotewutmontri and Alice Barkan. Dynamics of chloroplast translation during chloroplast differentiation in maize. *PLoS Genet*, 12(7):e1006106, 2016.
- [149] Yi Shao, Lihui Feng, Steven T Rutherford, Kai Papenfort, and Bonnie L Bassler. Functional determinants of the quorum-sensing non-coding rnas and their roles in target regulation. *The EMBO journal*, 32(15):2158–2171, 2013.
- [150] Alex S Shcheglov, Pavel A Zhulidov, Ekaterina A Bogdanova, and Dmitry A Shagin. Normalization of cDNA libraries. In *Nucleic Acids Hybridization Modern Applications*, pages 97–124. Springer, 2007.
- [151] Pavel A Zhulidov, Ekaterina A Bogdanova, Alex S Shcheglov, Laura L Vagner, George L Khaspekov, Valery B Kozhemyako, Mikhail V Matz, Ella Meleshkevitch, Leonid L Moroz, Sergey A Lukyanov, et al. Simple cDNA normalization using kamchatka crab duplex-specific nuclease. *Nucleic acids research*, 32(3):e37–e37, 2004.
- [152] Maarten H de Smit and J Van Duin. Secondary structure of the ribosome binding site determines translational efficiency: a quantitative analysis. *Proceedings of the National Academy of Sciences*, 87(19):7668–7672, 1990.
- [153] Daniel Camsund and Peter Lindblad. Engineered transcriptional systems for cyanobacterial biotechnology. *Frontiers in bioengineering and biotechnology*, 2:40, 2014.
- [154] Vivek K Mutalik, Joao C Guimaraes, Guillaume Cambray, Quynh-Anh Mai, Marc Juul Christoffersen, Lance Martin, Ayumi Yu, Colin Lam, Cesar Rodriguez, Gaymon Bennett, et al. Quantitative estimation of activity and quality for collections of functional genetic elements. *Nature methods*, 10(4):347–353, 2013.
- [155] Chunbo Lou, Brynne Stanton, Ying-Ja Chen, Brian Munsky, and Christopher A Voigt. Ribozyme-based insulator parts buffer synthetic circuits from genetic context. *Nature biotechnology*, 30(11):1137–1142, 2012.
- [156] R Kwok. Five hard truths for synthetic biology. *Nature*, 463:288–290, 2010.
- [157] Zachary Z Sun, Enoch Yeung, Clarmyra A Hayes, Vincent Noireaux, and Richard M Murray. Linear DNA for rapid prototyping of synthetic biological circuits in an *Escherichia coli* based tx-tl cell-free system. *ACS synthetic biology*, 3(6):387–397, 2013.

- [158] Zachary Z Sun, Clarmyra A Hayes, Jonghyeon Shin, Filippo Caschera, Richard M Murray, and Vincent Noireaux. Protocols for implementing an escherichia coli based tx-tl cell-free expression system for synthetic biology. *JoVE (Journal of Visualized Experiments)*, (79):e50762–e50762, 2013.
- [159] Kevin B Clairmont, William G Hagar, and Elizabeth A Davis. Manganese toxicity to chlorophyll synthesis in tobacco callus. *Plant physiology*, 80(1):291–293, 1986.
- [160] K Csatorday, Z Gombos, and B Szalontai. Mn²⁺ and co²⁺ toxicity in chlorophyll biosynthesis. *Proceedings of the National Academy of Sciences*, 81(2):476–478, 1984.
- [161] R Millaleo, M Reyes-Díaz, M Alberdi, AG Ivanov, M Krol, and NPA Hüner. Excess manganese differentially inhibits photosystem i versus ii in arabidopsis thaliana. *Journal of experimental botany*, 64(1):343–354, 2013.
- [162] R Hajiboland and BD Hasani. Effect of cu and mn toxicity on chlorophyll fluorescence and gas exchange in rice and sunflower under different light intensities. *Journal of Stress Physiology & Biochemistry*, 3(1), 2007.
- [163] Fernando Cebola Lidon, Maria Graça Barreiro, and José Cochicho Ramalho. Manganese accumulation in rice: implications for photosynthetic functioning. *Journal of plant physiology*, 161(11):1235–1244, 2004.
- [164] Ross O Nable, Robert L Houtz, and George M Cheniae. Early inhibition of photosynthesis during development of mn toxicity in tobacco. *Plant Physiology*, 86(4):1136–1142, 1988.
- [165] IE Papadakis, A Giannakoula, CP Antonopoulou, M Moustakas, E Avramaki, and IN Therios. Photosystem 2 activity of citrus volkameriana (l.) leaves as affected by mn nutrition and irradiance. *Photosynthetica*, 45(2):208–213, 2007.
- [166] CD Foy, RL t Chaney, and MC White. The physiology of metal toxicity in plants. *Annual Review of Plant Physiology*, 29(1):511–566, 1978.
- [167] John D Helmann. Specificity of metal sensing: iron and manganese homeostasis in bacillus subtilis. *Journal of Biological Chemistry*, 289(41):28112–28120, 2014.
- [168] Sumant Puri, Thomas H Hohle, and Mark R O’Brian. Control of bacterial iron homeostasis by manganese. *Proceedings of the National Academy of Sciences*, 107(23):10691–10695, 2010.
- [169] Eitan Salomon and Nir Keren. Acclimation to environmentally relevant mn concentrations rescues a cyanobacterium from the detrimental effects of iron limitation. *Environmental microbiology*, 17(6):2090–2098, 2015.
- [170] Anna Zorina, Maria A Sinetova, Elena V Kupriyanova, Kirill S Mironov, Irina Molkova, Lyudmila V Nazarenko, Vladislav V Zinchenko, and Dmitry A Los. Synechocystis mutants defective in manganese uptake regulatory system, mansr, are hypersensitive to strong light. *Photosynthesis research*, 130(1-3):11–17, 2016.
- [171] Simon A Jackson, Mark G Hinds, and Julian J Eaton-Rye. Solution structure of cyanop from synechocystis sp. pcc 6803: new insights on the structural basis for functional specialization amongst psbp family proteins. *Biochimica et Biophysica Acta (BBA)-Bioenergetics*, 1817(8):1331–1338, 2012.
- [172] Masaki Aoi, Yasuhiro Kashino, and Kentaro Ifuku. Function and association of cyanop in photosystem ii of synechocystis sp. pcc 6803. *Research on Chemical Intermediates*, 40(9):3209–3217, 2014.
- [173] Nir Keren, Hiroshi Ohkawa, Eric A Welsh, Michelle Liberton, and Himadri B Pakrasi. Psb29, a conserved 22-kd protein, functions in the biogenesis of photosystem ii complexes in synechocystis and arabidopsis. *The Plant Cell*, 17(10):2768–2781, 2005.

- [174] Peter J Nixon, Franck Michoux, Jianfeng Yu, Marko Boehm, and Josef Komenda. Recent advances in understanding the assembly and repair of photosystem ii. *Annals of botany*, page mcq059, 2010.
- [175] Dawn Smith and Christopher J Howe. The distribution of photosystem i and photosystem ii polypeptides between the cytoplasmic and thylakoid membranes of cyanobacteria. *FEMS Microbiology Letters*, 110(3):341–347, 1993.
- [176] Elena Zak, Birgitta Norling, Radhashree Maitra, Fang Huang, Bertil Andersson, and Himadri B Pakrasi. The initial steps of biogenesis of cyanobacterial photosystems occur in plasma membranes. *Proceedings of the National Academy of Sciences*, 98(23):13443–13448, 2001.
- [177] Steffen Heinz, Pasqual Liauw, Jörg Nickelsen, and Marc Nowaczyk. Analysis of photosystem ii biogenesis in cyanobacteria. *Biochimica et Biophysica Acta (BBA)-Bioenergetics*, 1857(3):274–287, 2016.
- [178] Steve Tottey, Carl J Patterson, Lucia Banci, Ivano Bertini, Isabella C Felli, Anna Pavelkova, Samantha J Dainty, Rafael Pernil, Kevin J Waldron, Andrew W Foster, et al. Cyanobacterial metallochaperone inhibits deleterious side reactions of copper. *Proceedings of the National Academy of Sciences*, 109(1):95–100, 2012.
- [179] Natalie Hoecker, Dario Leister, and Anja Schneider. Plants contain small families of upf0016 proteins including the photosynthesis affected mutant71 transporter. *Plant Signaling & Behavior*, (just-accepted):00–00, 2017.